A VARIATIONAL METHOD IN POTENTIAL FLOWS WITH A FREE SURFACE

Kwang June Bai

California University

Prepared for:

Department of the Navy

September 1972

A VARIATIONAL METHOD IN POTENTIAL FLOWS WITH A FREE SURFACE

by

Kwang June Bai

This research was carried out under the Naval Ship Systems Command General Hydromechanics Research Program Subproject SR 009 01 01, administered by the Naval Ship Research and Development Center

Report No. NA 72-2
Contract N00014-69-A-0200-1048
September 1972

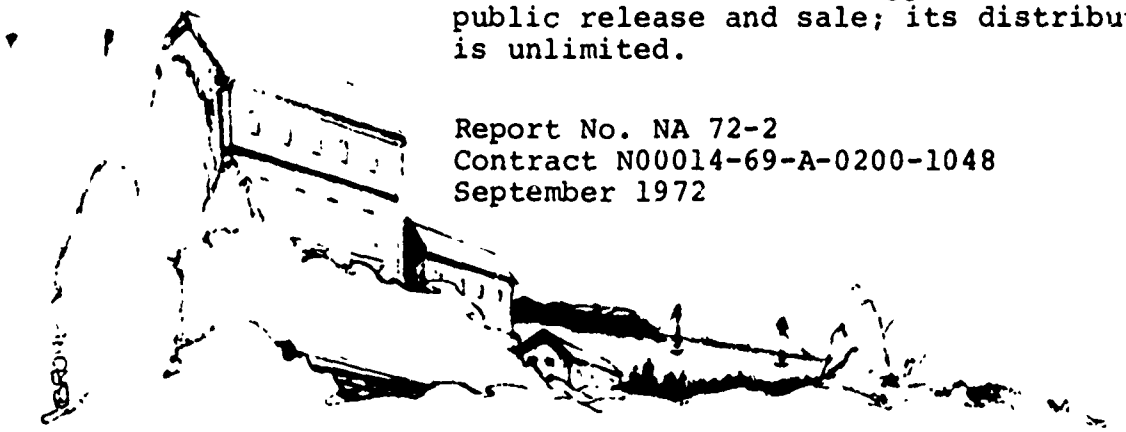

COLLEGE OF ENGINEERING

UNIVERSITY OF CALIFORNIA, Berkeley

Unclassified
Security Classification

DOCUMENT CONTROL DATA - R & D

(Security classification of title, body of abstract and indexing annotation must be entered when the overall report is classified)

1 ORIGINATING ACTIVITY (Corporate author)
University of California
College of Engineering
Berkeley, California

2a. REPORT SECURITY CLASSIFICATION
Unclassified

2b. GROUP

3 REPORT TITLE
A Variational Method in Potential Flows with a Free Surface

4 DESCRIPTIVE NOTES (Type of report and inclusive dates)
Final Technical Report

5 AUTHOR(S) (First name, middle initial, last name)
Kwang June Bai

6 REPORT DATE	7a. TOTAL NO OF PAGES	7b. NO OF REFS
September 1972	137 + vi	36

8a CONTRACT OR GRANT NO	9a. ORIGINATOR'S REPORT NUMBER(S)
N00014-69-A-0200-1048 b. PROJECT NO SR 009 01 01 c. d.	College of Engineering Report No. NA 72-2 9b OTHER REPORT NO(S) (Any other numbers that may be assigned this report)

10 DISTRIBUTION STATEMENT
This document has been approved for public release and sale; its distribution is unlimited.

11 SUPPLEMENTARY NOTES	12 SPONSORING MILITARY ACTIVITY
	Department of the Navy

13 ABSTRACT

The steady oscillatory irrotational motion of an inviscid incompressible fluid is described by a boundary-value problem of elliptic type. A variational form of this problem has been made here the basis of a numerical method. The problem is simplified assuming that the amplitudes of the generated waves are small compared with their wave lengths.

The numerical satisfaction of the radiation boundary condition has been investigated. Some sample problems with known solutions have been treated first in order to test the method. All the results for two-dimensional motion and for heaving motion of an axisymmetric body in infinite or finite depths show very good agreement with existing results. In addition, some diffraction problems in two dimensions with homogeneous fluid or stratified fluids are solved, and also a problem with non-uniform depth.

The main advantage of this method is that complex geometry of the boundary can be easily accommodated; for example, variable depth is no more difficult than constant depth. In principle, this method can solve any problem of elliptic partial differential equations with boundary conditions which are, partially or completely, of Dirichlet, Neumann, or mixed type.

14 KEY WORDS	LINK A		LINK B		LINK C	
	ROLE	WT	ROLE	WT	ROLE	WT
Finite Element						
Hydrodynamics						
Free Surface F low						
Ship Motions						
Diffraction						

A VARIATIONAL METHOD IN POTENTIAL FLOWS WITH A FREE SURFACE

by

Kwang June Bai

This research was carried out under the
Naval Ship Systems Command
General Hydromechanics Research Program
Subproject SR 009 01 01, administered by the
Naval Ship Research and Development Center

College of Engineering
University of California
Berkeley, California

September 1972

ABSTRACT

The steady oscillatory irrotational motion of an inviscid incompressible fluid is described by a boundary-value problem of elliptic type. The conventional variational form of this problem has been made here the basis of a numerical method in which an appropriate functional is minimized. The problem is simplified at the outset by replacing the nonlinear boundary conditions by linearized ones based on the assumption that the amplitudes of the generated waves are small compared with their wave lengths.

In order to optimize the numerical process, the decaying behavior of the local disturbance has been investigated and the results have been used to find an appropriate position for imposing the radiation boundary condition. Some sample problems with known solutions have been treated first in order to test this new method. All the results for two-dimensional motion and for heaving motion of an axisymmetric body in infinite or finite depths show very good agreement with existing results. In addition, some diffraction problems in two dimensions with homogeneous fluid or stratified fluids are solved, and also a problem with non-uniform depth.

The main advantage of this method is that complex geometry of the boundary can be easily accomodated; for example, variable depth is no more difficult than constant depth. In principle, this method can solve any problem of elliptic partial differential equations with boundary conditions which are, partially or completely, of Dirichlet, Neumann, or mixed type.

TABLE OF CONTENTS

		Page
	Abstract	i
	Table of Contents	ii
	Nomenclature	iv
	Introduction	1
I.	Mathematical Formulation	3
	1. Governing Equation and Boundary Conditions	3
	2. Pressure, Force, Moment and Wave Profile	13
II.	Local Disturbance, Propagating Waves and Radiation Condition	16
	1. Two-dimensional Problem	17
	a) Local Disturbance	17
	b) Propagating Waves and Radiation Condition	29
	2. Three-dimensional Problem	33
	a) Local Disturbance	33
	b) Propagating Waves and Radiation Condition	37
III.	Variational Method	43
IV.	Numerical Procedures	49
	1. Finite-element Discretization	49
	2. Truncation of the Infinite Boundaries	58
V.	Testing of the Method	61
	1. Pure Propagating Waves	61
	2. Pure Local Disturbance	62
	3. Oscillatory Pressure Given on the Free Surface	64

4. Forced Motion of Two-dimensional Cylinders in Water of Infinite and Finite Depths 65

5. Two-dimensional Diffraction Problem in Water of Infinite and Finite Depths. (Circular and Rectangular Sections) 67

6. Heaving Motion of Axi-symmetric Bodies (Sphere and Cylinder) 72

VI. New Problems 73

1. Forced Motion of Two-dimensional Cylinders in Water of Variable Depth 73

2. Two-dimensional Diffraction Problems in Water of Finite Depth (Triangular and Sinusoidal Sections, and Vertical Multi-barrier along the Free Surface) 75

VII. Discussion 77

Appendix A 80

Appendix B 84

Acknowledgement 87

Biblography 88

Figures 20 - 35 92

NOMENCLATURE

a	Maximum half beam of cylinder.
A	Submerged area of the cylinder in two dimensions.
A_w	Water plane area of the cylinder of unit length.
$[A]$, a_{ij}	Coefficient matrix and its components.
b_i , b_i^c, b_i^s	Value defined in (4-15).
$\mathcal{B}$, $\mathcal{B}_1$, $\mathcal{B}_2$	Body boundaries.
c , $\bar{c}$	Complex variables c=a + ib, and $\bar{c}$ = a - ib.
C_R , C_T	Reflection and transmission coefficients, respectively.
d	Decay factor.
$\mathcal{D}$, $\mathcal{D}_1$, $\mathcal{D}_2$	Bottom boundaries.
F , F^c, F^s	General functional, cosine- and sine-mode functionals, respectively.
$F^e(\phi)$	Functional defined in an element.
$\mathbf{F}$, $\mathbf{F}$, $\mathbf{F}_s$	Force vector, non-dimensional force vector and hydrostatic force vector, respectively.
$\mathcal{F}$, $\mathcal{F}_1$, $\mathcal{F}_2$	Free-surface boundaries.
$\mathcal{F}_p$	Free-surface boundary on which an oscillatory pressure distribution is specified.
g	Acceleration of Gravity.
$G(x,y,a,b)$	Green's function.
h	Draft of a floating body or distance from the free surface to the top of a submerged body.
h_{ij}	Defined in (4-14).
H, H_1, H_2	Depth of water.

J_n, Y_n, I_n, K_n	Bessel functions of the first kind, of the second kind, modified Bessel functions of the first kind and of the second kind, all of order n, respectively.
k_{ij}	Defined in (4-13).
m_i $(i=0,1,2,\cdots)$	Eigenvalues.
$\mathbf{M}$	Moment vector.
n	Normal vector.
$[N]$, or $N_1, N_2, \cdots$	Interpolation functions.
$p(x,y,t), p^c(x,y)$, p^s, $\bar{p}^c$, $\bar{p}^s$	Pressure, its cosine mode, its sine mode, and the nodal values of the cosine and sine modes, respectively.
p_0	Amplitude of the pressure.
R, R_1, R_2	Radiation boundaries.
(R, α, γ)	Polar coordinates in three dimensions.
s	Arc length on the body profile.
t	Time variables.
T	Period (second).
u, v (or V_x, V_y)	Velocity components in the x, y directions, respectively.
$\mathbf{V}(x,y,t), \mathbf{V}^c(x,y)$, $\mathbf{V}^s(x,y)$	Velocity vector, its cosine mode and sine mode, respectively.
$V_n^c, V_n^s, \bar{V}_n^c, \bar{V}_n^s$	Cosine- and sine-mode normal velocities and their nodal values, respectively.
x, y	Inertial Cartesian coordinates.
$\bar{x}(s), \bar{y}(s)$	Cartesian coordinates fixed in the body.
Y_0	Amplitude of the generated waves.
$Y(x,t), Y^c(x), Y^s(x)$	Wave profile, its cosine- and sine-mode wave profiles, respectively.
$\bar{Y}, \bar{Y}^c, \bar{Y}^s$	Non-dimensional wave profile, its cosine and sine-mode profiles, respectively.

$\gamma_D, \gamma_D^c, \gamma_D^s$	Diffracted-wave profile, its cosine- and sine-mode profiles, respectively.
$\gamma_x, \gamma_x^c, \gamma_x^s$	Incoming-wave profile, its cosine- and sine-mode profiles, respectively.
$\Upsilon^x, \Upsilon^A, \Upsilon^T$	Amplitudes of the incoming, reflected, and transmitted waves, respectively.
$x, \bar{x}$	Complex variables $z = x + iy$, $\bar{z} = x - iy$.
μ_{ij}, λ_{ij}	Added-mass and damping coefficients.
ξ, ξ_0, ξ_1, ξ_2	Amplitude of sway motion.
$\eta, \eta_0, \eta_1, \eta_2$	Amplitude of heave motion.
$\theta, \theta_0, \theta_1, \theta_2$	Amplitude of roll motion.
$\theta_D(x), \theta_T(x)$	Phase angles, for the diffracted and total waves, respectively.
ρ, ρ_1, ρ_2	Densities of the fluids.
$\Phi(x,y,t)$	Velocity potential.
Φ_x, Φ_D	Velocity potentials for the incoming and diffracted waves, respectively.
Φ_P, Φ_L	Velocity potentials corresponding to the propagating wave and the local disturbance, respectively.
$\varphi^c(x,y), \varphi^s(x,y)$	Cosine- and sine-mode velocity potentials, respectively.
$\varphi_{LS}, \varphi_{LI}$	Local-disturbance potential due to a source in the fluid and the image of the source in the upper plane, respectively.
δ_T	Phase lag of the transmitted wave.
τ	Tangential vector.
σ	Circular frequency (radian/sec.).
ε	Infinitesimal perturbation parameter.
ν	Wave number: $\nu = \sigma^2/g$ for infinite depth, and $\sigma^2/g = \nu \tanh \nu H$ in water of finite depth H.
$\Omega, \Omega_1, \Omega_2, \Omega_3$	Domain of definition.

Introduction

When we treat a steady oscillatory irrotational motion of an inviscid incompressible fluid described by a boundary-value problem, a method utilizing Green's function is used most often. But sometimes there are difficulties in carrying through computations which are involved with Green's functions and in addition the method has another drawback: it is not practical for a very complicated boundary geometry, i.e., for example, for a variable-depth problem , even though it could be done in principle.

In this paper another alternative method, a variational method, will be examined. This method is also called a finite-element method and has become a very useful method in the field of structural analysis in the last decade. The method has not been used much in other engineering fields.

There do exist some papers which treat problems of fluid flow. Zienkiewicz (1964), Matsuura and Kawakami (1968), Zienkiewicz and Newton (1969), Holand (1969) and Matsumoto (1970) treat oscillatory motions of the fluid and solve for the pressure as unknown variable in a finite tank since the pressure is the unknown variable in their formulations. Taylor, Patil and Zienkiewicz (1969) treated a problem of undamped harbor oscillation based on the shallow-water theory. Argyris, Mareczek and Scharpf (1969) and Doctors (1970) treated a potential-flow problem. Hunt (1970, 1971) treated a problem of sloshing water in a container based on a discrete-element structural theory of fluids.

In this paper the behavior of a local disturbance is

examined in considerable detail and the radiation condition is examined in the numerical calculations. The minimizing functional is defined as a function of the velocity potential, and the first-order linearized problem is treated. Several two-dimensional forced-motion problems and three-dimensional forced-heaving-motion problems of an axi-symmetric body are solved. Two-dimensional diffraction problems are also solved for quite a few different shapes of the obstacles. All the above problems are treated in water of finite and infinite depth. A two dimensional forced-motion problem is also treated in water of variable depth. A two-dimensional diffraction problem in the two fluids of different densities is treated.

Most results are compared with the results obtained by the other methods whenever they are available. Agreement is generally good.

A computer program has been written that can solve forced-motion problems or diffraction problems in a homogeneous fluid or in any number of stratified fluids for any complicated boundary geometries in two dimensions. Forced heaving motion of any axi-symmetric body in three dimensions can also be treated.

I. MATHEMATICAL FORMULATION

We assume that the fluid is inviscid, incompressible and its motion irrotational; surface tension is neglected. Then there exists a velocity potential which governs the kinematics of the fluid. Furthermore, we assume that the motion is sinusoidal in time, so that we can drop time dependency later. There is no further assumption necessary for the geometry of the boundaries.

The co-ordinate system is right-handed and rectangular. The y-axis is taken directed oppositely to the force of gravity, the x-axis coincides with the free surface when the fluid is at rest. The formulations given in this chapter are mainly for the two-dimensional case, but one can find the formulations for the three-dimensional case in the reference (Wehausen, 1960).

1. Governing Equation and Boundary Conditions

When we define a velocity potential $\Phi(x,y,t)$ in the fluid, this satisfies a Laplace equation throughout the fluid:

$$\nabla^2 \Phi(x,y,t) = 0, \tag{1-1}$$

where

$$\nabla^2 = \frac{\partial^2}{\partial x^2} + \frac{\partial^2}{\partial y^2},$$

$$u(x,y,t) = \frac{\partial \Phi}{\partial x}, \tag{1-2}$$

$$v(x,y,t) = \frac{\partial \Phi}{\partial y}.$$

In order to complete the free-surface boundary conditions, it is necessary to make use of one other condition besides the kinematic condition on the free surface, since the pressure is prescribed but the form of the surface is not prescribed a priori. Thus we use both kinematic and dynamic boundary conditions on the free surface. From them we obtain on the free surface, $y = Y(x,t)$, the boundary conditior

$$\Phi_{tt}(x,Y,t)+g\Phi_y+2\Phi_x\Phi_{xt}+2\Phi_y\Phi_{yt}+2\Phi_x\Phi_y\Phi_{xy}+\Phi_x^2\Phi_{xx}+\Phi_y\Phi_{yy}=0 . \quad (1\text{-}3)$$

For a moving boundary the kinematic boundary condition is

$$\frac{\partial\Phi}{\partial n} = \mathbf{n}\cdot\mathbf{V}(x,y,t) , \quad (1\text{-}4)$$

where $\mathbf{n}$ is a normal vector to the surface and $\mathbf{V}(x,y,t)$ may be taken as known. When the boundary is fixed in space, the equation (1-4) degenerates into the homogeneous boundary condition

$$\frac{\partial\Phi}{\partial n}(x,y,t) = 0 . \quad (1\text{-}5)$$

When the depth of the fluid is infinite, we have

$$\lim_{y\to-\infty} \frac{\partial\Phi}{\partial y} = 0. \quad (1\text{-}6)$$

The radiation condition requires the waves to be progressing outwards from the wave-generating source and imposes a uniqueness*

---

* A partial differential equation of elliptic type with boundary conditions of Dirichlet, Neumann or mixed type requires the boundary to be closed to ensure a unique and stable solution. See Morse and Feshbach (1953), pp. 706.

which would not otherwise be present.

Referring to Fig. 1, the cylinder is described parametrically by Cartesian coordinates $\bar{x} = \bar{x}(s)$, $\bar{y} = \bar{y}(s)$ in a system fixed in the cylinder such that this coordinate system coincides with the inertial coordinate system Oxy only when the body is at rest. The forced oscillation of the body is defined by giving the coordinates of the origin of the body coordinate system and the angle between Ox and $\bar{O}\bar{x}$:

$$\begin{aligned} \xi(t) &= \varepsilon\,\xi_0(t) = \varepsilon\,(\xi_1 \cos\sigma t + \xi_2 \sin\sigma t)\,, \\ \eta(t) &= \varepsilon\,\eta_0(t) = \varepsilon\,(\eta_1 \cos\sigma t + \eta_2 \sin\sigma t)\,, \\ \theta(t) &= \varepsilon\,\theta_0(t) = \varepsilon\,(\theta_1 \cos\sigma t + \theta_2 \sin\sigma t)\,, \end{aligned} \tag{1-7}$$

where $\xi_1, \xi_2, \eta_1, \eta_2, \theta_1, \theta_2$ are constants and $\xi(t)$, $\eta(t)$, $\theta(t)$ describe sway, heave, and roll motion, respectively. The infinitesimal perturbation parameter ε measures the relative size of body motion and hence of the motion of the fluid throughout the domain.

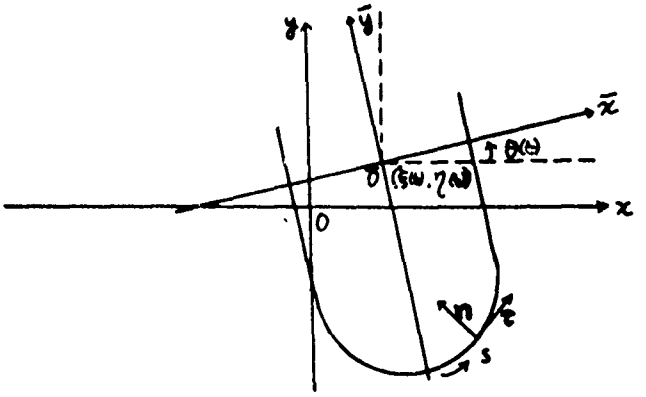

Fig. 1 Coordinate Systems

The motion of a point of the surface of the body described in terms of the inertial coordinates is as follows:

$$\begin{aligned} x(s,t) &= \bar{x}(s) + \varepsilon\,[\,\xi_0(t) - \bar{y}(s)\,\theta_0(t)\,] + O(\varepsilon^2)\,, \\ y(s,t) &= \bar{y}(s) + \varepsilon\,[\,\eta_0(t) + \bar{x}(s)\,\theta_0(t)\,] + O(\varepsilon^2)\,, \end{aligned} \tag{1-8}$$

and the normal velocity of the body surface is given by

$$\boldsymbol{n}\cdot\boldsymbol{V} = \varepsilon\Big[-\frac{d\xi_0(t)}{dt}\frac{d\bar{y}(s)}{ds} + \frac{d\eta_0}{dt}\frac{d\bar{x}}{ds} + \frac{d\theta_0}{dt}\Big(\bar{x}\frac{d\bar{x}}{ds} + \bar{y}\frac{d\bar{y}}{ds}\Big)\Big] + O(\varepsilon^2) \tag{1-9}$$

on (x(s,t), y(s,t)).

The boundary condition (1-9) is not yet a tractable boundary condition*, unless one solves this problem at the instantaneous position or as an initial-value problem because the boundary geometry is not fixed in space but moving as a function of time t. Hence the domain of definition in which a Laplace equation is to be satisfied is not fixed but is also moving as a function of time. To solve this as an initial-value problem is out of this paper's scope, therefore one should try to obtain a tractable boundary condition for a boundary fixed in space for all time. In order to express a normal velocity distribution on a boundary fixed in space, we shall make use of the analytic continuation of the velocity potential $\Phi(x,y,t)$, so that the potential evaluated on the body can be expanded in Taylor series in ε at a reference

---

* It is of interest to note that the differential operator for a Laplace equation does not have an operation with respect to time whereas a moving boundary is a function of time. A boundary condition on a moving 'material' boundary is always described in a Lagrangean representation rather than an Eulerian representation. However, in a diffraction problem with a fixed body in incoming waves, the boundary condition on the body is Eulerian. (See Eq. (1-25).

boundary (usually the average position is taken) fixed in space for all time and then in a perturbation series in ε in terms of the field variables:

$$\bar{\Phi}(x(s,t), y(s,t), t) = \bar{\Phi}(\bar{x}, \bar{y}, t) + O(\varepsilon) \quad , \tag{1-10}$$

$$\bar{\Phi}(x, y, t) = \varepsilon \bar{\Phi}^{(1)}(x, y, t) + \varepsilon^2 \bar{\Phi}^{(2)}(x, y, t) + \cdots \quad . \tag{1-11}$$

We obtain (1-12) for the normal derivative of the potential evaluated on the surface S_o, i.e., (x=x(s), y=y(s)) :

$$\frac{\partial \bar{\Phi}(\bar{x}, \bar{y}, t)}{\partial n} = \varepsilon \frac{\partial}{\partial n} \bar{\Phi}^{(1)}(\bar{x}, \bar{y}, t) + O(\varepsilon^2) \tag{1-12}$$

Equations (1-9) and (1-12) yield the required boundary condition on the body (1-4) for a forced motion.

Next we express the free surface Y(x,t) in a power series of ε:

$$Y(x,t) = \varepsilon Y^{(1)}(x,t) + \varepsilon^2 Y^{(2)}(x,t) + \cdots \quad . \tag{1-13}$$

Following the same procedure used to transfer the boundary condition for a moving body to a fixed boundary, we shall expand $\bar{\Phi}(x,Y,t)$ in a Taylor series about the neutral free surface y = 0 and substitute (1-13) in (1-3). Then we will obtain the following first-order free-surface boundary condition:

$$\bar{\Phi}^{(1)}_{tt}(x,0,t) + g \bar{\Phi}^{(1)}_{y} = 0 \quad . \tag{1-14}$$

When we drop the superscript in the potential $\bar{\Phi}^{(1)}$ for convenience and rewrite as a first-order problem, we have

$$\begin{aligned} &\nabla^2 \bar{\Phi}(x,y,t) = 0 && \text{(in the fluid)} \\ &\bar{\Phi}_{tt} + g \bar{\Phi}_y = 0 && \text{(on y=0)} \\ &\bar{\Phi}_n = -\frac{d\bar{\xi}_o}{dt}\frac{d\bar{y}}{ds} + \frac{d\bar{\eta}_o}{dt}\frac{d\bar{x}}{ds} + \frac{d\theta_o}{dt}\left(\bar{x}\frac{d\bar{x}}{ds} + \bar{y}\frac{d\bar{y}}{ds}\right) && (\text{on } S_o) \end{aligned} \tag{1-15}$$

Further, we assume that the potential $\Phi(x,y,t)$ can be decomposed into a cosine-mode potenti l and a sine-mode potential as follows:

$$\Phi(x,y,t) = \varphi^c(x,y)\cos\sigma t + \varphi^s \sin\sigma t \,. \tag{1-16}$$

From (1-7) and (1-9), we obtain

$$\begin{aligned} V_x(x,y,t) &= \sigma[(\xi_2 - y\theta_2)\cos\sigma t + (-\xi_1 + y\theta_1)\sin\sigma t], \\ V_y(x,y,t) &= \sigma[(\eta_2 + x\theta_2)\cos\sigma t - (\eta_1 + x\theta_1)\sin\sigma t], \end{aligned} \tag{1-17}$$

where

$$\mathbf{V} = (V_x, V_y)$$

From (1-15), (1-16) and (1-17) we obtain

$$\nabla^2\varphi^c(x,y)=0 \,, \quad \nabla^2\varphi^s(x,y)=0 \,, \tag{1-18}$$

$$\varphi^c_y - \frac{\sigma^2}{g}\varphi^c = 0 \,, \quad \varphi^s_y - \frac{\sigma^2}{g}\varphi^s = 0 \,. \ (\text{on } y=0), \tag{1-19}$$

$$\begin{aligned} &\varphi^c_n = \varphi^s_n = 0 \quad (\text{on a fixed body}) \,, \\ &\varphi^c_y = \varphi^s_y = 0 \quad (\text{on } y=-H. \text{ for finite depth } H), \end{aligned} \tag{1-20}$$

$$\lim_{y\to-\infty}\varphi^c_y = 0 \,, \quad \lim_{y\to-\infty}\varphi^s_y = 0 \quad (\text{for infinite depth}), \tag{1-21}$$

$$\frac{\partial\varphi^c}{\partial n} = \boldsymbol{n}\cdot\mathbf{V}^c \,, \quad \frac{\partial\varphi^s}{\partial n} = \boldsymbol{n}\cdot\mathbf{V}^s \,, \tag{1-22}$$

where

$$\begin{aligned} &\mathbf{V}(x,y,t) = \mathbf{V}^c(x,y)\cos\sigma t + \mathbf{V}^s(x,y)\sin\sigma t \,, \\ &\mathbf{V}^c = (\,\sigma(\xi_2 - y\theta_2)\,,\ \sigma(\eta_2 + x\theta_2)\,) \,, \\ &\mathbf{V}^s = (\,\sigma(-\xi_1 + y\theta_1)\,,\ -\sigma(\eta_1 + x\theta_1)\,) \,. \end{aligned} \tag{1-23}$$

As the radiation condition (Wehausen, p. 480; Stoker, p. 174) we can assume the asymptotic behavior:

$$\left.\begin{aligned} \varphi^c_x \pm \nu\varphi^s &\to 0 \\ \varphi^s_x \mp \nu\varphi^c &\to 0 \end{aligned}\right\} \quad \text{as} \quad x \to \pm\infty , \tag{1-24}$$

where ν is the wave number, i.e., $\nu = \sigma^2/g$ for infinite depth and $\sigma^2/g = \nu \tanh \nu H$ for finite depth H.

When we want to solve a diffraction problem due to a fixed body in the fluid with a homogeneous incoming wave, we assume that the total potential can be decomposed into a known potential of an incoming wave $\Phi_I(x,y,t)$ and a potential of a diffracted wave $\Phi_D(x,y,t)$. Then the boundary condition on the body for the diffracted-wave potential is

$$\frac{\partial}{\partial n}\Phi_D(x,y,t) = -\frac{\partial}{\partial n}\Phi_I(x,y,t) . \tag{1-25}$$

Let us next suppose that we have two fluids of densities ρ_1 , ρ_2 , one beneath the other, the common surface (when undisturbed) being plane and horizontal, as shown in Fig. 2.

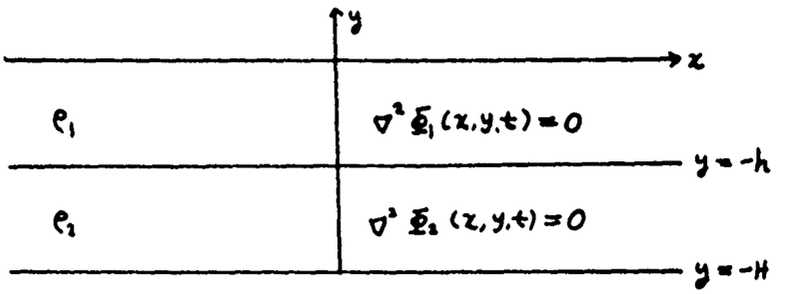

Fig. 2. Stratified Fluids

When we define the velocity potentials Φ_1 , Φ_2 in the upper and lower fluids, respectively, and when we use both kinematic and dynamic boundary conditions at the interface, we can write the first-order linearized boundary condition at the interface

of the two fluids, i.e., y = -h, as follows:

$$\begin{aligned} &\rho_2 \Phi_{2tt} - \rho_1 \Phi_{1tt} + (\rho_2 - \rho_1) g \Phi_{1y} = 0 , \\ &\rho_2 \Phi_{2tt} - \rho_1 \Phi_{1tt} + (\rho_2 - \rho_1) g \Phi_{2y} = 0 . \end{aligned} \tag{1-26}$$

When we define

$$\Phi_i = \varphi_i^c \cos \sigma t + \varphi_i^s \sin \sigma t , \quad i = 1, 2, \tag{1-27}$$

(1-26) becomes

$$\begin{aligned} &\varphi_{1y}^c + \frac{\sigma^2 \rho_1}{(\rho_2 - \rho_1) g} \varphi_1^c = \frac{\sigma^2 \rho_2}{(\rho_2 - \rho_1) g} \varphi_2^c \\ &\varphi_{1y}^s + \frac{\sigma^2 \rho_1}{(\rho_2 - \rho_1) g} \varphi_1^s = \frac{\sigma^2 \rho_2}{(\rho_2 - \rho_1) g} \varphi_2^s \end{aligned} \tag{1-28}$$

$$\begin{aligned} &\varphi_{2y}^c + \frac{\sigma^2 \rho_2}{(\rho_2 - \rho_1) g} \varphi_2^c = -\frac{\sigma^2 \rho_1}{(\rho_2 - \rho_1) g} \varphi_1^c \\ &\varphi_{2y}^s + \frac{\sigma^2 \rho_2}{(\rho_2 - \rho_1) g} \varphi_2^s = -\frac{\sigma^2 \rho_1}{(\rho_2 - \rho_1) g} \varphi_1^s \end{aligned} \tag{1-29}$$

It should be noted that (1-28) and (1-29) are mixed-type boundary conditions in the upper fluid and the lower fluid, respectively, and that they are coupled to each other.

When a pressure distribution is confined to a segment of the free surface, i.e.,

$$p(x,t) = \begin{cases} p^s \sin \sigma t, & |x| \le l, \\ 0, & |x| > l, \end{cases} \quad y=0, \tag{1-30}$$

with p^s a constant, we obtain the following boundary condition on the free surface from (1-16) and (1-30):

$$\begin{aligned} \varphi^c_y - \frac{\sigma^2}{g}\varphi^c &= \begin{cases} c, & |x| \le l, \\ 0, & |x| > l, \end{cases} \quad y=0, \\ \varphi^s_y - \frac{\sigma^2}{g}\varphi^s &= 0, \quad -\infty < x < +\infty, \ y=0, \end{aligned} \tag{1-31}$$

where

$$c = -p^s \sigma / \rho g$$

Three dimensions will be considered very briefly here. When we consider the three-dimensional problem analogous to (1-18) - (1-31) for two dimensions, we can still use most of the two-dimensional formulations. We take the velocity potential $\Phi(x,y,z,t)$ in rectangular coordinates or $\Phi(R,\alpha,y,t)$ in cylindrical coordinates. The Laplace operator becomes

$$\nabla^2 = \frac{\partial^2}{\partial x^2} + \frac{\partial^2}{\partial y^2} + \frac{\partial^2}{\partial z^2},$$

or

$$\nabla^2 = \frac{1}{R}\frac{\partial}{\partial R}\left(R\frac{\partial}{\partial R}\right) + \frac{1}{R^2}\frac{\partial^2}{\partial \alpha^2} + \frac{\partial^2}{\partial y^2},$$

where

$$x = R\cos\alpha, \quad z = R\sin\alpha$$

In (2-22) we now have $V^c = V^c(x,y,z)$, $V^s = V^s(x,y,z)$, and (1-23) will take a different form because the given motion has now six degrees of freedom.

As the radiation condition in three dimensions, we assume the following asymptotic behavior:

$$\lim_{R\to\infty} \sqrt{R}\,\left(\frac{\partial \phi}{\partial R} - i\nu\phi\right) = 0, \tag{1-32}$$

where

$$\begin{aligned} \Phi(x,y,z,t) &= \mathrm{Re}\left(\phi(x,y,z)\, e^{-i\sigma t}\right) \\ &= \varphi^c \cos\sigma t + \varphi^s \sin\sigma t, \\ \phi(x,y,t) &= \varphi^c(x,y,z) + i\,\varphi^s(x,y,z) \end{aligned} \tag{1-33}$$

or equivalently

$$\begin{aligned} &\lim_{R\to\infty} \sqrt{R}\left(\frac{\partial \varphi^c}{\partial R} + \nu\varphi^s\right) = 0, \\ &\lim_{R\to\infty} \sqrt{R}\left(\frac{\partial \varphi^s}{\partial R} - \nu\varphi^c\right) = 0. \end{aligned} \tag{1-34}$$

2. Pressure, Force, Moment, and Wave Profile

The velocity potential $\Phi(x,y,t)$ defined earlier does not give any dynamic properties of the flow unless Euler's integral is utilized. The pressure p is determined by Euler's integral,

$$p(x,y,t) = -\rho \Phi_t - \rho g y \tag{1-35}$$

with the term $\frac{1}{2}\rho|\nabla\Phi|^2$ suppressed as being of higher order. The first term in (1-35) is a hydrodynamic pressure and the second a hydrostatic pressure. Then the force on a body submerged in the fluid is given by

$$\mathbf{F} = \int_{S_0} p\,\mathbf{n}\,ds \tag{1-36}$$

and the moment with respect to the origin by

$$\mathbf{M} = \int_{S_0} p\,\mathbf{r}\times\mathbf{n}\,ds\ , \tag{1-37}$$

where S_0 describes the interface of the body and the fluid and $\mathbf{n}$ is the normal vector into the body.

If the free surface is described by $y = Y(x,t)$, then

$$Y = -\frac{1}{g}\Phi_t(x,0,t) \tag{1-38}$$

When we decompose Y into a cosine and sine mode in time,

$$Y(x,t) = Y^c(x)\cos\sigma t + Y^s(x)\sin\sigma t\ , \tag{1-39}$$

then we obtain, from (1-16), (-38) and (1-39)

$$Y^c(x) = -\frac{\sigma}{g}\varphi^s(x,0) \quad , \quad Y^s(x) = \frac{\sigma}{g}\varphi^c(x,0). \tag{1-40}$$

When a body is undergoing a forced oscillation, it is more convenient to use non-dimensional quantities for (1-35) - (1-40). If we assume the forced motion has only heave motion with amplitude η , then we can define

$$\begin{aligned} \bar{p} &= p_0/\rho g \eta \ , \\ F &= F_0/\rho g \eta A_w \ , \\ \bar{Y} &= Y_0/\eta \ , \ \bar{Y}^c = Y^c/\eta \ , \ \bar{Y}^s = Y^s/\eta \ , \end{aligned} \tag{1-41}$$

where A_w is water plane area and p_0, F_0, Y_0 are the amplitudes of the pressure p , of the force F and of the generated waves Y, respectively, these being sinusoidal in time t . The added mass μ_{22} and damping coefficient λ_{22} can be defined as follows*:

$$\begin{aligned} \mu_{22} &= -\int_{S_0} \varphi^c(x,y)\, n_2\, ds / A\eta\sigma \ , \\ \lambda_{22} &= -\int_{S_0} \varphi^s(x,y)\, n_2\, ds / A\eta\sigma \ , \end{aligned} \tag{1-42}$$

$$\mathbf{n} = (n_1, n_2)$$

---

* The notation μ_{22} and λ_{22} has been introduced here in order to conform with the more general notation μ_{ij} , λ_{ij} used when all degrees of freedom are present. Such problems can also be handled by the method to be described.

where A is the subjerged area of the body in two dimensions.

One can define all these non-dimensional quantities and hydrodynamic coefficients for other modes of motion in two dimensions or in three dimensions, but these will not be given here.

II. LOCAL DISTURBANCE, PROPAGATING WAVE AND RADIATION CONDITION

In this chapter an attempt is made to obtain a more tractable form for the radiation condition in order to facilitate applying a numerical method. One main difficulty in the radiation condition is that it should be applied as $x \to \infty$ (or $R \to \infty$). But one cannot, of course, go to infinity and an infinite boundary has always to be truncated at some ' sufficiently large' distance in a numerical method. In this chapter some criteria are developed to determine how near to the moving body (or a fixed body in a diffraction problem) one can construct an imaginary boundary on which one can apply a more tractable version of the radiation condition. The two-dimensional case will be treated first.

In order to examine the behavior of a local disturbance, we make use of two fundamental tools in potential theory. The first is the eigenfunction expansion, and the second is the potential of a pulsating source, since the source is the slowest-decaying singularity among all orders of singularities. It seems to be easier to use a pulsating source in the case of infinite depth, whereas both can be used in the finite-depth problem and give the same result.

In two- and three-dimensional cases much is very similar. Therefore in section two of this chapter, treating the three-dimensional case, details will be mostly omitted.

1. Two-dimensional Problem

a) A Local Disturbance

In order to make use of the eigenfunction expansion in the finite-depth problem, we construct two imaginary vertical boundaries* $\mathcal{B}_1$, $\mathcal{B}_2$ which extend from the bottom to the free surface, including any moving body in between. First we assume the depth is constant at y = -H. One can subdivide the region Ω bounded by y=0, y=-H, $\mathcal{R}_1$ and $\mathcal{R}_2$ into three subregions $\Omega_1, \Omega_2, \Omega_3$ as shown in Fig. 3 so that

$$\Omega = \Omega_1 + \Omega_2 + \Omega_3 \quad . \tag{2-1}$$

Once we have solved the original problem with given motion on the moving body, we know the solution $\Phi(x,y,t)$ everywhere in the fluid. Suppose the function $\partial \Phi(x,y,t)/\partial n$ on $\mathcal{B}_2$ is computed from this solution $\Phi(x,y,t)$. With this we may now solve a new boundary-value problem in the subregion Ω_2 with the boundary condition on $\mathcal{B}_2$ derived from the original formulation. We should obtain a solution identical with the original solution in the

---

* One can also construct only one vertical imaginary boundary which pierces the body and extends the original domain of definition to include the immersed part of the body. Then we separate the original problem into two problems for which the domains extend to infinity on the left-hand side and right-hand side, respectively. One assumes that there exist normal-velocity distributions for each sub-region which represent the body motion with an appropriate restriction on the body geometry. In the three-dimensional case one can construct an imaginary vertical circular cylinder which contains the body and extends to the bottom.

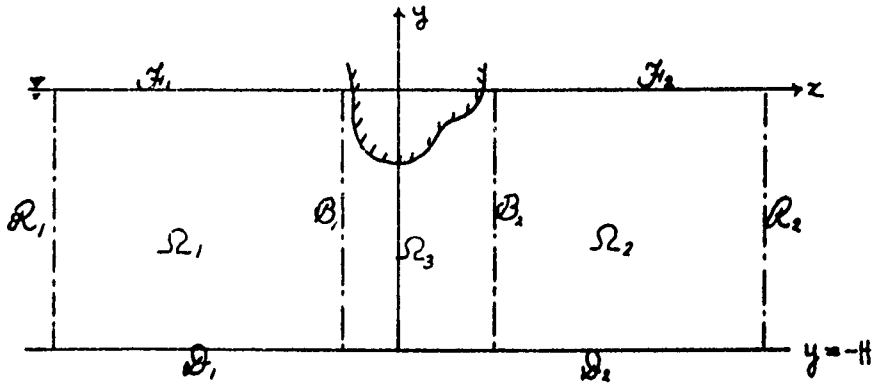

Fig. 3. Imaginary Boundaries, $\mathcal{B}_1$ and $\mathcal{B}_2$

sub-region Ω_2 due to the uniqueness theorem. A similar procedure can be applied for the sub-region Ω_1 .

Let us consider solving the problem in the sub-region where the boundaries consist of a free surface $\mathcal{F}_2$, the fictitious moving boundary $\mathcal{B}_2$, the bottom $\mathcal{D}_2$, and the boundary $\mathcal{R}_2$ ($x = \infty$). We may shift the y-axis without loss of generality, as shown in Fig. 4.

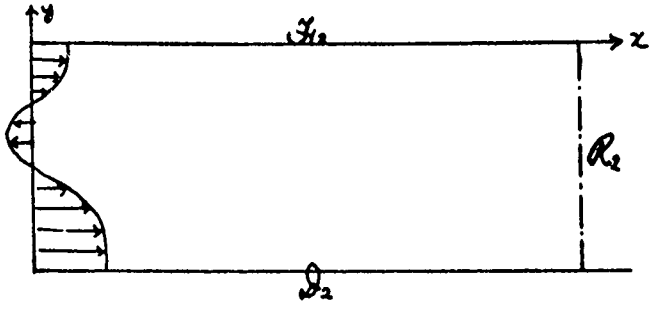

Fig. 4. Normal Velocity Distributions on an Imaginary Boundary

Now this new problem can be interpreted as a flexible-wall wave-maker. In order to solve this problem one can use a classical method, i.e. the separation of variables. By this

method one can easily obtain the eigenfunctions (Wehausen, pp. 472-475). The eigenfunctions are

$$\{ \cosh m_0(y+H),\ \cos m_i(y+H) \}, \tag{2-2}$$

where

$$\begin{aligned} \sigma^2/g &= m_0 \tanh m_0 H \\ \sigma^2/g &= -m_i \tan m_i H \quad (i=1,2,\cdots). \end{aligned} \tag{2-3}$$

Fig. 5 shows the relations (2-3) for the eigenvalues, and the functions (2-2) may be shown easily by direct computation to be orthogonal on the interval $-H \le y \le 0$. Both orthogonality and completeness are consequences of the Sturm-Liouville theory.

By making use of these eigenfunctions, one can obtain the solution of this problem as follows:

$$\begin{aligned} \Phi(x,y,t) &= \varphi^c \cos\sigma t + \varphi^s \sin\sigma t \\ &= \frac{a_0}{m_0} \cosh m_0(y+H) \sin(m_0 x - \sigma t) \\ &\quad - \sum_{i=1}^{\infty} \frac{a_i}{m_i} e^{-m_i x} \cos m_i(y+H) \cos\sigma t \end{aligned} \tag{2-4}$$

where

$$\Phi_n(x,y,t)\Big|_{B_0} = f(y) \cos\sigma t,$$

$$\begin{aligned} a_0 &= \frac{4 m_0}{\sinh 2m_0 H + 2 m_0 H} \int_{-H}^{0} f(y) \cosh m_0(y+H)\, dy, \\ a_i &= \frac{4 m_i}{\sin 2 m_i H + 2 m_i H} \int_{-H}^{0} f(y) \cos m_i(y+H)\, dy. \end{aligned} \tag{2-5}$$

$$(i = 1, 2, \cdots)$$

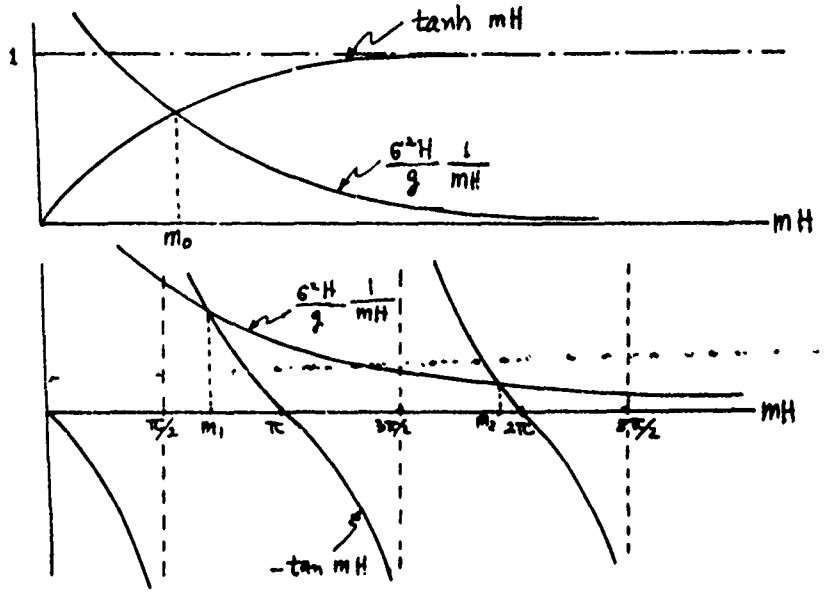

Fig. 5. Eigenvalues

Further, the potential Φ can be decomposed into two parts: one represents a propagating wave system, the other a pure local disturbance*, i.e.,

$$\Phi(x,y,t) = \Phi_p(x,y,t) + \Phi_L(x,y,t) , \qquad (2\text{-}6)$$

where

$$\Phi_p(x,y,t) = \frac{a_0}{m_0}\cosh m_0(y+H)\sin(m_0 x - \sigma t) , \qquad (2\text{-}7)$$

$$\Phi_L(x,y,t) = \sum_{i=1}^{\infty}\frac{a_i}{m_i} e^{-m_i x}\cos m_i(y+H)\cos\sigma t . \qquad (2\text{-}8)$$

Let us consider the behavior of the local disturbance expressed in the equation (2-8). How far should one go along the x-axis in order to have the local disturbance reduced to, say, 0.5% of the maximum (x=0)? To determine this we have to examine the

* One can also obtain the solution for the local disturbance Φ_L (x,y,t) by imposing $\Phi_L(x,y,t) \to 0$ as $x \to \infty$. In this case one will obtain $\{\cos m_i(y+H)\}$, $i=1,2,\cdots$, as eigenfunctions.

values of m_i $(i=1,2,\cdots)$. The value $m_1 H$ is the smallest among $m_i H$ $(i=1,2,\cdots)$ since m_1 is the smallest eigenvalue. From Fig. 5 the following inequalities hold:

$$\begin{aligned} \pi/2 &< m_1 H < \pi, \\ 3\pi/2 &< m_2 H < 2\pi, \\ &\vdots \\ (2k-1)\pi/2 &< m_k H < k\pi. \end{aligned} \tag{2-9}$$

Let us define the decay factor from (2-8) by

$$d \equiv e^{-m_1 x} . \tag{2-10}$$

When we non-dimensionalize the variable x by taking H as a non-dimensionalizing length scale, we have

$$d = e^{-m_1 H \bar{x}} \tag{2-11}$$

where

$$\bar{x} = x/H \tag{2-12}$$

From (2-9) and (2-11) one obtains

$$e^{-\pi \bar{x}} < d < e^{-\frac{\pi}{2}\bar{x}} . \tag{2-13}$$

Now one can see that for finite depth the decay factor is independent of the frequency of the motion, i.e. of σ or $2\pi g/\sigma^2$. For example, when one wants to assure $d < e^{-2\pi}$, then one must have $\bar{x} > 4$, that is, x should be at least four times the depth. When one considers a particular frequency such

that the wave length is four times the depth H, then the local disturbance decreases to $e^{-2\pi}$ times its original size in a half wave length away from the wave maker. Another extreme example is the case in which the frequency of the motion is so high that the wave length is a tenth of the depth H. Then the local disturbance decreases to $e^{-20\pi}$ times its original size in forty wave lengths away from the wave maker. Fig. 6 shows qualitatively these two extreme cases.

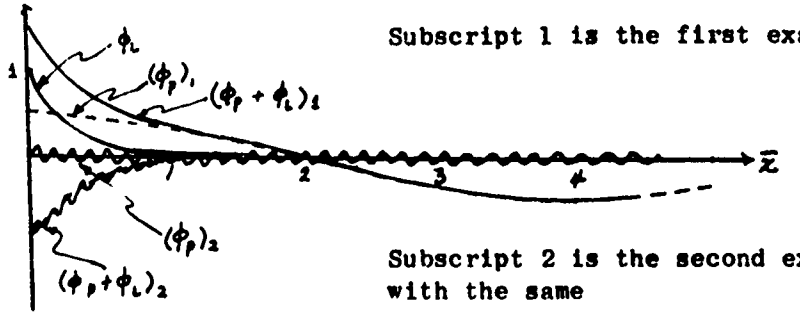

Fig. 6

It was mentioned at the beginning of this chapter that an estimate of the extent of the local disturbance could also be obtained from a source of pulsating strength. For the case of infinite depth we shall use this alternative. A source with pulsating strength $\cos \sigma t$ at (a,b) is given (Wehausen, p. 481) as follows:

$$\Phi(x,y,a,b,t) = Re\left\{ \frac{1}{2\pi}\left[\log\frac{\bar{z}-\bar{c}}{z-c} + 2\int_0^\infty \frac{e^{-ik(z-\bar{c})}}{k-\nu}\,dk\right]\cos\sigma t \right.$$
$$\left. - e^{-i\nu(z-\bar{c})}\sin\sigma t\right\}, \qquad (2\text{-}14)$$

where

$$z = x + iy \quad ,$$
$$c = a + ib \quad ,$$
$$\bar{c} = a - ib \quad ,$$
$$\nu = \sigma^2/g \quad .$$

After making use of a contour integral in the complex plane and some manipulations, one can reduce (2-14) to (2-15) and obtain (2-16) from (2-6). The procedure for deriving (2-15) from (2-14) is given in Appendix A.

$$\Phi_L(x,y,a,b,t) = \frac{1}{\pi}\left[\frac{1}{2}\log\frac{\rho_1}{\rho_2} + \int_0^\infty \frac{(\gamma - \nu\rho_2\sin\theta_2)\, e^{-\gamma}\, d\gamma}{(\gamma - \nu\rho_2\sin\theta_2)^2 + (\nu\rho_2\cos\theta_2)^2}\right]\cos\sigma t,$$

$$\Phi_p(x,y,a,b,t) = e^{\nu(y+b)}\sin[\nu(x-a) - \sigma t] \qquad (2\text{-}15)$$

where

$$z - c = \rho_1 e^{i\theta_1} \quad , \quad z - \bar{c} = \rho_2 e^{i\theta_2} \quad .$$

Now one can examine a local disturbance defined in the first equation of (2-15) and one can utilize the Gauss-Laguerre formulas [Abramowitz and Stegun, 1967] for the numerical integrations. One can further decompose

$$\Phi_L(x,y,t) = \frac{1}{\pi}(\varphi_{LS} + \varphi_{LI})\cos\sigma t \quad , \qquad (2\text{-}16)$$

where

$$\varphi_{LS} = \frac{1}{2}\log\frac{\rho_1}{\rho_2} \quad , \qquad (2\text{-}17)$$

$$\varphi_{LI} = \int_0^\infty \frac{(\xi - \sin\theta_2)\, e^{-\xi\nu\rho_2}}{(\xi - \sin\theta_2)^2 + \cos^2\theta_2}\, d\xi \quad . \qquad (2\text{-}18)$$

φ_{Ls} is the potential due to the source and φ_{Lx} is due to the image of the source, i.e. a sink in upper half-plane. In the case of infinite depth, one can obviously define the decay factor, but Figures 7 to 10 show the values of the potential for a local disturbance directly; this gives enough information about its behavior.

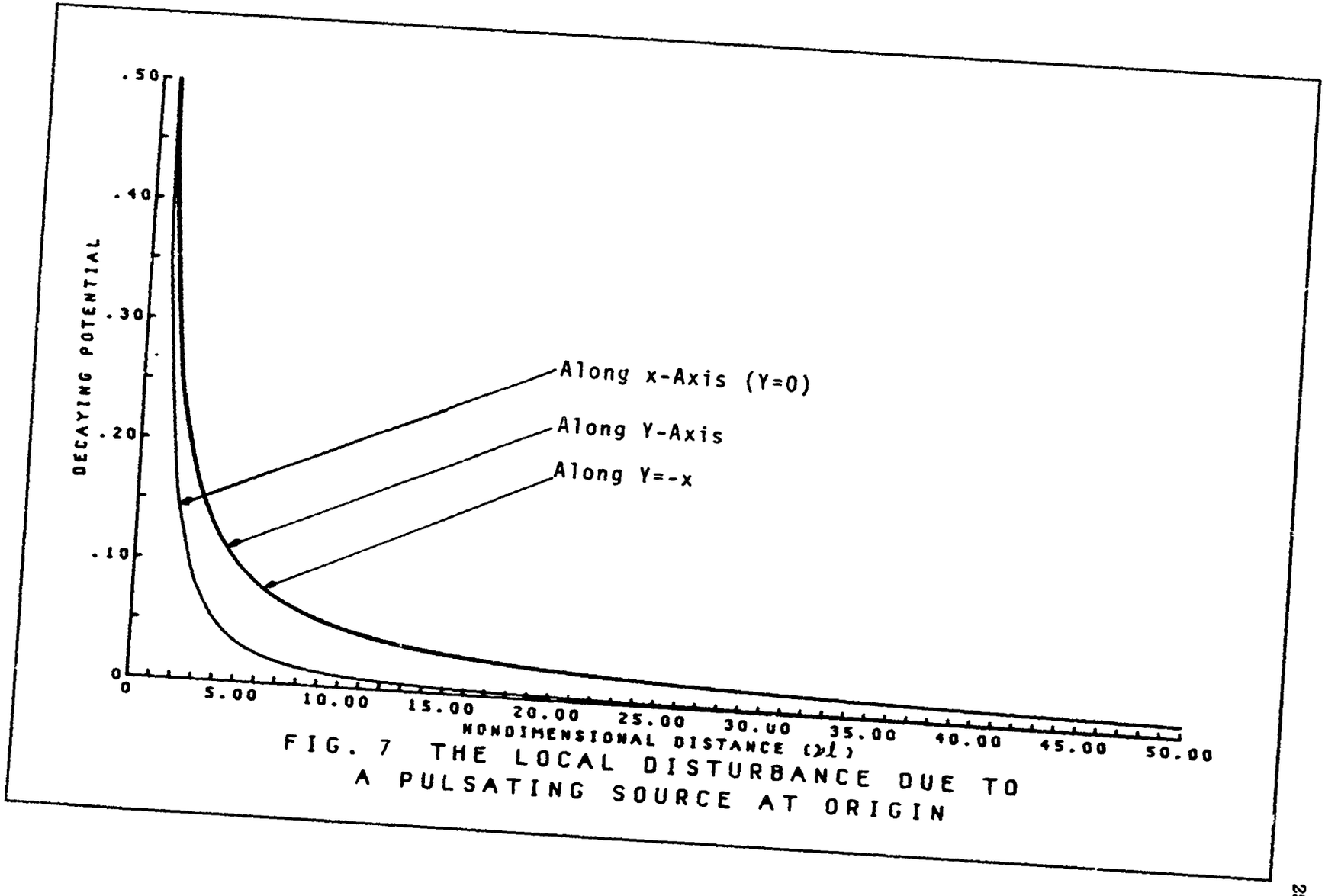

FIG. 7 THE LOCAL DISTURBANCE DUE TO A PULSATING SOURCE AT ORIGIN

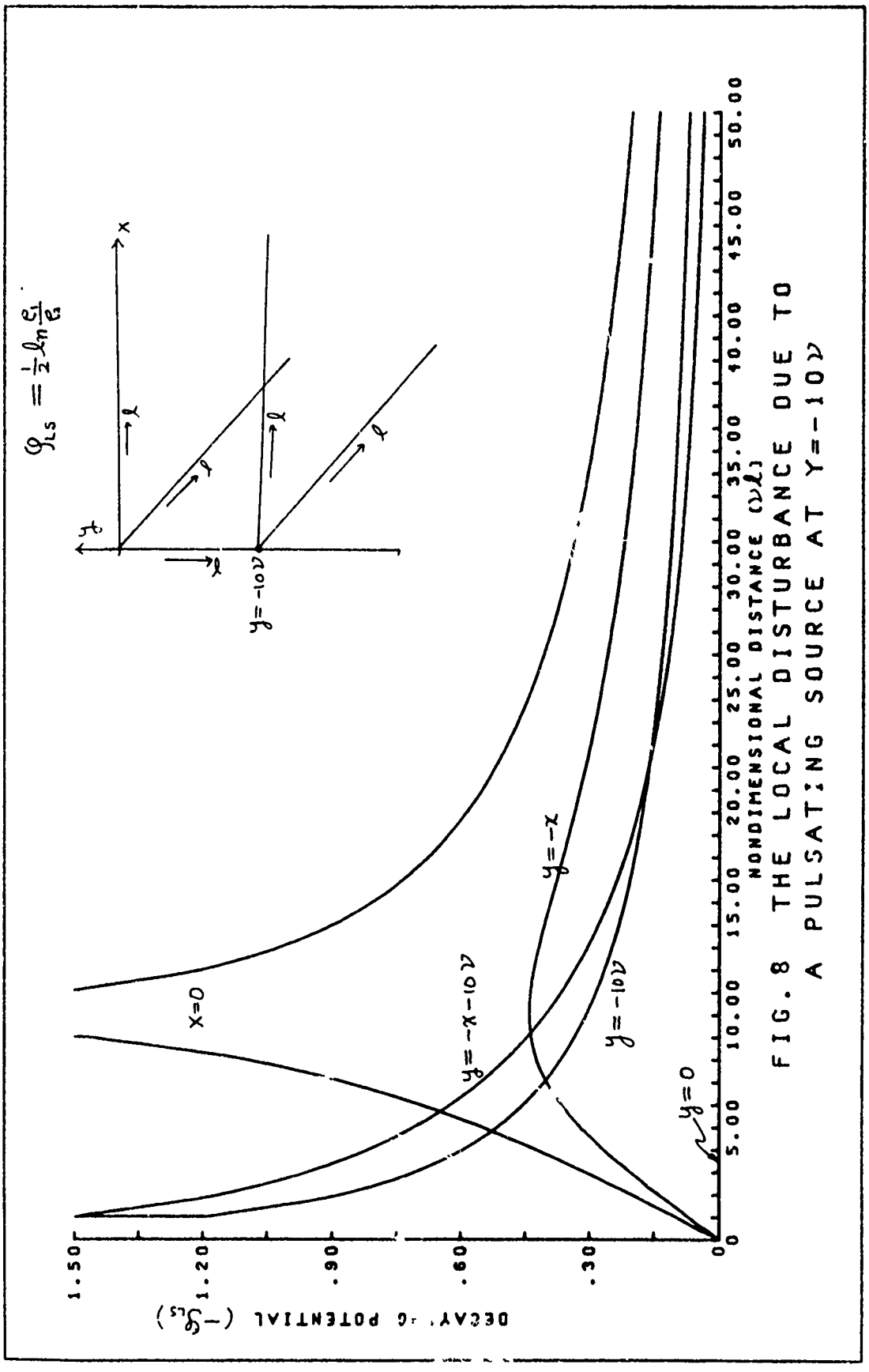

FIG. 8 THE LOCAL DISTURBANCE DUE TO A PULSATING SOURCE AT Y=-10ν

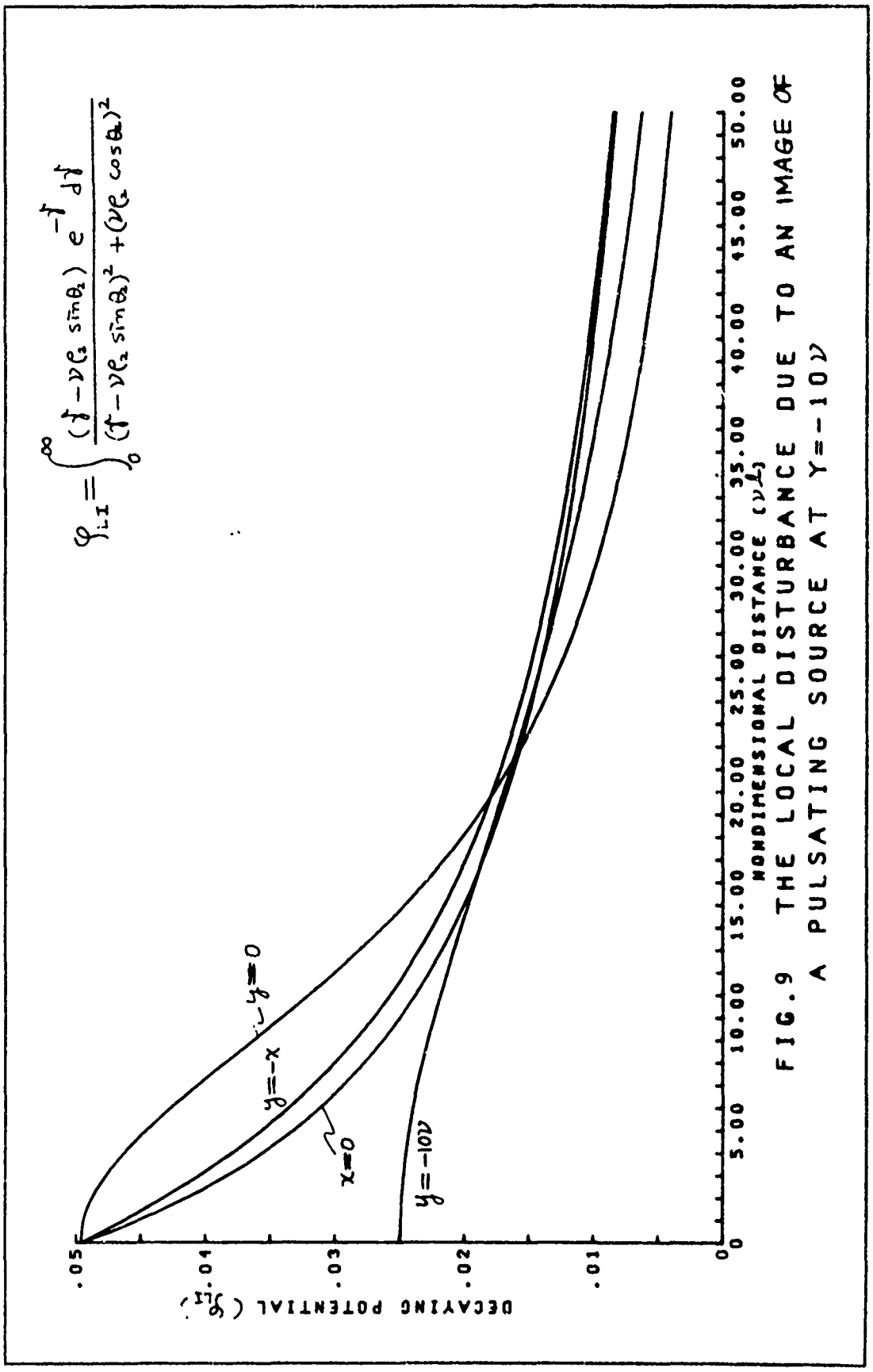

FIG. 9 THE LOCAL DISTURBANCE DUE TO AN IMAGE OF A PULSATING SOURCE AT Y=−10ν

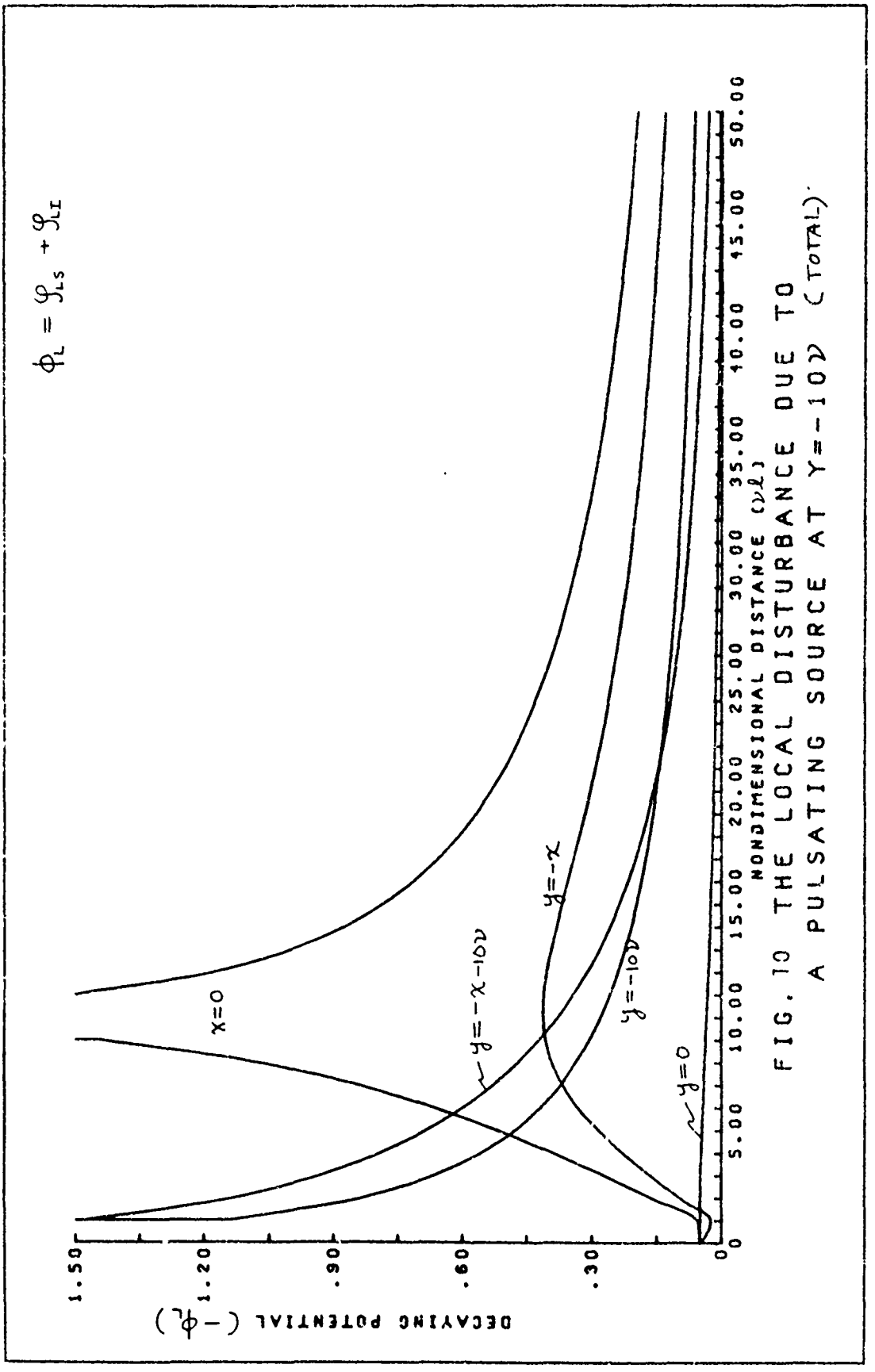

FIG. 10 THE LOCAL DISTURBANCE DUE TO A PULSATING SOURCE AT Y=-10ν (TOTAL)

b) Propagating Waves and Radiation Condition

From the previous sub-section, one sees that the velocity potential can be represented as a sum of a potential of a local disturbance and a potential of propagating waves. This decomposition is unique. Now we can examine a pure propagating wave which is the solution for a homogeneous boundary condition with no body in the fluid and with uniform constant depth or infinite depth. The solutions are given in many books on hydrodynamics (e.g., Lamb p. 369). They are as follows:

for finite depth,

$$\Phi_p(x,y,t) = A \cosh \nu(y+H) \cos(\nu x - \sigma t) , \qquad (2\text{-}19)$$

where

$$A = -ga/\sigma \cosh \nu H, \quad \sigma^2/g = \nu \tanh \nu H, \quad a = \text{wave amplitude}$$

for infinite depth

$$\Phi_p = B e^{\nu y} \cos(\nu x - \sigma t) , \qquad (2\text{-}20)$$

where

$$B = -a/\sigma, \quad \nu = \sigma^2/g, \quad a = \text{wave amplitude}$$

In the formulation in Chapter One, the radiation condition simply states the asymptotic behavior of the generated waves at a large distance from the moving body, but for a numerical method, we need a more tractable boundary condition than (1-24) or (1-34), which simply state an asymptotic behavior at infinity. Therefore in this subsection we will try to obtain a more tractable radiation condition from the examination of pure propagating waves in order to apply it to the numerical scheme.

Let us try to derive a boundary condition from (2-19) or (2-20). First (2-19) and (2-20) are slightly changed in (2-21) by defining φ_p^c, φ_p^s which correspond to the cosine and sine modes, respectively:

$$\bar{\Phi}_p = \varphi_p^c \cos\sigma t + \varphi^s \sin\sigma t \tag{2-21}$$

where

for finite depth,

$$\begin{aligned} \varphi_p^c &= A \cosh \nu(y+H) \cos \nu x \ , \\ \varphi_p^s &= A \cosh \nu(y+H) \sin \nu x \ , \end{aligned} \tag{2-22}$$

for infinite depth,

$$\begin{aligned} \varphi_p^c &= B e^{\nu y} \cos \nu x \ , \\ \varphi_p^s &= B e^{\nu y} \sin \nu x \ . \end{aligned} \tag{2-23}$$

Since the formulation in Chapter One is given for the potentials $\varphi^c(x,y)$ and $\varphi^s(x,y)$ after the time has been precipitated out, one obviously may try to make a condition (a coupled relation between φ_p^c and φ_p^s) from (2-22) or (2-23). One readily sees that a coupled relation cannot be made from them unless the derivative terms are taken into consideration. The first derivatives with respect to x and y are as follows:

for finite depth,

$$\begin{aligned}
\frac{\partial}{\partial x}(\varphi_p^c) &= -A\nu \cosh \nu(y+H) \sin \nu x , \\
\frac{\partial}{\partial y}(\varphi_p^c) &= A\nu \sinh \nu(y+H) \cos \nu x , \\
\frac{\partial}{\partial x}(\varphi_p^s) &= A\nu \cosh \nu(y+H) \cos \nu x , \\
\frac{\partial}{\partial y}(\varphi_p^s) &= A\nu \sinh \nu(y+H) \sin \nu x ;
\end{aligned} \tag{2-24}$$

for infinite depth,

$$\begin{aligned}
\frac{\partial}{\partial x}(\varphi_p^c) &= -B\nu e^{\nu y} \sin \nu x , \\
\frac{\partial}{\partial y}(\varphi_p^c) &= B\nu e^{\nu y} \cos \nu x , \\
\frac{\partial}{\partial x}(\varphi_p^s) &= B\nu e^{\nu y} \cos \nu x , \\
\frac{\partial}{\partial y}(\varphi_p^s) &= B\nu e^{\nu y} \sin \nu x .
\end{aligned} \tag{2-25}$$

From (2-22) and (2-24) or (2-23) and (2-25) the following coupled first-order differential equations can be obtained for finite or infinite depths:

$$\begin{aligned}
\frac{\partial}{\partial x}(\varphi_p^c) &= -\nu \varphi_p^s , \\
\frac{\partial}{\partial x}(\varphi_p^s) &= \nu \varphi_p^c .
\end{aligned} \tag{2-26}$$

Our main concern in this section is to derive a more tractable radiation condition, as mentioned before, which would be a boundary condition of Dirichlet, Neumann or mixed type. If one takes the boundary to be normal to the x-axis, then (2-26) becomes a mixed type boundary condition, since in this case we can replace $\frac{\partial}{\partial n}$ by $\frac{\partial}{\partial x}$.

The equation (2-26) can be written as

$$\left.\begin{aligned} \frac{\partial}{\partial n}(\varphi_p^c) &= -\nu \varphi_p^s \\ \frac{\partial}{\partial n}(\varphi_p^s) &= \nu \varphi_p^c \end{aligned}\right\} \quad \text{on } x = \text{const.} \tag{2-26'}$$

It is of interest to note that, for the infinite-depth case, one can obtain the coupled relation (2-27) below for a more general boundary than (2-26) or (2-26'). And this boundary could be any simply connected line from the free surface to a sufficient depth that could represent the infinite-depth problem for numerical computation:

$$\begin{aligned} \frac{\partial}{\partial n}(\varphi_p^c) &= \nu(-n_1 \varphi_p^s + n_2 \varphi_p^s) \quad , \\ \frac{\partial}{\partial n}(\varphi_p^s) &= \nu(n_1 \varphi_p^c + n_2 \varphi_p^s) \quad , \end{aligned} \tag{2-27}$$

or

$$\begin{aligned} \frac{\partial}{\partial n}(\varphi_p^c) - \nu n_2 \varphi_p^c &= -\nu n_1 \varphi_p^s \quad , \\ \frac{\partial}{\partial n}(\varphi_p^s) - \nu n_2 \varphi_p^s &= \nu n_1 \varphi_p^c \quad , \end{aligned} \tag{2-28}$$

where $\mathbf{n} = (n_1, n_2)$ is the outward normal vector from the fluid on the boundary.

It should be noted that (2-27) or (2-28) is reduced to (2-26) or (2-26') if the boundary is chosen to be vertical, i.e., $\mathbf{n} = (1,0)$.

2. Three-dimensional Problem

As mentioned before, most of the procedures in this section are similar to the previous section in this chapter. Thus a brief treatment will be given. However, a derivation of a new radiation condition will be given in some detail.

Cylindrical coordinates will be used throughout this section.

a) Local Disturbance

The finite-depth problem will be treated first. It is assumed that the motion (normal-velocity distribution) is given on $R=R_o$ * (refer to Fig. 11).

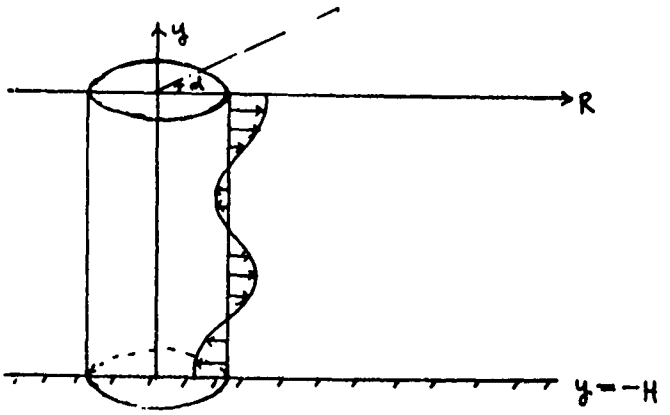

Fig. 11

In order to solve this problem with a simple geometry, one can use the method of separation of the variables as in the previous section. Then one obtains the elementary solutions (Wehausen, p. 475) as follows:

---

* See the footnote on page 17.

$$\cosh m_0(y+H)\,[A J_n(m_0 R) + B Y_n(m_0 R)] \cos(n\alpha+\delta)\cos(\sigma t+\tau),$$

$$\cos \nu_i(y+H)\,[A I_n(m_i R) + B K_n(m_i R)] \cdot \cos(n\alpha+\delta)\,(\cos\sigma t+\tau) \quad (2\text{-}29)$$

$$(i = 1,2,\cdots)$$

where A, B, δ, τ are constants, where the eigenvalues m_o, m_i $(i = 1,2,\cdots)$ are defined in (2-3) and where n is an integer because of the juncture condition (continuity condition) along the α-direction unless there is a radial-plane cut pivoted on the y-axis.

Without actually constructing a solution for a given normal velocity distribution on the body by using the above eigenfunctions, one can examine the behavior of a local disturbance in general. In the first equation of (2-29), J_n is the only bounded function and represents a standing wave with a fixed phase at infinity, whereas one can find bounded standing waves of arbitrary phase in two dimensions. Whenever one wants to construct a wave of arbitrary phase* at infinity, one must also admit the singular Bessel function Y_n; in other words, one should permit a logarithmic singularity at the axis R=0. Therefore, the first equation in (2-29) can be used to construct a propagating wave. In the second equation in (2-29), I_n is bounded at R=0 but increases exponentially as $R \to \infty$ whereas K_n is singular at R=0 but bounded for other values of R and decreases exponentially as

---

* Only when there is a standing wave of arbitrary phase can one construct an outgoing wave which can be expressed in the form
$\phi = f(x-ct)$ for one spatial dimension and in the form
$\phi = f_1(x) f_2(x-ct)$ for two spatial dimensions.

$R \to \infty$. There is no function which is bounded everywhere and represents a local disturbance in three dimensions. In general, one may expect that the solution of a boundary-value problem will require the functions K_n and hence a singularity at R=0. The function K_n will represent the local disturbance.

In order to investigate the behavior of a local disturbance one may then simply examine the function $K_n(m_i R)$. The functions $J_n(\chi)$, $Y_n(\chi)$, and $K_n(\chi)$ have well known asymptotic representations as $\chi \to \infty$. These asymptotic representations are

$$\begin{aligned} J_n(\chi) &\sim \sqrt{\frac{\pi}{2\chi}} \cos(\chi - \delta_n) , \\ Y_n(\chi) &\sim \sqrt{\frac{\pi}{2\chi}} \sin(\chi - \delta_n) , \\ K_n(\chi) &\sim \sqrt{\frac{\pi}{2\chi}} e^{-\chi} , \end{aligned} \tag{2-30}$$

where

$$\delta_n = \frac{n\pi}{2} + \frac{\pi}{4} .$$

When n is quite small, say, n=0,1,2,3, these asymptotic formulas give very good approximations for these real functions, even when the variable χ is not so large. For example, when n = 0 the asymtotic formulas for $J_0(\chi)$ and $Y_0(\chi)$ give such good approximate ones after about one wave length.

When an axisymmetric body is heaving vertically, n = 0, and when the body is surging, n = 1, and so on. The more complicated one makes the motion, the higher the order of the Bessel functions contained in the solution. We restrict ourselves to the case n = 0 for simplicity, but in principle a general type of motion can be treated in the same way and there will be

only a change in the region in which the asymptotic formulas will be useful for the approximation.

From the above considerations one can readily adopt the two-dimensional results (2-9)-(2-13) for a local disturbance expressed in $K_n(m;R)$ by replacing x by R.

For infinite depth, we shall examine a source with pulsating strength $\cos \sigma t$ at y=b on the y-axis (Wehausen, p. 477). The potential* is

$$\Phi(R,y,b) = \left[\frac{1}{r}+\frac{1}{r_1}+2\nu e^{\nu y}\int_{\infty}^{y}\frac{e^{-\nu y}}{r_1}dy\right]\cos\sigma t + 2\pi\nu e^{\nu(y+b)}\left[J_0(\nu R)\sin\sigma t - Y_0(\nu R)\cos\sigma t\right], \tag{2-31}$$

where

$$r^2 = R^2 + (y-b)^2 \quad , \quad r_1^2 = R^2 + (y+b)^2 \, .$$

For convenience we define

$$\Phi(R,y,b) = \Phi_L + \Phi_T \quad , \tag{2-32}$$

$$\Phi_L(R,y,b) = (\varphi_{LS} + \varphi_{LT})\cos\sigma t \, , \tag{2-33}$$

where

$$\varphi_{LS} = \frac{1}{r}+\frac{1}{r_1}$$
$$\varphi_{LT} = 2\nu e^{\nu y}\int_{\infty}^{y}\frac{e^{-\nu y}}{r_1}dy \, . \tag{2-34}$$

For the computation of the integral in (2-34) the Gauss-Laguerre quadrature formula has been used as was done for the two-dimensional computations (see Appendix A).

---

* If we take a higher-order singularity, then we get higher-order Bessel functions.

b) Propagating Waves and Radiation Condition

We have already remarked in the previous sub-section that one must have a pair of J_n and Y_n in order to construct a propagating wave and that the asymptotic formulas for J_n, Y_n, and K_n have a very wide range of validity as approximations. Thus we shall construct a new relation between the approximate expressions for J_n and Y_n, which will be used as a radiation condition later. Since the radiation condition is nothing but a condition for the departing phase in space, one may suppress the factor $R^{-\frac{1}{2}}$ in the asymptotic representations in considering the oscillatory parts. Now let us define the first term of the asymptotic expansions as functions to be used in the derivation of a new form of the radiation condition more suitable for numerical calculations:

$$\hat{J}_n(\nu R) \equiv \sqrt{\frac{2}{\pi \nu R}} \cos(\nu R - \delta_n), \qquad (2\text{-}35)$$

$$\hat{Y}_n(\nu R) \equiv \sqrt{\frac{2}{\pi \nu R}} \sin(\nu R - \delta_n),$$

where

$$\left.\begin{aligned} J_n(\nu R) - \hat{J}_n(\nu R) &\longrightarrow 0 \\ Y_n(\nu R) - \hat{Y}_n(\nu R) &\longrightarrow 0 \\ \delta_n = \tfrac{n\pi}{2} + \tfrac{\pi}{4} &. \end{aligned}\right\} \quad \text{as} \quad R \longrightarrow \infty,$$

Define $\hat{\varphi}^c$ and $\hat{\varphi}^s$ as follows:

$$\hat{\varphi}^c = \sqrt{R} \cdot \hat{J}_n = A \cos(\nu R - \delta_n), \qquad (2\text{-}36)$$

$$\hat{\varphi}^s = \sqrt{R}\ \hat{Y}_n = A \sin(\nu R - \delta_n),$$

where

$$A = \sqrt{\frac{2}{\pi c \nu}} = \text{constant}.$$

From the condition of departing phase and (2-36), in a manner similar to the derivation of the two-dimensional case we obtain

$$(\hat{\varphi}^c)_R = -\nu\hat{\varphi}^s\,,$$
$$(\hat{\varphi}^s)_R = \nu\hat{\varphi}^c\,. \tag{2-37}$$

From (2-36),

$$(\hat{\varphi}^c)_R = \frac{\partial}{\partial R}(\sqrt{R}\cdot\hat{J}_n) = \tfrac{1}{2}R^{-\frac{1}{2}}\hat{J}_n + R^{\frac{1}{2}}(\hat{J}_n)_R\,,$$
$$(\hat{\varphi}^s)_R = \frac{\partial}{\partial R}(\sqrt{R}\,\hat{Y}_n) = \tfrac{1}{2}R^{-\frac{1}{2}}\hat{Y}_n + R^{\frac{1}{2}}(\hat{Y}_n)_R\,. \tag{2-38}$$

From (2-37) and (2-38), we obtain the following:

$$\tfrac{1}{2}R^{-\frac{1}{2}}\hat{J}_n + R^{\frac{1}{2}}(\hat{J}_n)_R = -\nu R^{\frac{1}{2}}\hat{Y}_n\,,$$
$$\tfrac{1}{2}R^{-\frac{1}{2}}\hat{Y}_n + R^{\frac{1}{2}}(\hat{Y}_n)_R = \nu R^{\frac{1}{2}}\hat{J}_n\,, \tag{2-39}$$

or

$$\sqrt{R}\,[\,(\hat{J}_n)_R + \tfrac{1}{2R}\hat{J}_n + \nu\hat{Y}_n\,] = 0\,,$$
$$\sqrt{R}\,[\,(\hat{Y}_n)_R + \tfrac{1}{2R}\hat{Y}_n - \nu\hat{J}_n] = 0\,. \tag{2-40}$$

We finally propose as a new radiation condition for numerical computation

$$\sqrt{R}\left[(\varphi_p^c)_R + \tfrac{1}{2R}\varphi_p^c + \nu\varphi_p^s\right] = 0\,,$$
$$\sqrt{R}\left[(\varphi_p^s)_R + \tfrac{1}{2R}\varphi_p^s - \nu\varphi_p^c\right] = 0\,, \tag{2-41}$$

where

$$\Phi_p(R,\alpha,y,t) = \varphi_p^c(R,\alpha,y)\cos\sigma t + \varphi_p^s(R,\alpha,y)\sin\sigma t.$$

At this stage one may start to have doubts about the new radiation condition (2-41) because the second terms (in the bracket) in (2-41) are $O(R^{-3/2})$ whereas only the first term in the asymptotic expansions for $J_n(\nu R)$ and $Y_n(\nu R)$ was taken in the derivation of (2-41). If the neglected terms are of order less than or equal to $O(R^{-3/2})$ in the asymptotic expansions, those terms should have been taken into account in the derivation of (2-41). In order to examine this, we write down the complete asymptotic expansions for $J_n(x)$ and $Y_n(x)$ (Watson, p. 199; Whittaker and Watson, pp. 368-371):

$$\begin{aligned} J_n(x) &\sim \sqrt{\frac{2}{\pi x}}\,[U(x)\cos(x-\delta_n) - V(x)\sin(x-\delta_n)], \\ Y_n(x) &\sim \sqrt{\frac{2}{\pi x}}\,[U(x)\sin(x-\delta_n) + V(x)\cos(x-\delta_n)], \end{aligned} \tag{2-42}$$

where δ_n is defined in (2-30) and

where

$$\begin{aligned} U(x) &= \left\{1 + \sum_{m=1}^{\infty} \frac{(-)^m\{4n^2-1^2\}\{4n^2-3^2\}\cdots\{4n^2-(4m-1)^2\}}{(2m)!\;2^{6m}\cdot x^{2m}}\right\}, \\ V(x) &= \sum_{m=1}^{\infty} \frac{(-)^m\{4n^2-1^2\}\{4n^2-3^2\}\cdots\{4n^2-(4m-3)^2\}}{(2m-1)!\;2^{6m-3}\;x^{2m-1}}. \end{aligned} \tag{2-43}$$

From (2-42) if we take two terms in the expansions, we will have

$$\begin{aligned} J_n(x) &\sim A_0\,x^{-1/2}\cos(x-\delta_n) - B_1\,x^{-3/2}\sin(x-\delta_n) + O(x^{-5/2}), \\ Y_n(x) &\sim A_0\,x^{-1/2}\sin(x-\delta_n) + B_1\,x^{-3/2}\cos(x-\delta_n) + O(x^{-5/2}), \end{aligned} \tag{2-44}$$

where A_0 and B_1 are constants defined in (2-43). From (2-44) it can be seen readily that the second term is $O(R^{-3/2})$

and should have been taken into account in the derivation of (2-41) if all terms through this order are retained. Fortunately these worries turn out to be unnecessary, for, if one substitutes these two-term expansions (2-44) into (2-41), the terms of $O(R^{-3/2})$ introduced by retaining the second term of $O(R^{-3/2})$ cancel each other, and the lowest order left is $O(R^{-5/2})$. Thus we have the following:

$$\begin{aligned} (J_n)_R + \frac{1}{2R} J_n + \nu Y_n &= O(R^{-5/2}) \ , \\ (Y_n)_R + \frac{1}{2R} Y_n - \nu J_n &= O(R^{-5/2}) \ . \end{aligned} \tag{2-45}$$

As mentioned earlier, the first term in the expansions, i.e., the equations (2-35), are very good approximations for J_n and Y_n, but if we take the two terms as defined in (2-44) the approximations will be far better. Even most mathematical tables do not give the Bessel functions J_0 and Y_0 for $x>15.9$, for example, but give the formula (2-44) instead (e.g., McLachlan, pp. 215-217). This is even less than three wave lengths in our problem ($x = \nu R$). Therefore the relations (2-41) are valid to the same extent that (2-44), neglecting the terms of $O(R^{-5/2})$, is valid. This is then the new radiation condition that we shall use.

If we take the limit $R\to\infty$, (2-41) reduces to the conventional radiation condition (1-34). Therefore one can interpret this new radiation condition as a boundary condition which gives a better approximation than the conventional radiation condition and does not require R to be so large for its application.

If one takes a boundary R = constant, the derivative with respect to R in (2-41) becomes a Neumann-type boundary condition, which we were hoping to obtain for later application of a variational principle.

It is also of interest to note that the new radiation condition (2-41) can be obtained without using the elementary solutions, i.e., the Bessel functions J_n and Y_n, but through physical observations and much simpler mathematics. When we observe steady-state outgoing ring waves in a pond which are generated at a point or in a small region in the center of the pond, at some distance away from the wave-making region (or point) we can assume

$$Y(R,t) = A(R) \cos(\nu R - \sigma t) , \tag{2-46}$$

where Y is the elevation of the free surface and the amplitude A is a function of R. Since we have assumed that the motion of the fluid is a steady oscillatory one, then the energy flux across an arbitrary concentric circular cylinder in one period must remain a constant. From this consideration we obtain

$$A(R) = c/\sqrt{R} , \tag{2-47}$$

where c is a constant.

If we had started with the above equation (2-47) in the derivation of the new radiation condition, we could have obtained the same equation (2-41) without having considered the asymtotic behavior of the Bessel functions. This method does not seem to be mathematically rigorous, but is still based on observation of the real phenomena, and hence it shouldn't be disparaged.

III. VARIATIONAL METHOD

Most problems of applied physics encountered in engineering are formulated in the form of a differential equation which governs the behavior of a typical, infinitesimal region in the domain of definition, and which can be solved analytically or numerically. To solve such problems analytically one may use the method of separation of variables for a very simple geometry or the method of integral representations by using Green functions. In ship-hydrodynamics problems, the latter is used most often. Sometimes, however, there are difficulties in carrying through computations which are involved with Green functions. Furthermore, the method has another drawback, in that it is not practical for a very complicated boundary geometry, i.e., for example, for a variable-depth problem, even though it could be done in principle.

In this chapter we shall discuss an alternative method, a so-called variational method. A formulation in a variational form can be obtained directly from the fundamental physics of the problem, e.g., the energy method in a structural problem. In a slightly different way, it can also be obtained mathematically from the fundamental differential equations. It is not always possible to find a variational form for a given problem. When a variational form is not known for a differential equation that we wish to solve, we can still use a numerical technique to minimize a 'pseudo-variational form' or any approximate functional

constructed for the differential equation (Zienkiewicz, pp. 38-40, 1971).

There exist variational principles for the motion of a fluid either in an Eulerian representation or in a Lagrangean representation (Eckart, 1960; Luke, 1966). Since our formulation, Equations (1-18) - (1-23) and the radiation conditions (2-26') and (2-41), consists of Laplace's equation with boundary conditions, partly, of Neumann type and, partly of mixed type, we shall simply adopt a well-known variational form for this problem (Mikhlin, pp. 138-151, 1964).

Let us consider Laplace's equation

$$\nabla^2 \phi(x,y) = 0 \quad (\text{in } \Omega), \tag{3-1}$$

with a boundary condition, of the form

$$\phi_n + \alpha \phi = \beta \quad (\text{on } \partial\Omega),$$

where $\alpha(x,y)$ and $\beta(x,y)$ are known functions. The variational form for this problem requires introduction of the following functional:

$$F(\phi) = \iint_{\Omega} \tfrac{1}{2} |\nabla \phi|^2 dx dy + \int_{\partial\Omega} (\tfrac{1}{2}\alpha\phi^2 - \beta\phi) ds . \tag{3-2}$$

A function ϕ that minimizes the functional F is a solution of (3-1), and vice versa. The proof that the function ϕ which minimizes the functional $F(\phi)$ is the solution of (3-1), is also in Mikhlin (pp. 115-116, 1964).

In three dimensions one has a similar form. Let ϕ satisfy

$$\nabla^2\phi(x,y,z) = 0 \qquad (\text{in } \Omega),$$
$$\phi_n(x,y,z) + \alpha\phi = \beta \qquad (\text{on } \partial\Omega), \tag{3-3}$$

where $\alpha(x,y,z)$ and $\beta(x,y,z)$ are known functions. Then the corresponding functional $F(\phi)$ is

$$F(\phi) = \iiint_{\Omega} \frac{1}{2}|\nabla\phi|^2 \, dx\,dy\,dz + \iint_{\partial\Omega} \left(\frac{1}{2}\alpha\phi^2 - \beta\phi\right) dA \tag{3-4}$$

It is of interest to note a special case in which the general form of the functional $F(\phi)$ in (3-2) or (3-4) can degenerate to the boundary integral only when we distribute Green functions along the boundary (Bessho, 1970). The application of this degenerate case is given in Sao, Maeda and Hweng (1971). In this case the computation will be similar to the scheme used by Frank (1967).

In our problem, from (1-18) - (1-23) we can readily see that we will have two functionals, one for a cosine-mode and the other for a sine-mode, and that these two functionals to be minimized are coupled on the boundary on which the radiation condition, (2-26') or (2-41), is imposed, i.e., the integral along the boundary in (3-2). Due to this coupling on a boundary, the final matrix, which is the coefficient matrix in a set of algebraic equations obtained from the finite-element discretization to be discussed in the next chapter, is not symmetric, when we combine two sets of the algebraic equations, for the cosine-mode and the sine-mode, respectively, whereas in most structural problems they are symmetric. However, we can obtain

the two functionals $F^c(\varphi^c)$, $F^s(\varphi^s)$, for the functions φ^c and φ^s, respectively, from (3-2), (1-8) - (1-23), and (2-26') and Fig. 12 as follows:

$$F^c(\varphi^c) = \iint_\Omega \tfrac{1}{2}|\nabla\varphi^c|^2 dx\,dy - \frac{\sigma^2}{g}\int_{\mathcal{F}_1\cup\mathcal{F}_2}(\varphi^c)^2 dx - \int_{\mathcal{B}}(n\cdot V^c)\,\varphi^c ds - \nu\int_{\mathcal{R}_1\cup\mathcal{R}_2}\varphi^s\varphi^c dy \,, \tag{3-5}$$

$$F^s(\varphi^s) = \iint_\Omega \tfrac{1}{2}|\nabla\varphi^s|^2 dx\,dy - \frac{\sigma^2}{g}\int_{\mathcal{F}_1\cup\mathcal{F}_2}(\varphi^s)^2 dx - \int_{\mathcal{B}}(n\cdot V^s)\,\varphi^s ds + \nu\int_{\mathcal{R}_1\cup\mathcal{R}_2}\varphi^c\varphi^s dy \,, \tag{3-6}$$

where the integrals along the bottom $\mathcal{B}$ vanish in both cases unless the bottom is moving. As mentioned before, the last integrals along the 'radiation boundary' in (3-5) and (3-6) show the coupling relation between F^c and F^s; therefore the minimizing functions φ^c and φ^s must be found at the same time, not one after another, unless we can decouple them.

When a pressure distribution $p^c \cos\sigma t + p^s \sin\sigma t$ is specified in a segment on the free surface, then we obtain the new functionals after we add

$$\int_{\mathcal{F}_p}(p^s\sigma/\rho g)\,\varphi^c dx \tag{3-7}$$

to (3-5) and add

$$-\int_{\mathcal{H}_p} (\rho^c \sigma / eg)\, \rho^s \, dx \qquad (3\text{-}8)$$

to (3-6). When we have stratified fluids, the boundary integrals along the interface, for the upper fluid and for lower fluid (see (1-28) and (1-29), will show the coupling relation between the upper fluid and the lower fluid in each cosine-mode and sine-mode functionals, F^c and F^s, respectively.

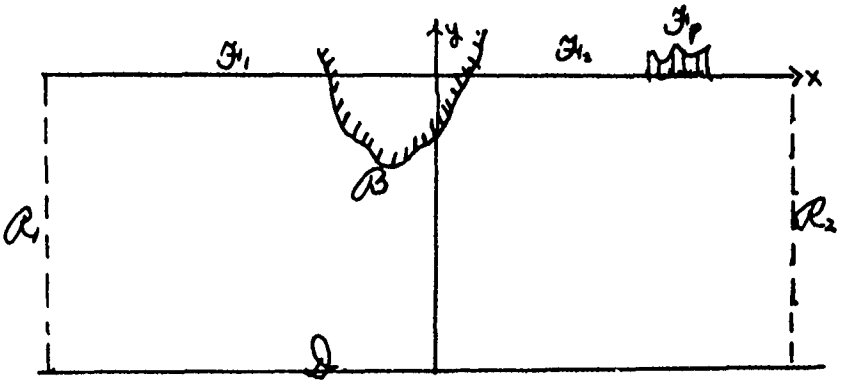

Fig. 12.

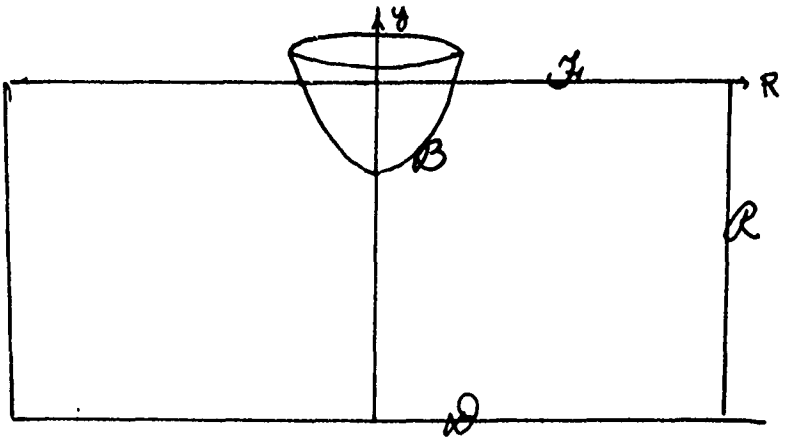

Fig. 13.

In three dimensions heaving motion of an axi-symmetric body, which can be formally reduced to the two-dimensional problem, will be treated here for simplicity. But a general three-dimensional problem can be described in a straightforward way. From the formulations in the first chapter and the new radiation condition (2-41), we obtain two coupled functionals $F^c(\varphi^c)$ and $F^s(\varphi^s)$ (refer to Fig. 1.3) as follows:

$$F^c(\varphi^c) = 2\pi \iint_{\Omega} R \cdot \tfrac{1}{2}\left[(\varphi_R^c)^2 + (\varphi_y^c)^2\right] dy\, dR - \frac{2\pi\sigma^2}{g}\int_{\mathcal{F}} R(\varphi^c)^2 dR$$
$$-2\pi \int_{\mathcal{B}} R(n\cdot V^c)\varphi^c ds - \pi\int_{\mathcal{L}} (\varphi^c)^2 dy - 2\pi\nu \int_{\mathcal{R}} \varphi^s R \varphi^c dy, \tag{3-9}$$

$$F^s(\varphi^s) = 2\pi \iint_{\Omega} R \cdot \tfrac{1}{2}\left[(\varphi_R^s)^2 + (\varphi_y^s)^2\right] dy\, dR - \frac{2\pi\sigma^2}{g}\int_{\mathcal{F}} R(\varphi^s)^2 dR$$
$$-2\pi \int_{\mathcal{B}} R(n\cdot V^s)\varphi^s ds - \pi\int_{\mathcal{L}} (\varphi^s)^2 dy + 2\pi\nu \int_{\mathcal{R}} \varphi^c R \varphi^s dy, \tag{3-10}$$

or, by dividing (3-9), (3-10) by π and redefining F^c and F^s,

$$F^c(\varphi^c) = \iint_{\Omega} R\left[(\varphi_R^c)^2 + (\varphi_y^c)^2\right] dy\, dR - \frac{2\sigma^2}{g}\int_{\mathcal{F}} R(\varphi^c)^2 dR$$
$$-2\int_{\mathcal{B}} R(n\cdot V^c)\varphi^c ds - \int_{\mathcal{L}} (\varphi^c)^2 dy - 2\nu \int_{\mathcal{R}} R\varphi^s\varphi^c dy, \tag{3-11}$$

$$F^s(\varphi^s) = \iint_{\Omega} R\left[(\varphi_R^s)^2 + (\varphi_y^s)^2\right] dy\, dR - \frac{2\sigma^2}{g}\int_{\mathcal{F}} R(\varphi^s)^2 dR$$
$$-2\int_{\mathcal{B}} R(n\cdot V^s)\varphi^s ds - \int_{\mathcal{L}} (\varphi^s)^2 dy + 2\nu \int_{\mathcal{R}} R\varphi^c\varphi^s dy. \tag{3-12}$$

IV. NUMERICAL PROCEDURES

In this chapter a brief description of the method of finite-element discretization will be given in the first section. How an infinite boundary can be truncated in the numerical procedure will be discussed in the second section.

1. Finite-element Discretization

A reader can find a very extensive and detailed exposition in Zienkiewicz (1971). Therefore we will give only a very brief description here. The convergence of the numerical solution of Laplace's equation is discussed by Reid (1972).

To begin with, the functional $F(\phi)$ of a single function $\phi(x,y)$* defined in (3-2) will be treated first with the goal of developing a numerical procedure for finding the function ϕ that minimizes the functional F. The coupled case, which we have in (3-5) and (3-6) or (3-11) and (3-12), will be discussed later.

Let the region occupied by fluid, up to the place at which the radiation condition is to be imposed, be subdivided by lines or surfaces into a (not necessarily rectangular) grid. Each connected piece within the subdivision will be called an 'element'. We suppose ϕ to be a function that is continuous and bounded (but see the discussion in chapter VII) in the subdivided region.

---

* The function ϕ defined in (3-1) and (3-2) can be any integrable function and it should not be understood as the velocity potential defined in (1-33).

One of the important steps in the procedure is the introduction of a set of interpolation functions $N_i(x,y)$, $i = 1, \cdots, N$, associated with <u>each</u> element and of such a character that ϕ can be approximated as a sum of these functions, each multiplied by the value of ϕ at, say, a node of the grid associated with the element ($\bar{\phi}_i$; at the i-th node). However, these values of $\bar{\phi}_i$ need not be nodal values of ϕ but may be other values (parameters) characterizing ϕ in the element, for our numerical scheme requires minimizing a functional which is represented in integral form rather than directly with the values of function itself. Let us write the set of interpolation functions as a row vector

$$[N] = [N_1, N_2, \cdots, N_N] \tag{4-1}$$

and the set of 'nodal' values as a column vector

$$\{\bar{\phi}\}^e = [\bar{\phi}_1^e, \bar{\phi}_2^e, \cdots, \bar{\phi}_N^e]^T \tag{4-2}$$

in an N-node element. The superscript e on $\{\bar{\phi}\}$ or on $\bar{\phi}_1, \cdots \bar{\phi}_N$ means that these values are considered in an individual element. We may then approximate ϕ in each element by the sum

$$\phi \cong [N]\{\bar{\phi}\}^e \tag{4-3}$$

We shall give below an example for a rectangular element, a very simple element shape, for the purpose of illustration. However, in our actual computations we used more elaborate elements, a four-node quadrilateral and eight-node quadrilateral (see Appendix B).

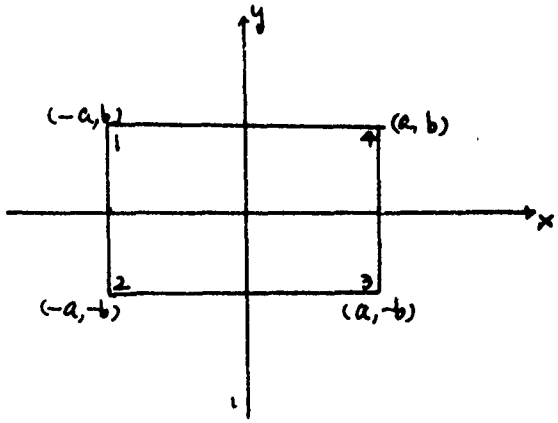

We can write ϕ as in (4-3)

$$\phi \cong N_1 \bar{\phi}_1 + N_2 \bar{\phi}_2 + N_3 \bar{\phi}_3 + N_4 \bar{\phi}_4 \,, \tag{4-4}$$

where

$$\begin{aligned} N_1(x,y) &= \frac{1}{4ab}(a-x)(b+y) \,, \\ N_2(x,y) &= \frac{1}{4ab}(a-x)(b-y) \,, \\ N_3(x,y) &= \frac{1}{4ab}(a+x)(b-y) \,, \\ N_4(x,y) &= \frac{1}{4ab}(a+x)(b+y) \,. \end{aligned} \tag{4-5}$$

In order to minimize the functional $F(\phi)$ in (3-2) with respect to the total number of parameters (or nodal values) associated with the whole domain, we can write a system of equations

$$\frac{\partial F}{\partial \{\bar{\phi}\}} = \begin{Bmatrix} \frac{\partial F}{\partial \bar{\phi}_1} \\ \frac{\partial F}{\partial \bar{\phi}_2} \\ \vdots \end{Bmatrix} = 0 \,. \tag{4-6}$$

Let an element in Ω be denoted by Ω^e . Then we may decompose F as follows:

$$F(\phi) = \iint_{\Omega} + \int_{\partial\Omega} = \sum_e \left[\iint_{\Omega^e} + \int_{\partial\Omega^e \cap \partial\Omega} \right]$$
$$= \sum_e F^e(\phi) \qquad (4\text{-}7)$$

We now approximate F^e within each element:

$$F^e(\phi) \cong F^e([N]\{\bar{\phi}\}) \qquad (4\text{-}8)$$

Henceforth we shall simply write F^e for the approximate value. It now becomes evident that the interpolation functions N_i must be chosen in conformity with the nature of the functional F . In particular, they should be chosen so that at the interfaces the approximation to ϕ is such that it and its derivatives of one order less than those occurring in the integrands of F are continuous. This assures that there is no contribution to the integral from the interfaces.

Then from (4-6) and (4-7) we obtain (4-9)

$$\frac{\partial F}{\partial \bar{\phi}_n} = \sum_e \frac{\partial F^e}{\partial \bar{\phi}_n} = 0. \qquad (4\text{-}9)$$

For any node we can write, by differentiating (3-2) with respect to $\bar{\phi}_i$ $(i = 1, 2, \ldots)$,

$$\frac{\partial F^e}{\partial \bar{\phi}_i} = \iint_{\Omega^e} \left(\phi_x \frac{\partial \phi_x}{\partial \bar{\phi}_i} + \phi_y \frac{\partial \phi_y}{\partial \bar{\phi}_i} \right) dx\, dy$$
$$+ \int_{\partial\Omega^e \cap \partial\Omega} \left[\alpha \phi \frac{\partial \phi}{\partial \bar{\phi}_i} - \beta(x,y) \frac{\partial \phi}{\partial \bar{\phi}_i} \right] ds, \qquad (4\text{-}10)$$

where the second integral is present only if the element has a boundary on which the boundary condition in (3-1) is specified.

Noting that $\{\bar{\phi}\}$ is no longer a function of x and y but that [N] is now a function of x and y,

$$\frac{\partial \phi}{\partial x} = \left[\frac{\partial N_i}{\partial x}, \frac{\partial N_j}{\partial x}, \cdots\right]\{\bar{\phi}\}^e,$$

$$\frac{\partial \phi}{\partial y} = \left[\frac{\partial N_i}{\partial y}, \frac{\partial N_j}{\partial y}, \cdots\right]\{\bar{\phi}\},$$

$$\frac{\partial}{\partial \bar{\phi}_i}\left(\frac{\partial \phi}{\partial x}\right) = \frac{\partial N_i}{\partial x}, \tag{4-11}$$

$$\frac{\partial \phi}{\partial \bar{\phi}_i} = N_i, \text{ etc.}$$

finally we obtain in the whole region

$$\frac{\partial F}{\partial \{\bar{\phi}\}} = [A]\{\bar{\phi}\} - [B] = 0, \tag{4-12}$$

or

$$[A]\cdot\{\bar{\phi}\} = [B], \tag{4-12'}$$

where

$$a_{ij} = k_{ij} + h_{ij},$$

$$k_{ij} = \iint_{\Omega}\left(\frac{\partial N_i}{\partial x}\frac{\partial N_j}{\partial x} + \frac{\partial N_i}{\partial y}\frac{\partial N_j}{\partial y}\right)dx\,dy \tag{4-13}$$

$$= \sum_e \iint_{\Omega^e}\left(\frac{\partial N_i}{\partial x}\frac{\partial N_j}{\partial x} + \frac{\partial N_i}{\partial y}\frac{\partial N_j}{\partial y}\right)dx\,dy,$$

$$h_{ij} = \int_{\partial\Omega} \alpha N_i N_j \, ds \ , \tag{4-14}$$

$$b_i = \int_{\partial\Omega} \beta N_i \, ds \ . \tag{4-15}$$

The formulated problem has now been reduced to the equation (4-12') a set of linear simultaneous algebraic equations. The coefficient matrix [A] has the nice properties of being symmetric, as one can see readily from the equations (4-13) and (4-14) and of being banded if nodes are properly numbered.

The numerical computations of the integrals (4-13), (4-14) and (4-15) for four- and eight-node quadrilateral elements are briefly discussed in Appendix B.

Now let us consider the finite-element discretization for the coupled functionals $F^c(\varphi^c)$ and $F^s(\varphi^s)$ in (3-5) and (3-6) or (3-11) and (3-12). Since we can use (4-8) in two dimensions without change and also since we can write with a slight change in three dimensions

$$k_{ij} = \iint_{\Omega} R\left(\frac{\partial N_i}{\partial R}\frac{\partial N_j}{\partial R} + \frac{\partial N_i}{\partial y}\frac{\partial N_j}{\partial y}\right) dR\,dy \ , \tag{4-16}$$

where $N_i = N_i(R,y)$, let us consider next the boundary integral involving $\alpha(x,y)$, defined in (3-1) and reduced to (4-14) in the final matrix equation (4-12'). In two dimensions α occurs only on the free surface, where $\alpha = -\omega^2/g$, a constant*. Then,

---

* When we have two fluids, we also have at the interface of the two fluids, α and β (see (1-28) and (1-29).

referring to Fig. 12, we obtain from (4-14)

$$h_{ij} = -\frac{\sigma^2}{g}\int_{\mathcal{S}_1} N_i N_j \, dx \tag{4-17}$$

both for $F^c(\varphi^c)$ and $F^s(\varphi^s)$.

In three dimensions there are two boundaries on which α occurs, on the free surface and on the 'radiation boundary'. Thus we obtain an analogous form to (4-14) for both F^c and F^s (see Fig. 13):

$$h_{ij} = -\frac{\sigma^2}{g}\int_{\mathcal{S}_1} R N_i N_j \, dR + \frac{1}{2}\int_{\mathcal{R}} N_i N_j \, dy . \tag{4-18}$$

Next let us consider the boundary integrals involving $\beta(x,y)$. The value of α considered above was constant in our problem, but β may be a function. We can express analogously to (4-3) as

$$\beta = [N]\{\bar{\beta}\} = [N_1, N_2, \cdots N_n]\begin{Bmatrix}\bar{\beta}_1\\ \bar{\beta}_2\\ \vdots\\ \bar{\beta}_n\end{Bmatrix}, \tag{4-19}$$

where [N] are the interpolation functions as before and $\{\bar{\beta}\}$ are the nodal values of the function β. From (4-15) and (4-19) we obtain

$$b_i = \int_{\partial\Omega} [N]\{\bar{\beta}\} N_i \, ds = \left(\int_{\partial\Omega} [N] N_i \, ds\right)\{\bar{\beta}\} . \tag{4-20}$$

The equation (4-20) becomes in two dimensions

$$b_i = \left(\int_{\mathcal{B}} [N] N_i ds\right)\{\bar{\beta}\} + \left(\int_{\mathcal{R}_1 \cup \mathcal{R}_2} [N] N_i ds\right)\{\bar{\beta}\} . \tag{4-21}$$

In two dimensions we obtain

from $F^c(\varphi^c)$:

$$b_i = \left(\int_{\mathcal{B}} [N]\, N_i ds\right)\left\{\bar{V}_n^c\right\} - \left(\frac{\varepsilon}{c_g}\int_{\mathcal{B}_p} [N]\, N_i dx\right)\left\{\bar{P}^s\right\} - \nu\left(\int_{\mathcal{R}_1 \cup \mathcal{R}_2} [N]\, N_i dy\right)\left\{\bar{\varphi}^s\right\}, \qquad (4\text{-}22)$$

and from $F^s(\varphi^s)$:

$$b_i = \left(\int_{\mathcal{B}} [N]\, N_i ds\right)\left\{\bar{V}_n^s\right\} + \left(\frac{\varepsilon}{c_g}\int_{\mathcal{B}_p} [N]\, N_i dx\right)\left\{\bar{P}^c\right\} + \nu\left(\int_{\mathcal{R}_1 \cup \mathcal{R}_2} [N]\, N_i dy\right)\left\{\bar{\varphi}^c\right\} \qquad (4\text{-}23)$$

In three dimensions we obtain

from $F^c(\varphi^c)$:

$$b_i = \left(\int_{\mathcal{B}} [N]\, N_i R ds\right)\left\{\bar{V}_n^c\right\} - \nu R\left(\int_{\mathcal{R}} [N]\, N_i dy\right)\left\{\bar{\varphi}^s\right\} \qquad (4\text{-}24)$$

and from $F^s(\varphi^s)$:

$$b_i = \left(\int_{\mathcal{B}} [N]\, N_i R ds\right)\left\{\bar{V}_n^s\right\} + \nu R\left(\int_{\mathcal{R}} [N]\, N_i dy\right)\left\{\bar{\varphi}^c\right\} \qquad (4\text{-}25)$$

where

$$\mathbf{n}\cdot\mathbf{v}^c = [N]\left\{\bar{V}_n^c\right\}, \qquad \mathbf{n}\cdot\mathbf{v}^s = [N]\left\{\bar{V}_n^s\right\},$$

$$\varphi^c = [N]\left\{\bar{\varphi}^c\right\}, \qquad \varphi^s = [N]\left\{\bar{\varphi}^s\right\},$$

$$p^c = [N]\left\{\bar{P}^c\right\}, \qquad p^s = [N]\left\{\bar{P}^s\right\}.$$

The values of $\{\bar{\beta}\}$, that is, the normal-velocity distributions are known and the computation of the integrals along the body boundary in (4-20) and (4-21) is straightforward. These become the components of [B] in (4-12'). For convenience let the matrix equation be understood such that the right-hand side, [B], is known, whereas the unknown values are on the left-hand side, as is conventional. Now let us consider the integrals along the boundary $\mathcal{R}_1 + \mathcal{R}_2$ or $\mathcal{R}$ in the expressions (4-22) to (4-25) for both cases, i.e., the cosine mode and sine mode, the boundary integral contains the values of the sine-mode potentials. First we compute all b_i and next we move those terms which contain the opposite-mode potentials to the left-side hand. In order to combine the cosine-mode potentials $\bar{\varphi}^c$ and the sine-mode potentials $\bar{\varphi}^s$ we rearrange both potentials into one array as follows:

$$\left\{\begin{array}{c} \bar{\varphi}_1^c \\ \bar{\varphi}_1^s \\ \bar{\varphi}_2^c \\ \bar{\varphi}_2^s \\ \vdots \\ \vdots \end{array}\right\} \qquad (4\text{-}26)$$

This arrangement minimizes the bandwidth of the coefficient matrix after combination. The coefficient matrix will now be no longer symmetric.

Further, if we denote the integrals along $\mathcal{B}$ and $\mathcal{J}_p$ in (4-22) and (4-25) as b_i^c, and those in (4-23) and (4-25) as b_i^s, the final form of the matrix equation becomes:

$$[A] \begin{Bmatrix} \varphi_1^c \\ \varphi_1^s \\ \varphi_2^c \\ \varphi_2^s \\ \vdots \end{Bmatrix} = \begin{Bmatrix} b_1^c \\ b_1^s \\ b_2^c \\ b_2^s \\ \vdots \end{Bmatrix} . \qquad (4\text{-}27)$$

When an oscillatory-pressure distribution is specified on a segment of the free surface or when there are two fluids of densities ρ_1 , ρ_2 , all the procedures for obtaining (4-27) will be very similar to those explained earlier. It is of interest to note that the interface condition in the two fluids (see (1-28) and (1-29)) makes the coefficient matrix [A] in (4-27) asymmetric due to the coupled interface boundary condition between the upper fluid and the lower fluid.

2. Truncation of the Infinite Boundaries

In Chapter II, the decaying behavior of the local disturbance has been considered and a new radiation condition was derived which can be applied where the local disturbance is negligibly small compared with the propagating waves. We can state a few criteria for the subdivision of the domain occupied by the fluid (or fluids) and for the truncation of the infinite boundaries.

Criterion 1. One should subdivide each wave length by at least ten approximately equidistant points along the horizontal direction.

Criterion 2. The truncation of the infinite boundaries should be made after examination of the behavior of the local disturbance discussed in Chapter II.

It is difficult to state definite and detailed criteria for the general problems, but one can sensibly determine the truncation of the infinite boundaries and the proper subdivisions in the domain case by case after understanding the specific problem which is dealt with. For example, if the bottom is not uniform as shown in Fig. 14, then the subdivisions and the truncation of the infinite boundaries should be different along the left-hand side and the right-hand side as shown in Fig. 14, since we know the asymptotic form of the propagating waves on each side.

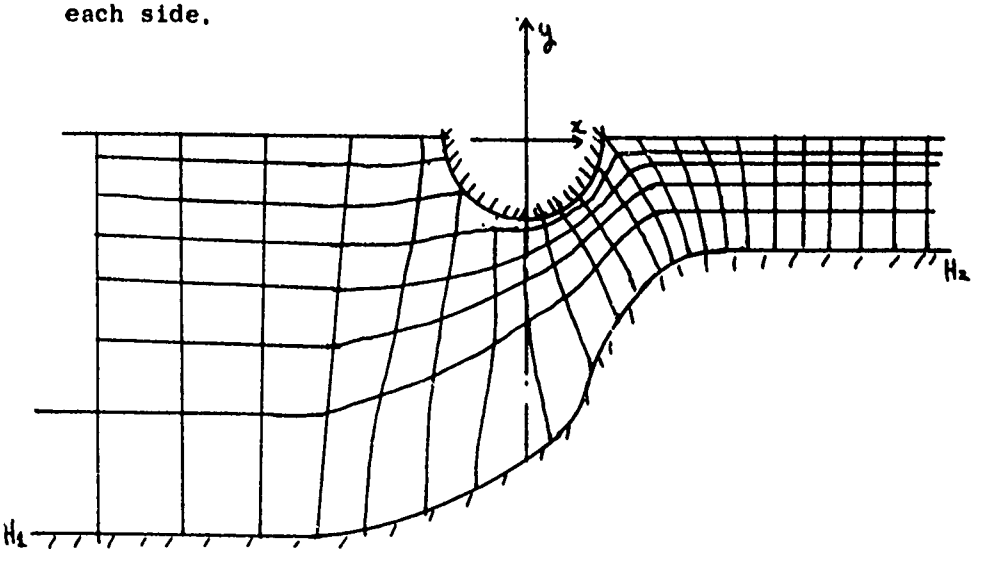

FIG. 14. Subdividing Meshes in the Fluid

In this case ν in the radiation condition is, of course, different on the left-hand side and on the right-hand side, i.e. $\nu=\nu_1$, on the left-hand side and $\nu=\nu_2$ on the right-hand side, where

$$\begin{aligned} \sigma^2/g &= \nu_1 \tanh \nu_1 H_1 , \\ \sigma^2/g &= \nu_2 \tanh \nu_2 H_2 . \end{aligned} \tag{4-28}$$

V. TESTING OF THE METHOD

1. Pure Propagating Waves

In this section simple tests are made to examine the radiation condition. Let us consider a fictitious wall on which a normal velocity is defined as

$$n \cdot V = (\Phi_p)_n \tag{5-1}$$

where Φ_p is defined in (2-19) in two dimensions. The numerical results for the boundary condition (5-1) on a fictitious wall have been compared with the exact solution (2-19) for many cases. For example, in one case the radiation condition is applied right next to the wall; in other words, one discretized element has both boundaries, a fictitious-motion boundary on one side and the radiation boundary condition on the opposite side. All the numerical results give very good agreement with the exact solutions whenever we subdivide the domain of the fluid properly into finite elements. Consider a thin strip one hundredth of a wave length wide subdivided into one hundred elements in the vertical direction. If the fictitious motion is applied at the left-hand side of the strip and the radiation condition at the right-hand side, then the numerical results agree with the exact values to six or seven decimal places if eight-node quadrilateral elements are used.

In three dimensions, propagating ring waves are tested with the local disturbance artificially suppressed,

i.e. the boundary condition on a fictitious vertical cylinder $R = R_o$ is taken as follows:

$$\left.\frac{\partial \varphi^c}{\partial R}\right|_{R=R_o} = -\nu \frac{\cosh \nu(y+H)}{\cosh \nu H} J_1(\nu R_o),$$
$$\left.\frac{\partial \varphi^s}{\partial R}\right|_{R=R_o} = -\nu \frac{\cosh \nu(y+H)}{\cosh \nu H} Y_1(\nu R_o), \qquad (5\text{-}2)$$

where H is the depth.

The exact solution for the boundary condition (5-2) is simply

$$\Phi(R,y,t) = \varphi^c \cos\sigma t + \varphi^s \sin\sigma t$$
$$= \frac{\cosh \nu(y+H)}{\cosh \nu H} (J_o \cos\sigma t + Y_o \sin\sigma t) \qquad (5\text{-}3)$$

where $R \geq R_o$, $-H \leq y \leq 0$. In this three-dimensional case the numerical results are compared with the exact solutions (Bessel's functions) given by Abramowitz and Stegun (1967) and shown in Fig. 20 for y=0. The radiation condition is applied at $R=R_1$, which was taken as less than one and a half wave lengths for the two cases considered. The numerical results are identical up to three significant digits with the Bessel functions.

2. Pure Local Disturbance

As we have seen in Chapter two, if we apply the radiation condition on a boundary which is so close to the moving body that the local-disturbance potential Φ_1 has not

decayed sufficiently, then we will obtain a numerical solution not for the original problem but for a completely different problem. For, when we take the conventional radiation condition, which states the asymptotic behavior at infinity, then the local disturbance potential Φ_L trivially satisfies the radiation condition. Therefore no special difficulties in connection with the local disturbance arise in an analytic method. On the other hand, in numerical scheme, the treatment of the local disturbance is the most cumbersome.

In this section the radiation condition is applied at various distances at which the local disturbance remains of considerable magnitude, in order to obtain some idea as to how close the truncation of the infinite boundary may be applied.

Let us consider an example in two dimensions with the exact solution

$$\Phi(x,y,t) = A_0 e^{-m_1 x} \cos m_1(y+H) \cos \sigma t, \qquad (5\text{-}4)$$

where m_1 is given in (2-3) and A_0 is a constant. The two components of Φ are

$$\varphi^c(x,y) = A_0 e^{-m_1 x} \cos m_1(y+H),$$
$$\varphi^s(x,y) = 0, \qquad (5\text{-}5)$$

where $-H \le y \le 0$ and $0 \le x < \infty$. Then on a fictitious wall at $x=0$ the boundary condition will be:

$$\varphi_x^c\big|_{x=0} = -m_1 A_0 \cos m_1 (y+H),$$
$$\varphi_x^s\big|_{x=0} = 0. \qquad (5\text{-}6)$$

We apply the radiation condition at $x=x_1$.

Fig. 21 shows the potentials φ^c and φ^s with the radiation condition imposed at various distances from the plane x=0 and shows that the numerical solution agrees very well in this case when the radiation boundary is taken such that x/H≥3. However when we impose the radiation condition too close to the moving body, then the numerical solution gives a non-zero sine-mode potential $\varphi^s(x,y)$, although this is identically zero in the exact solution.

3. Oscillatory Pressure Given on the Free Surface

Let an oscillatory pressure be given on a segment $2l$ of the free surface; the boundary condition on the free surface is then given in (1-31). Stoker (pp. 58-66) has applied complex-variable theory to give the solution for the propagating waves, i.e. for Φ_p, as an asymptotic solution at a large distance. If we adopt the Green function for this problem and make use of Green's theorem, the solution can be given as

$$\Phi(x,y,t) = -c\int_{-l}^{l} \varphi(x,0,a,0,t)\,da \qquad (5\text{-}7)$$

where G is defined in (2-14) and C is defined in (1-31). For finite depth G is given in Wehausen (1960); it would not be difficult to extend (5-7) to three dimensions.

In this section, two cases in water of infinite depth are compared with the solution computed from (5-7) and given in Fig. 22. Fig. 23 shows the same two cases for finite depth.

It is of interest to remark that a problem with the non-homogeneous free-surface boundary condition must be solved whenever we treat higher-order problems.

4. Forced Motion of Two-dimensional Cylinders in Water of Infinite and Finite Depths

A circular cylinder of radius a oscillating in a free surface has been tested for infinite depth for five non-dimensional wave numbers νa = 0.5, 1.0, 1.5, 2.0, 3.0, and compared with Porter's results (Porter, 1960). They give very good agreement in all cases. Table 1 shows the comparisons between Porter's results and the results by this numerical method for the case νa = 1.

For finite depth, H = 2a a half-immersed circular cylinder has been tested for two non-dimensional wave numbers νa = 0.1, 0.5 and compared with the results obtained by another method (C. H. Kim, 1969). The added-mass coefficients and wave-amplitude ratio for heave do not give good agreement for either case.

	Added Mass μ_{22}	Damping Coeff. λ_{22}	Asympt. Wave Amp. ($\bar{\Upsilon}$),	Force ($\bar{F}$)
Porter	.60	.40	.79	.42
This Method	.59688	.40356	.7936	.4063

Non-dimensional Pressure in Phase with the Acceleration

	Angle* 0°	10°	20°	30°	40°	50°	60°	70°	80°	90°
Porter	.70	.68	.63	.55	.45	.32	.17	.030	-.097	-.18
This Method	.69408	.67946	.62773	.54949	.44063	.31447	.17512	.0360	-.08730	-.16213

Non-dimensional Pressure in Phase with the Velocity

	Angle 0°	10°	20°	30°	40°	50°	60°	70°	80°	90°
Porter	.23	.24	.25	.27	.31	.35	.42	.51	.62	.75
This Method	.23496	.23874	.25215	.27484	.31096	.35795	.42624	.51366	.62722	.76001

* The angle is measured from the negative y-axis.

Table 1.

5. Two-dimensional Diffraction Problems in Water of Infinite and Finite Depth (Circular, Rectangular Sections)

The incoming wave is assumed to be

$$\begin{aligned} Y_I(x,t) &= \sin(\nu x - \sigma t) \\ &= \sin \nu x \cos \sigma t - \cos \nu x \sin \sigma t \end{aligned} \tag{5-8}$$

with the amplitude being unity. Following the definition (1-39), for the incoming wave, we write

$$Y_I(x,t) = Y_I^c \cos \sigma t + Y_I^s \sin \sigma t \tag{5-9}$$

where

$$Y_I^c = \sin \nu x \ , \quad Y_I^s = -\cos \nu x .$$

From (1-40) we define the free-surface wave profile due to a fictitious forced motion given in (1-25):

$$Y_D(x,t) = Y_D^c \cos \sigma t + Y_D^s \sin \sigma t \ ,$$

where

$$\begin{aligned} Y_D^c &= -\frac{\sigma}{g} \varphi_D^s(x,0) \ , \\ Y_D^s &= \frac{\sigma}{g} \varphi_D^c(x,0) \ , \end{aligned} \tag{5-10}$$

and

$$\Phi_D(x,y,t) = \varphi_D^c \cos \sigma t + \varphi_D^s \sin \sigma t .$$

then the total velocity potential Φ_T is given as

$$\Phi_T = \Phi_I + \Phi_D \tag{5-11}$$

and the wave profile on the free surface is

$$Y_T(x,t) = Y_I(x,t) + Y_D(x,t)$$

and

$$Y_T(x,t) = Y_T^c \cos \sigma t + Y_T^s \sin \sigma t . \tag{5-12}$$

In order to describe the phase relation between Y_D^c and Y_D^s ,

we define the phase angle

$$\theta_D(x) = \tan^{-1}\left(-Y_D^c / Y_D^s\right) \; ; \tag{5-13}$$

similarly

$$\theta_T(x) = \tan^{-1}\left(-Y_T^c / Y_T^s\right) \tag{5-14}$$

where the arc tangent is understood to take its principal value, i.e., $-\pi/2 \le \theta_D, \theta_T \le \pi/2$

If $|Y^I|, |Y^T|, |Y^R|$ are the amplitudes at infinity of the incoming, transmitted, and reflected waves, respectively, then we define the reflection and transmission coefficients by

$$C_R = |Y^R| / |Y^I| , \qquad C_T = |Y^T| / |Y^I| \tag{5-15}$$

and obtain as a consequence of conservation of energy,

$$C_R^2 + C_T^2 = 1 . \tag{5-16}$$

we can also express the transmitted wave at infinity similarly to (5-8),

$$Y^T = |Y^T| \sin(\gamma x - \sigma t - \delta_T),$$

where δ_T is the phase lag of the transmitted wave to the incoming wave at infinity.

Diffraction of homogeneous incoming waves on a submerged circular cylinder was taken as a test computation since this problem has been treated analytically by various people (Dean, 1948; Ursell, 1950; Ogilvie, 1963). It is well-known that the reflection coefficient of a submerged circular cylinder in water of infinite depth is zero in the first-order

theory. Thus the model is taken for the numerical calculation to be identical with the one Dean and Ursell computed, as shown in Fig. 15.

The results for $\nu_a = \frac{\pi}{3}$ are shown in Fig. 24. The transmitted wave lags behind the incoming wave by about 82 degrees; Ursell found about 90 degrees.

A diffraction problem with a rectangular cylinder (refer to Fig. 16) in water of finite depth has been tested for some frequencies and compared with the results obtained by another method (Mei and Black, 1969). The results show very good agreements for both submerged and surface obstacles. Fig. 25 - Fig. 28 show the results for these obstructions.

Each figure giving the results of the diffraction problems consists mostly of four sheets of figures; for example, Fig. 25 consists of Fig. 25a, Fig. 25b, Fig. 25c, and Fig. 25d. The first figure shows the diffracted waves $Y_D(x)$. The upper part of the second one shows the phase angle $\theta_D(x)$ between the cosine-mode wave Y_D^c and the sine-mode wave Y_D^s. This figure shows the transmitted waves on the right-hand side and the sum of the incoming wave and the reflected wave on the left-hand side. The fourth figure is arranged in a similar fashion to the second figure except for the total waves. The phase angle θ_T shows the phase lag of the transmitted waves with respect to the incoming waves at the far right-hand side; it is hard to give a physical interpretation to θ_T on the left-hand side when the reflection coefficient C_R is large, as, e.g., in Fig. 32d. The lower part of the fourth figure shows the reflection and

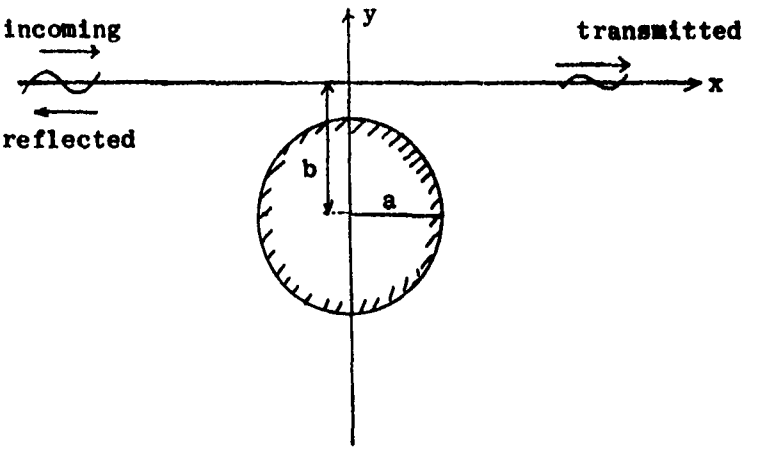

Fig. 15

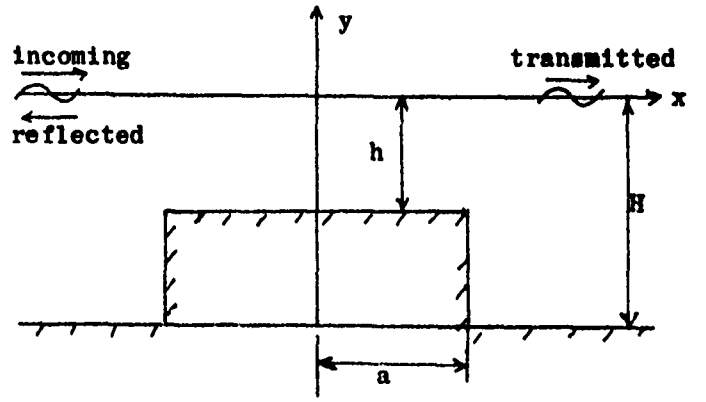

(a)

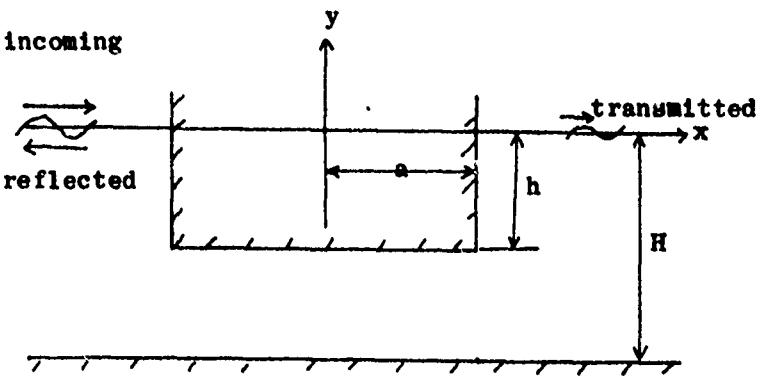

(b)

Fig. 16

transmission coefficients at the far left-hand and far right-hand sides, respectively. It is easy to prove analytically that $|Y_T|_{max}$ on the left-hand side has a sharp trough and a smooth crest and that the average of two values of $|Y_T|_{max}$ at the crest and trough is one. But sometimes, for example, Fig. 26d does not show a very sharp trough, but is chopped off in the plotting by the computer due to the lack of a sufficient number of data points near the trough.

6. Heaving Motion of Axi-Symmetric Bodies (Sphere and V rtical Cylinder)

A hemisphere in heave motion in water of infinite depth has been tested for two frequencies, $\nu a = 0.5, 1.0$, and compared with the results obtained by other methods (Cumming, 1963). The results show very good agreement.

The waves and wave forces generated by vertical circular cylinder of draft/radius = 0.5 in heave motion in water of infinite depth have been computed for few frequencies, $\nu a = 0.5, 1.0$. The results have been compared with those of Sao, Maeda and Hwang (1971), but they are not in good agreement. In view of the good agreement between our results and those computed by many others for other configurations, we are inclined to favor our results in case of disagreement.

VI. NEW PROBLEMS

Once this method has been proved to be a useful numerical method, one can utilize it for solving any problem within the scope of its applicability, however complicated its boundary may be. In this chapter only a few sample problems will be treated since any one can make use of the method for cases of interest to him.

1. Forced Motion of Two-dimensional Cylinders in Water of Variable Depth

Forced motion of a rectangular cylinder in the free surface with a vertical cliff submerged under the heaving cylinder is treated. As shown in Fig. 17, we have an infinite depth on the left-hand side and a finite depth on the right-hand side. Hence we have two different lengths of the waves which propagate to each direction. Due to the asymmetry of the bottom with respect to the y-axis, we may expect a non-zero force component in the x-direction, even though the cylinder and the motion are symmetric with respect to the y-axis. The numerical computation for $\sigma^2 a/g = 0.1$ shows that the amplitude of the x-component of the hydrodynamic force is about one fifth of that of the y-component. Fig. 29 shows the wave profiles for this case.

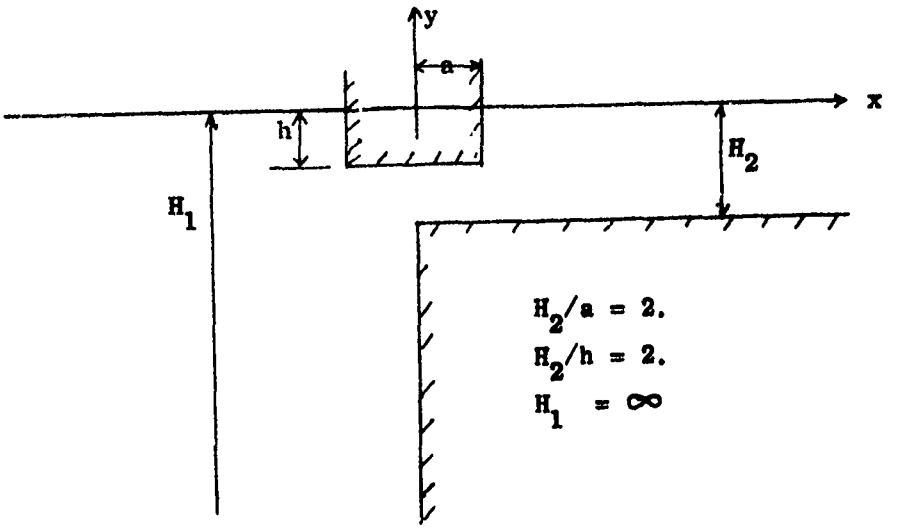

Fig. 17

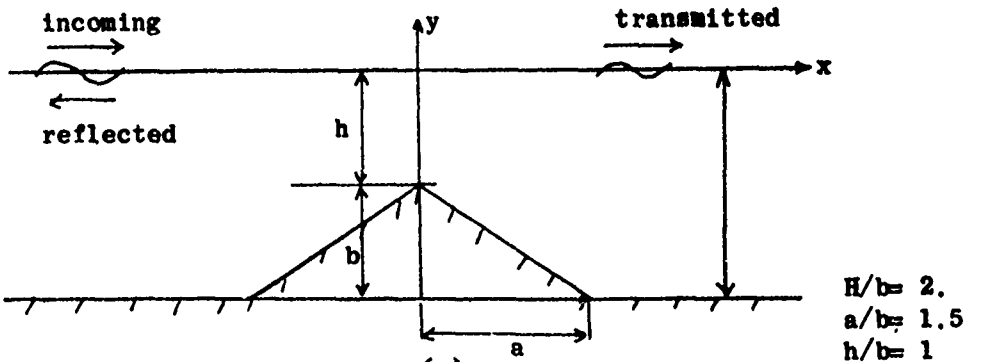

(a)

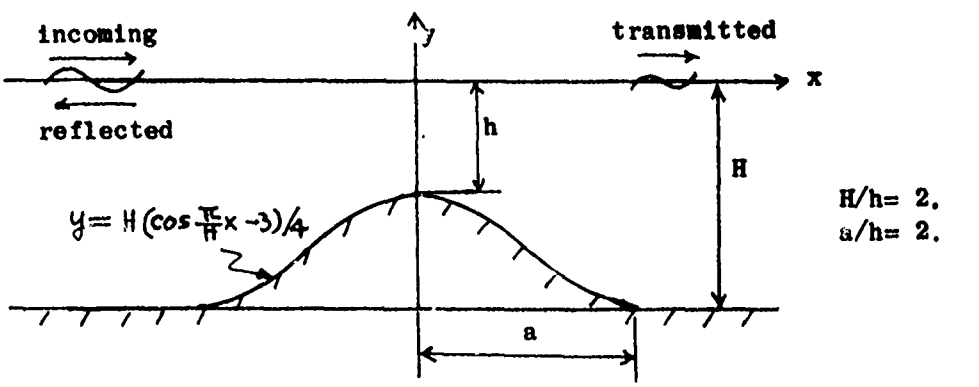

(b)

Fig. 18

2. Diffraction Problems in Water of Finite Depth (Triangular, and Sinusoidal Section and Vertical Multi-barrier along the Free Surface)

The geometries of the triangular- and sinusoidal-shaped obstructions on the bottom are shown in Fig. 18. The results for the triangular-shaped obstacle on the bottom are given for $\nu h = 1.0$ in Fig. 30. The results for the sinusoidal hump on the bottom are given in Fig. 31 for $\nu h = 0.5$.

A diffraction problem for two vertical flat plates piercing the free surface was treated in some detail and this problem was extended to the case of two fluids of different densities, ρ_1 and ρ_2 (corresponding to oil contained between two vertical flat plates (see Fig. 19). Experimental results (Raissi, 1972) are available for these problems. The results are obtained for four different frequencies for a homogeneous fluid and are compared with the experiments. Agreement is good. The results for two fluids are obtained for a frequency which is near one of the resonant frequencies of the internal waves. The maximum amplitude of the internal waves is about six times higher than that of the surface waves on the oil. Fig. 32 shows the results for a homogeneous fluid for period T = 1 sec. ($\nu h = 0.6404$) and a/h = 2.34. Fig. 33 - Fig. 35 show the results for the two fluids for T = 1.84 sec. (h=0.2704) and a/h = 2.34.

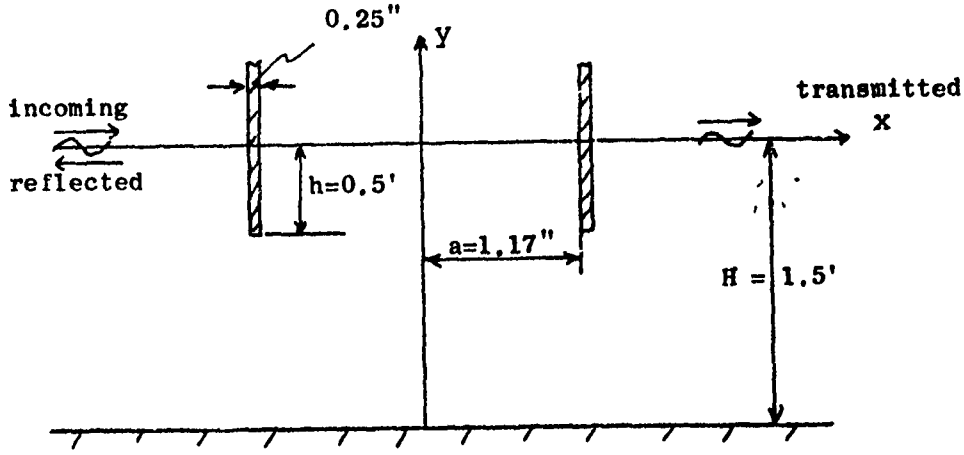
0.25"
y
incoming
reflected
transmitted
x
h=0.5'
a=1.17"
H = 1.5'

(a)

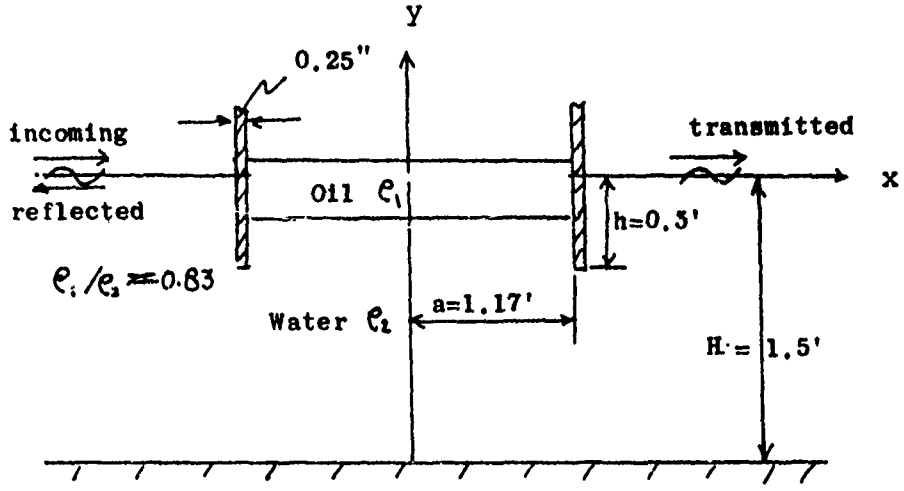
y
0.25"
incoming
reflected
transmitted
x
Oil ρ_1
h=0.5'
$\rho_1/\rho_2 = 0.83$
Water ρ_2
a=1.17'
H = 1.5'

(b)

Fig. 19

VII. DISCUSSION

The main purpose of this paper is rather the testing of a numerical method than anything else. Therefore the testing of this method has been carried out for a variety of different problems, varying from homogeneous wave propagation to a diffraction problem due to two vertical flat plates piercing the free surface when oil is contained between two vertical plates.

Most results obtained by this method agree with those obtained by other methods, either analytic, numerical or experimental. But there were two types of problems which did not agree very well: one is the forced motion of a two-dimensional circular cylinder in water of finite depth and the other is the heaving vertical circular cylinder in water of infinite depth. It seems to be worthwhile to compute the complete results since we checked only a few frequencies. One can also easily compute the forced motion of the axi-symmetric vertical cylinder in water of finite depth.

In addition to the fact that any degree of complicated boundary geometry can be handled easily by this method, there is still a further degree of freedom in that one can express the velocity potentials on a mathematically singular plate (in which the potentials are discontinuous across the boundary) through numbering of the nodes for each element. One can easily construct a 'numerical Riemann-surface branch cut' by making two adjacent elements which have the singular boundary

in common have different nodal numbers at that boundary, even though the coordinates of the nodes on the boundary are identical.

At this stage we may ask ourselves, what happens at the ends of the flat plate which are submerged. Does this method give the correct behavior at the singularity? The solution of the velocity potential at the singular point breaks down unless we introduce a proper interpolation function to represent the near field including the singularity. If we use a linear- or quadratic-interpolation function in the near field, then we always obtain a finite value at the singularity, because the singularity, which is $O(x^{-\frac{1}{2}})$ in the near field, is integrable and our numerical method minimizes a functional which is represented in integral form rather than dealing with the function itself.

It would seem to be worthwhile to develop a proper interpolation function to represent the near field, including the singularity, in order to obtain a correct solution at the singularity.

It would be very interesting to extend this method to the ship-resistance problem. In this case it may be difficult to express the radiation condition in moving coordinates in a tractable form.

A computer program can probably never be made as efficient or as general as possible. However, we have made

considerable effort to attain such a goal. As mentioned in Chapter IV, our computer program solves the coupled equations of cosine-mode potential and sine-mode potential simultaneously. Accordingly, the band width of the final coefficient matrix is double the band width of the either potential of either mode. It would be worthwhile to try to decouple them and to solve them separately. This might result in a saving of computer time.

It is possible to extend this method to a general three-dimensional boundary geometry without much difficulty. However, the band width of the coefficient matrix will then be very large. Hence the computing time will also be very large. If we modify the present computer program slightly, we can solve diffraction problems with an axi-symmetric body in three dimensions and a plane incoming wave. Other modes of motion than heave can also be treated for the axi-symmetric body.

APPENDIX A

The potential $\Phi(x, y, a, b, t)$ due to a source with pulsating strength $\cos \sigma t$ at (a,b) is given in (2-14), i.e.,

$$\Phi(x,y,a,b,t) = \mathrm{Re}\left\{ \left[\frac{1}{2\pi} \log \frac{z-c}{z-\bar{c}} + \frac{1}{\pi} \int_0^\infty \frac{e^{-ik(z-\bar{c})}}{k-\nu} dk \right] \cos \sigma t - e^{-i\nu(z-\bar{c})} \sin \sigma t \right\}, \tag{A-1}$$

where $c = a + ib$, $\bar{c} = a - ib$, $z = x + iy$.

Let us consider a contour integral $\oint_C \frac{e^{-ik(z-\bar{c})}}{k-\nu} dk$ in the complex K - plane (as shown below)

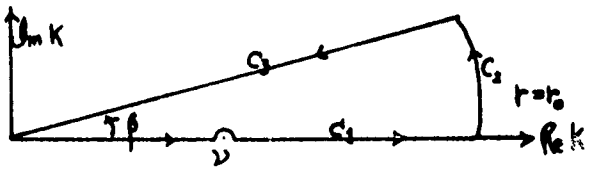

where $\oint_C = \int_{C_1} + \int_{C_2} + \int_{C_3}$. (A-2)

From the cauchy integral theorem, we have

$$\oint_C \frac{e^{-ik(z-\bar{c})}}{k-\nu} dk = 0 . \tag{A-3}$$

Let us define,

$$z-c = \rho_1 e^{i\theta_1} ,$$
$$z-\bar{c} = \rho_2 e^{i\theta_2} , \tag{A-4}$$

$$K = re^{i\alpha}$$

$$I_1 = \int_{C_1} \frac{e^{-ik(z-\bar{z})}}{K-\nu} dK$$

$$= \int_{C_1} \frac{\exp(-ire^{i\alpha}\rho_2 e^{i\theta_2})}{re^{i\alpha}-\nu} (e^{i\alpha}dr + ire^{i\alpha}d\alpha)$$

$$= \int_{C_1} \frac{\exp[r\rho_2\{\sin(\alpha+\theta_2) - i\cos(\alpha+\theta_2)\}]}{r-\nu e^{-i\alpha}} (dr + ird\alpha)$$

$$I_2 = \int_{C_2} \frac{\exp[r\rho_2\{\sin(\alpha+\theta_2) - i\cos(\alpha+\theta_2)\}]}{r-\nu e^{i\alpha}} (dr + ird\alpha) \qquad \text{(A-5)}$$

$$I_3 = \int_{C_3} \frac{\exp[r\rho_2\{\sin(\alpha+\theta_2) - i\cos(\alpha+\theta_2)\}]}{r-\nu e^{i\alpha}} (dr + ird\alpha)$$

From (A-2) and (A-3) we obtain:

$$I_1 = -(I_2 + I_3) \qquad \text{(A-6)}$$

In order to make the computation of I_2 and I_3 easy, we shall try to make $I_2 \to 0$ as $r_\infty \to \infty$ and shall choose the path of integration in I_3 along $\alpha = \beta$ from $r = 0$ to $r = \infty$ so that the integrand becomes non-oscillatory in r. From this we obtain

$$\beta + \theta_1 = -\tfrac{\pi}{2} \quad .$$

$$\beta = -\tfrac{\pi}{2} - \theta_1 \quad .$$

then we take the limit as $r_0 \to 0$, the integral I_3 becomes

$$I_3 = \int_\infty^0 \frac{e^{-ir\rho_1}}{r - \nu e^{-i(\frac{\pi}{2} + \theta_1)}} \, dr$$

$$= -\int_0^\infty \frac{e^{-ir\rho_1} \, dr}{r - \nu \sin\theta_1 - i\nu\cos\theta_1}$$

$$= -\int_0^\infty \frac{[r - \nu\sin\theta_1 - i\nu\cos\theta_1] \, e^{-ir\rho_1}}{(r - \nu\sin\theta_1)^2 + \nu^2\cos^2\theta_1} \, dr \,, \qquad (A\text{-}8)$$

and

$$I_2 \longrightarrow 0 .$$

Now let us go back to the equation (A-1), and use the above results. The Cauchy principal-value integral in (A-1) becomes

$$\int_{-\infty}^{\infty} \frac{e^{-ik(a-z)}}{k-\nu} \, dk = \int_{\zeta_1} \frac{e^{-ik(a-z)}}{k-\nu} \, dk + i\pi e^{-i\nu(a-z)} \qquad (A\text{-}9)$$

and (A-1) becomes

$$\Phi(x,y,a,b,t) = \mathrm{Re}\left\{ \left[\frac{1}{2\pi i} \left(\ln \frac{\rho_1}{\rho} + i(\theta_1 - \theta_2) \right) + \frac{1}{2\pi} I_1 \right] \cos\sigma t \right.$$
$$\left. + i\, e^{-i\nu(a-z)} \cos\sigma t - e^{-i\nu(a-z)} \sin\sigma t \right\}$$

$$= \left[\frac{1}{2\pi} \ln \frac{\rho_1}{\rho} + \frac{1}{2\pi} \mathrm{Re}\{-I_3\} \right] \cos\sigma t \qquad (A\text{-}10)$$
$$+ e^{\nu(y+b)} \sin[\nu(x-a) - \sigma t] \,,$$

where

$$\mathcal{R}e\,(-I_3) = \int_0^\infty \frac{(r-\nu\sin\theta_2)\, e^{-r\rho_2}}{(r-\nu\sin\theta_2)^2+\nu^2\cos^2\theta_2}\,dr$$

$$= \int_0^\infty \frac{\gamma-\sin\theta_2\; e^{-\gamma\nu\rho_2}}{(\gamma-\sin\theta_2)^2+\cos^2\theta_2}\,d\gamma$$

$$= \int_0^\infty \frac{\gamma-\nu\rho_2\sin\theta_2\; e^{-\gamma}\,d\gamma}{(\gamma-\nu\rho_2\sin\theta_2)^2+(\nu\rho_2\cos\theta_2)^2}\,. \qquad \text{(A-11)}$$

It is of interest to note two simple cases, i.e. $\theta_2 = 0$ and $\theta_2 = -\pi/2$

$$\mathcal{R}e\,(-I_3) = \int_0^\infty \frac{\gamma\, e^{-\gamma}\,d\gamma}{\gamma^2+(\nu\rho_2)^2} \qquad (\theta_2 = 0;\ \text{along x-axis } x>0) \quad \text{(A-12)}$$

$$\mathcal{R}e\,(-I_3) = \int_0^\infty \frac{e^{-\gamma}\,d\gamma}{\gamma-\nu\rho_2} \qquad (\theta_2 = -\tfrac{\pi}{2},\ \text{along y axis } y<0) \quad \text{(A-13)}$$

From (A-12), (A-13) we can see the integral decrease as $(\nu\rho_2)^{-2}$ along the x-axis and $(\nu\rho_2)^{-1}$ along the y-axis for large $(\nu\rho_2)$.

In order to compute (A-11), one may use the Gauss-Laguerre formula whenever the error bound for the numerical integration is permissible. For completeness this well-known formula (Abramowitz and Stegun, 1967) is stated here:

$$\int_0^\infty f(x)\, e^{-x}\,dx = \sum_{i=1}^{n} w_i\, f(x_i) + \mathcal{R}_n\,, \qquad \text{(A-14)}$$

where

x_i is the i-th zero of the Laguerre Polynomial $\mathcal{L}_n(x)$

$$w_i = \frac{(n!)^2\, x_i}{(n+1)^2\,[\mathcal{L}_{n+1}(x_i)]^2}\,,$$

$$\mathcal{R}_n = \frac{(n!)^2}{(2n)!}\, f^{(2n)}(\xi) \qquad (0<\xi<\infty).$$

APPENDIX B

We shall give a very brief description of general quadrilateral elements. A reader can find much more detail in Zienkiewicz (1971, pp. 103-170) and Ergatoudis, Irons and Zienkiewicz (1968). The procedure for the numerical integrations in (4-12), (4-13) and (4-14) will also be described briefly.

Let us consider a four-node quadrilateral element in the physical plane. We introduce a new coordinate system in such a way that the element in the xy plane maps, one-to-one, into a square in the new coordinates ($\xi\,\eta$ - plane) shown in Fig. A-1. Then we can express a function ϕ in terms of a set of the interpolation functions $[\bar{N}]$, which are functions of ξ and η .

$$\phi \cong \bar{N}_1(\xi,\eta)\,\bar{\phi}_1 + \bar{N}_2\,\bar{\phi}_2 + \bar{N}_3\,\bar{\phi}_3 + \bar{N}_4\,\bar{\phi}_4 \qquad \text{(B-1)}$$

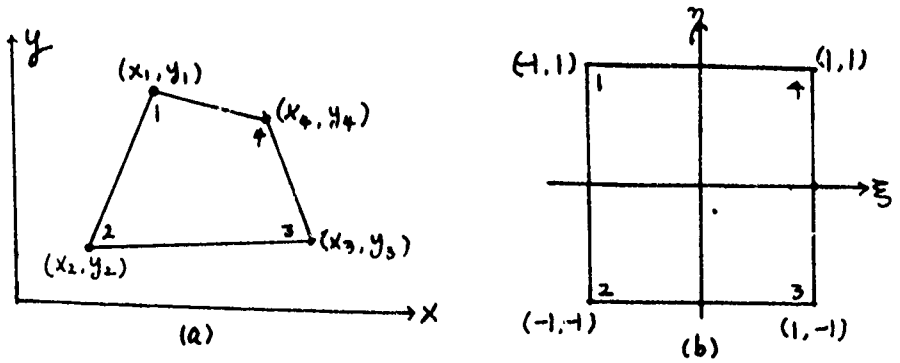

Fig. A-1

Similarly we can write

$$x = \bar{N}_1 x_1 + \bar{N}_2 x_2 + \bar{N}_3 x_3 + \bar{N}_4 x_4 \qquad \text{(B-2)}$$

$$y = \bar{N}_1 y_1 + \bar{N}_2 y_2 + \bar{N}_3 y_3 + \bar{N}_4 y_4$$

where

$$\begin{aligned} \bar{N}_1 &= (1-\xi)(1+\eta)/4 \ , \\ \bar{N}_2 &= (1-\xi)(1-\eta)/4 \ , \\ \bar{N}_3 &= (1+\xi)(1-\eta)/4 \ , \\ \bar{N}_4 &= (1+\xi)(1+\eta)/4 \ . \end{aligned} \tag{B-3}$$

$[\bar{N}]$ contains the interpolation functions in the new coordinates. Hence this may be different from [N] in the physical plane.

When we have a general quadrilateral element, it is more convenient to perform the integrals in (4-12), (4-13) and (4-14) in the new coordinate system. From the coordinate transformation, we have

$$\begin{aligned} \frac{\partial}{\partial \xi} &= \frac{\partial x}{\partial \xi}\frac{\partial}{\partial x} + \frac{\partial y}{\partial \xi}\frac{\partial}{\partial y} \ , \\ \frac{\partial}{\partial \eta} &= \frac{\partial x}{\partial \eta}\frac{\partial}{\partial x} + \frac{\partial y}{\partial \eta}\frac{\partial}{\partial y} \ , \end{aligned}$$

or in matrix notation

$$\begin{Bmatrix} \frac{\partial}{\partial \xi} \\ \frac{\partial}{\partial \eta} \end{Bmatrix} = [J] \begin{Bmatrix} \frac{\partial}{\partial x} \\ \frac{\partial}{\partial y} \end{Bmatrix} \quad \text{and} \quad \begin{Bmatrix} \frac{\partial}{\partial x} \\ \frac{\partial}{\partial y} \end{Bmatrix} = [J]^{-1} \begin{Bmatrix} \frac{\partial}{\partial \xi} \\ \frac{\partial}{\partial \eta} \end{Bmatrix}$$

in which [J] is the Jacobian matrix,

$$[J] = \begin{bmatrix} \frac{\partial x}{\partial \xi} & \frac{\partial y}{\partial \xi} \\ \frac{\partial x}{\partial \eta} & \frac{\partial y}{\partial \eta} \end{bmatrix} = \frac{1}{4} \begin{bmatrix} -(1+\eta) & -(1-\eta) & (1-\eta) & (1+\eta) \\ (1-\xi) & -(1-\xi) & -(1+\xi) & (1+\xi) \end{bmatrix} \begin{bmatrix} x_1 & y_1 \\ x_2 & y_2 \\ x_3 & y_3 \\ x_4 & y_4 \end{bmatrix}$$

The integration with respect to x and y in (4-12) can simply be changed to integration with respect to ξ and η, with a simplification of the limits of integration, which now are simply from -1 to 1 in both variables, and with the change

$$dx\,dy = |J|\, d\xi\, d\eta \ ,$$

where $|J|$ is the determinant of $[J]$. Similarly the boundary integrals defined in (4-13) and (4-14) can also be carried out in the new coordinates with a change of variables,

$$ds = \sqrt{dx^2(\xi) + dy^2(\xi)} = \sqrt{\left(\frac{dx}{d\xi}\right)^2 + \left(\frac{dy}{d\xi}\right)^2}\, d\xi$$

or

$$ds = \sqrt{dx^2(\eta) + dy^2(\eta)} = \sqrt{\left(\frac{dx}{d\eta}\right)^2 + \left(\frac{dy}{d\eta}\right)^2}\, d\eta$$

with limits from -1 to 1.

All the integrations are performed numerically using the well-known Gaussian quadrature formula (Abramowitz and Stegun, pp. 916-917).

In our computer program, the element shapes that we used were four-node and eight-node quadrilateral elements. The procedure for computing K_{ij}, h_{ij} and b_i in (4-12), (4-13) and (4-14) for the case of an eight-node quadrilateral element is very similar to that for a four-node element. Therefore this will not be given here.

In writing the computer program, a computer program made for structural problems (Wilson, 1970) has been helpful.

ACKNOWLEDGEMENT

I am greatly indebted to Professor John V. Wehausen not only for his patient guidance throughout this work but also for his continuous encouragement throughout my graduate studies.

I am grateful to Professor J. R. Paulling for his guidance and encouragement in my experimental research during my graduate work. I would like to thank Professor R. L. Wiegel for reviewing the manuscript.

Finally, I am indeed grateful for the moral and partly financial support of my brother and my family and for the unlimited understanding of my wife throughout my years of schooling at Berkeley.

BIBLIOGRAPHY

Abramowitz, M.; Stegun, I. A.

Handbook of mathematical functions. Dover Publications, New York, 1967, xiv + 1046 pp.

Argyris, J. H.; Mareczek, C.; Scharpf, D. W.

Two and three dimensional flow using finite elements. J. Roy. Aero. Soc. 73(1969), 961-964.

Bessho, Masatoshi

Variational approach to steady ship wave problem. 8th Sym. Naval Hydrodynamics, Pasadena, Calif., 1970, 36 pp.

Cumming, Richard A.

The experimental determination of forces and pressures acting on a hemisphere oscillating on a free surface. Univ. of Calif., Berkeley, Coll. of Engrg. Rep. No. NA-63-1 (March 1963), iii + 42 pp.

Dean, W. R.

On the reflection of surface waves by a submerged circular cylinder. Proc. Cambridge Phil. Soc. 44 (1948), 483-491.

Doctors, L. J.

An application of the finite element technique to boundary value problems of potential flows. Int. J. Num. Meth. Eng. 2(1970), 243-252.

Eckart, Carl.

Variation principles of hydrodynamics. Physics of fluids 3, No. 3(1960), 421-427.

Ergatoudis, I.; Irons, B. M.; Zienkiewicz, O. C.

Curved isoparametric 'quadrilateral' elements for finite element analysis. Int. J. Solids & Struct. 4(1968), 31-42.

Frank, W.

Oscillation of cylinders in or below the free surface of deep fluids. N. S. R. D. C., Rep. 2375 (1967), vi + 42 pp.

Holand, Ivar.

Finite elements for the computation of hydrodynamic mass. Proc. of Symp. on finite element Techniques held at the University of Stuttgart, Germany, June 10-12, 1969. (4th International Ship Structures Congress).

Hunt, D. A.

Discrete element idealization of an incompressible liquid for vibration analysis. AIAA J. 8, no. 6 (June 1970), 1001-1004.

Discrete element structural theory of fluids. AIAA J. 9, no. 3 (March 1971), 451-461.

Kim, Cheung, H.

Hydrodynamic forces and moments for heaving swaying, and rolling cylinders on water of finite depth. J. Ship Res. 13(1969), 137-154.

Lamb, H.

Hydrodynamics. 6th ed. Cambridge Univ. Press, 1932, xv + 738 pp.

Luke, J. C.

A variational principle for a fluid with a free surface. J. Fluid Mech. 27(1967), 395-397.

Matsumoto, Kouhei.

Application of finite element method to added virtual mass of ship hull vibration. J. Soc. Naval Arch. Japan 127(1970), 83-90.

Matsuura, Yoshikazu; Kawakami, Hajime

Calculation of added virtual mass and added virtual mass moment of inertia of ship hull vibration by the finite element method. J. Soc. Naval Arch. Japan 38 (1968), 281-291.

McLachlan, N. W.

Bessel functions for engineers. 2nd ed. Oxford Univ. Press, London, 1954, xii + 239 pp.

Mei, Chiang C.; Black, Jared L.

Scattering of surface waves by rectangular obstacles in waters of finite depth. J. Fluid Mech. 38(1969), 499-511.

Mikhlin, S. G.

Variational methods in mathematical physics. (Translated by Boddington, T.) Macmillan Company, New York, 1964, xxxii + 582 pp.

Morse, P. M.; Feshbach, H.

Methods of theoretical physics. Part I. McGraw-Hill, New York, 1953, xxii + 997 + xl.

Ogilvie, T. Francis

First- and second-order forces on a cylinder submerged under a free surface. J. Fluid Mech. 16(1963), 451-472.

Porter, W. R.

Pressure distributions, added mass and damping coefficients for cylinders oscillating in a free surface. Inst. Engrg. Res., Univ. Calif., Berkeley, Series 82, Issue 16(1960), x + 181 pp.

Raissi, H.

Use of two- and three-dimensional bottomless cylinders for harbor and oil storage tanks (tentative name). Dissertation, Univ. Calif., Berkeley, Dept. of Civil Engineering (Hydraulic Lab.), To be published in Dec. 1972.

Reid, J. K.

On the construction and convergence of a finite-element solution of Laplace's equation. J. Inst. Maths Applics 9(1972), 1-13.

Sao, Kunihisa; Maeda, Hisaaki; Hwang, J. H.

On the heaving oscillation of a circular dock. J. Soc. Naval Arch. Japan 130(1971), 127-130.

Stoker, J. J.

Surface waves. Interscience Publishers, New York, 1957, xxviii + 567 pp.

Taylor, C.; Patil, B. S., Zienkiewicz, O. C.

Harbour oscillation: a numerical treatment for undamped natural modes. Proc. Inst. Civil Eng. 43(1969), 141-156.

Ursell, F.

Surface waves on deep water in the presence of a submerged circular cylinder. I. Proc. Cambridge Phil. Soc. 46(1950), 141-152.

Watson, G. N.

Theory of Bessel functions. 2nd ed. Cambridge Univ. Press, 1966, vi + 804 pp.

Wehausen, J. V.; Laitone E. V.

Surface waves. Encyclopedia of Physics, vol. IX, 1960, Springer-Verlag, Berlin. 446-778.

Whittaker, E. T.; Watson, G. N.

Modern Analysis. 4th ed., Cambridge Univ. Press, 1963, 608 pp.

Wilson, E. L.; Pretorius, P. C

A computer program for the analysis of prismatic solids, Univ. of Calif., Berkeley, Dept. of Civil Engineering, Sept. 1970, ii + 50 pp.

Zienkiewicz, O. Z.

Hydrodynamic pressures due to earthquakes. Water Power, Sept. 1964, 382-388.

Zienkiewicz, O. Z.; Newton, R. E.

Coupled vibrations of a structure submerged in a conpressible fluid. Proc. Int. Symp. on Finite Element Techniques, Stuttgart, 1969, 359-379.

Zienkiewicz, O. Z.

The finite element method in engineering science. McGraw-Hill, London, 1971, xiv + 521 pp.

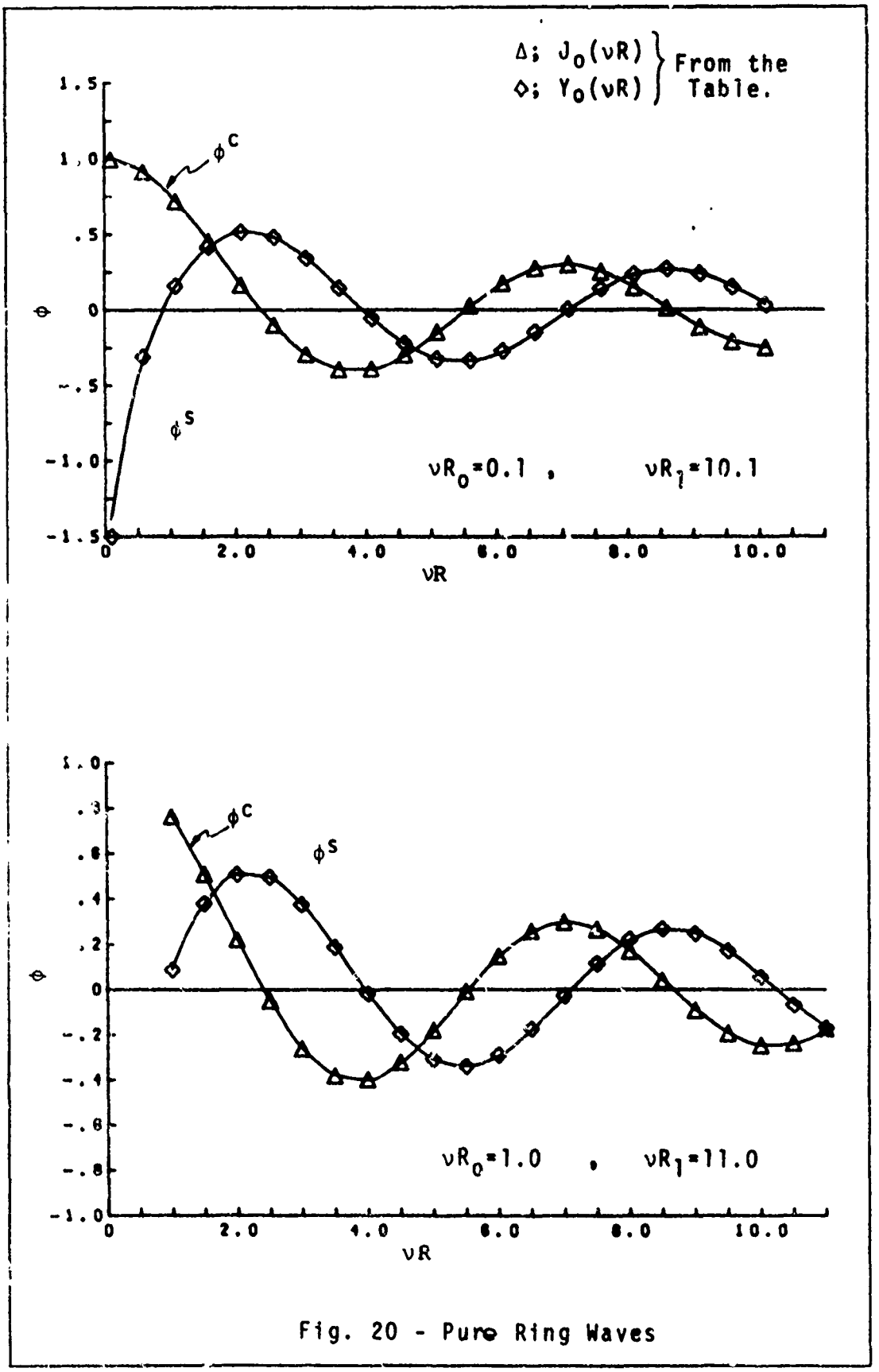

Fig. 20 - Pure Ring Waves

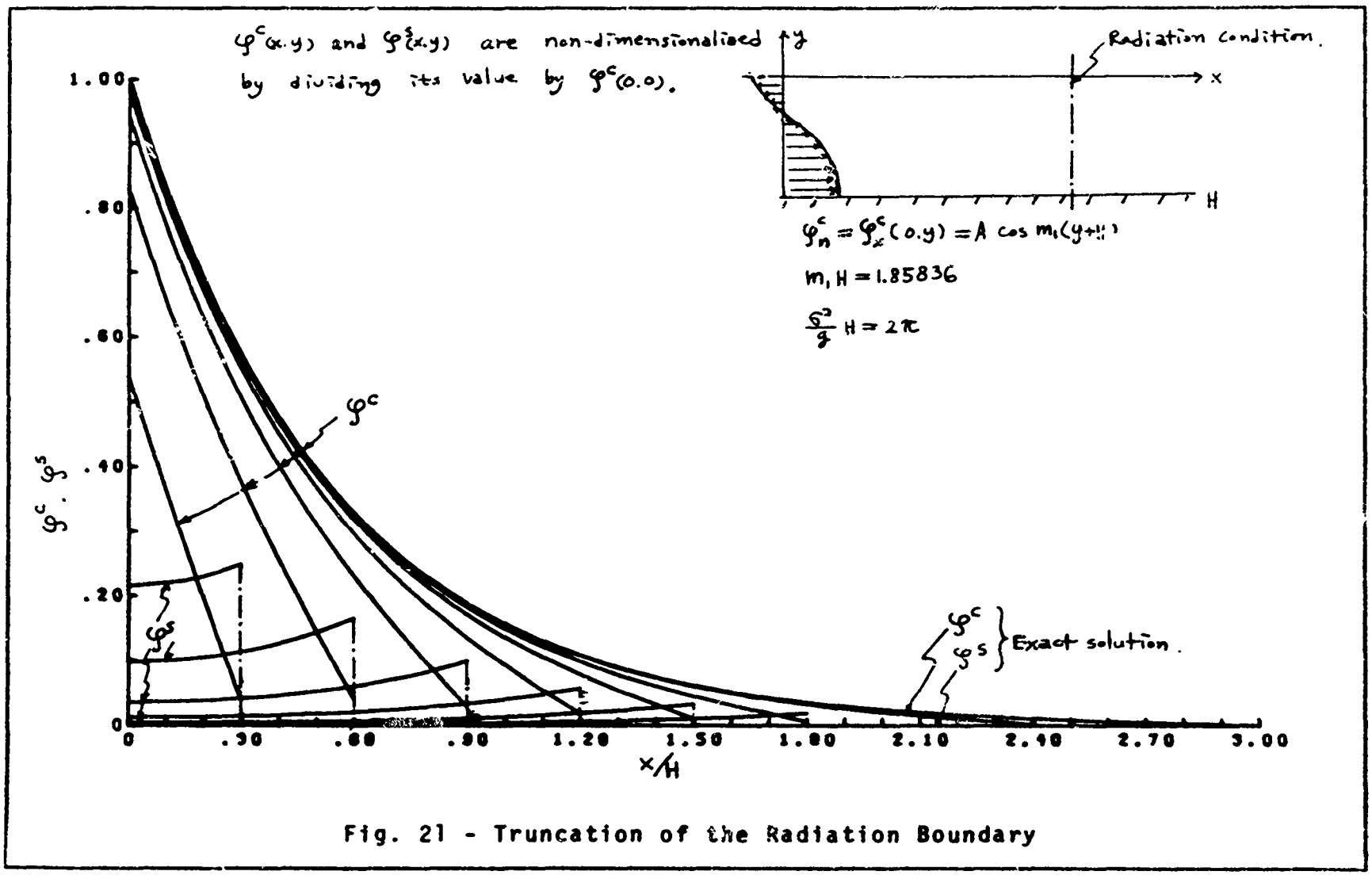

Fig. 21 - Truncation of the Radiation Boundary

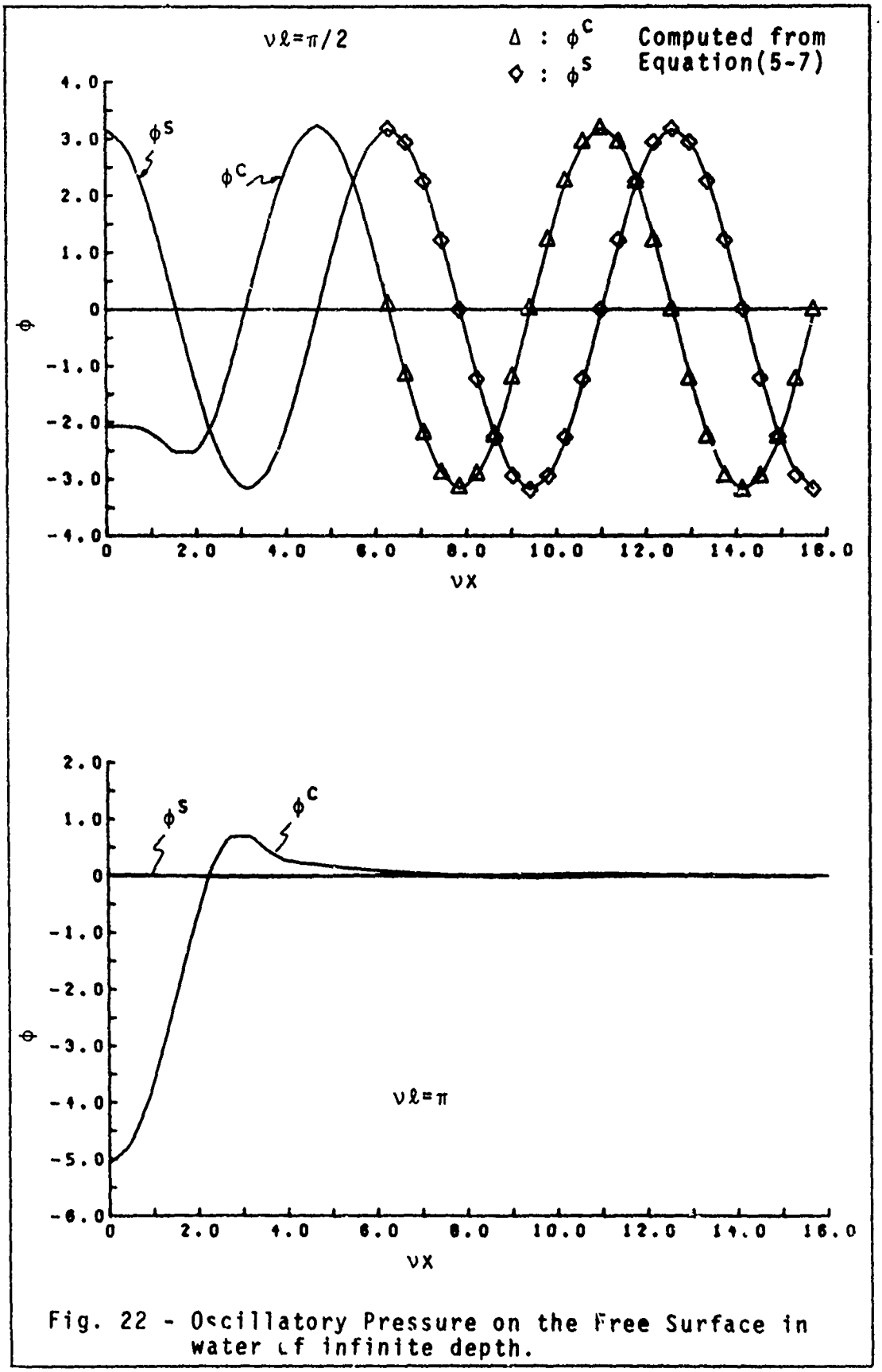

Fig. 22 - Oscillatory Pressure on the Free Surface in water of infinite depth.

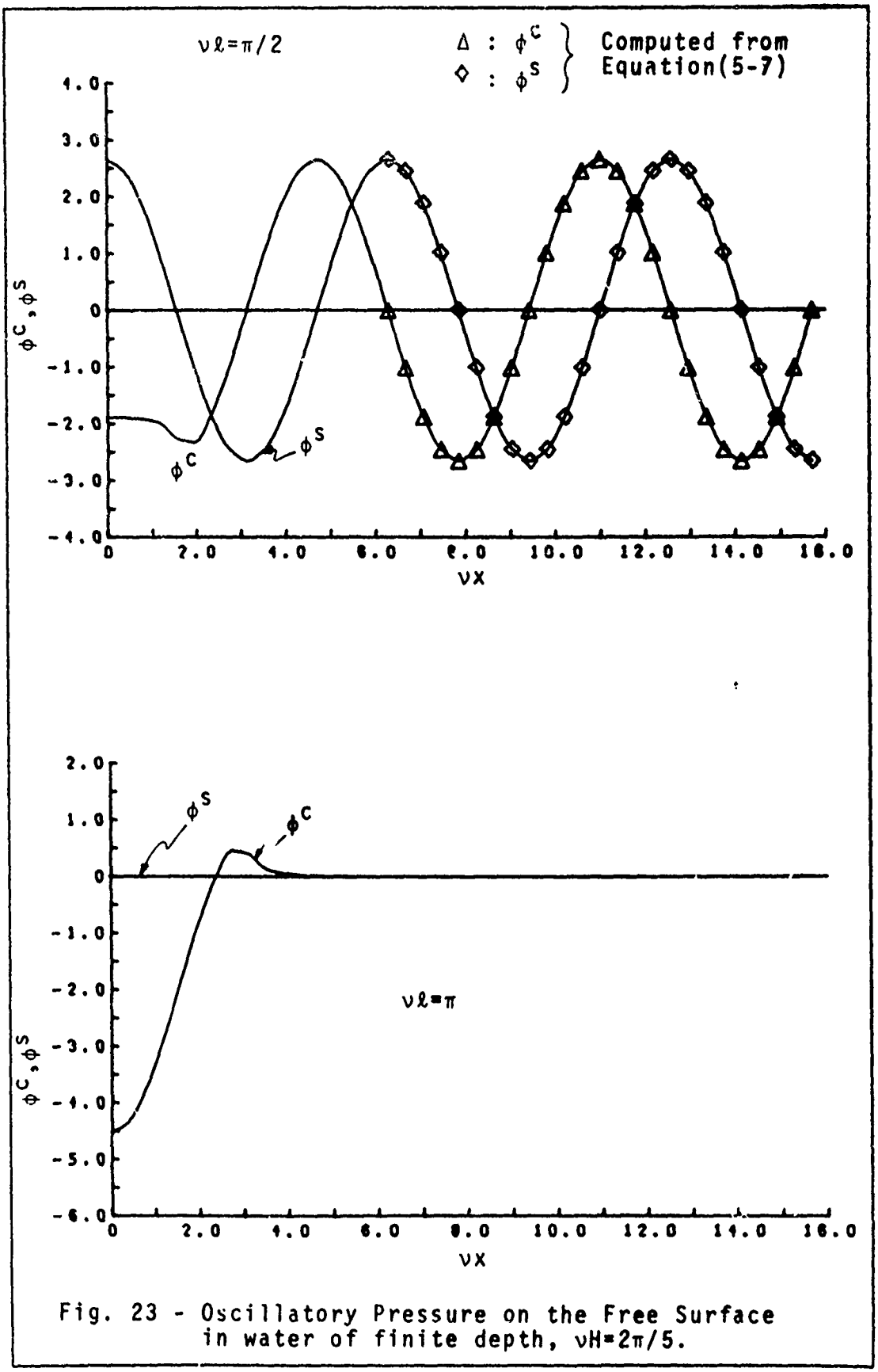

Fig. 23 - Oscillatory Pressure on the Free Surface in water of finite depth, νH=2π/5.

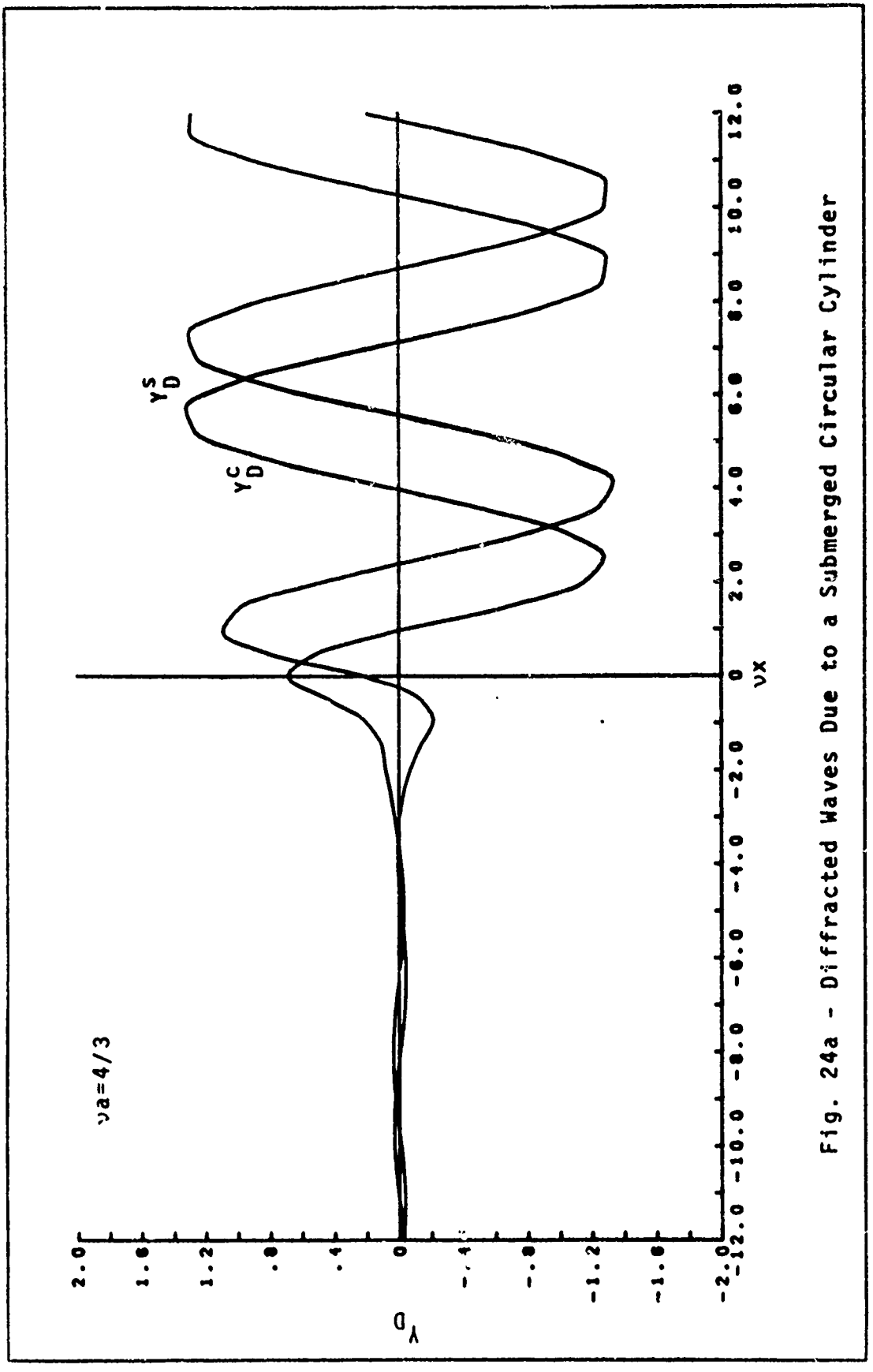

Fig. 24a - Diffracted Waves Due to a Submerged Circular Cylinder

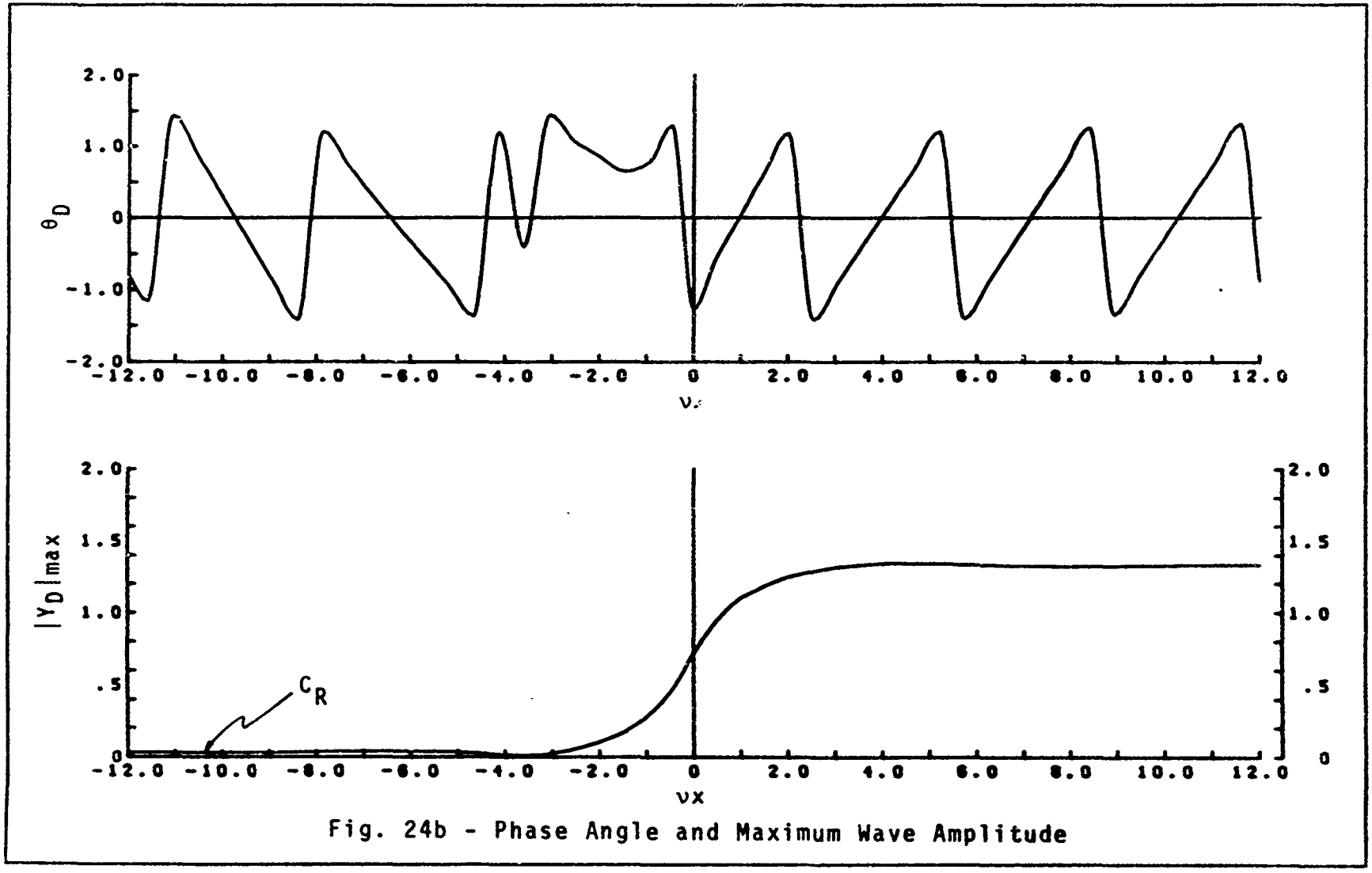

Fig. 24b - Phase Angle and Maximum Wave Amplitude

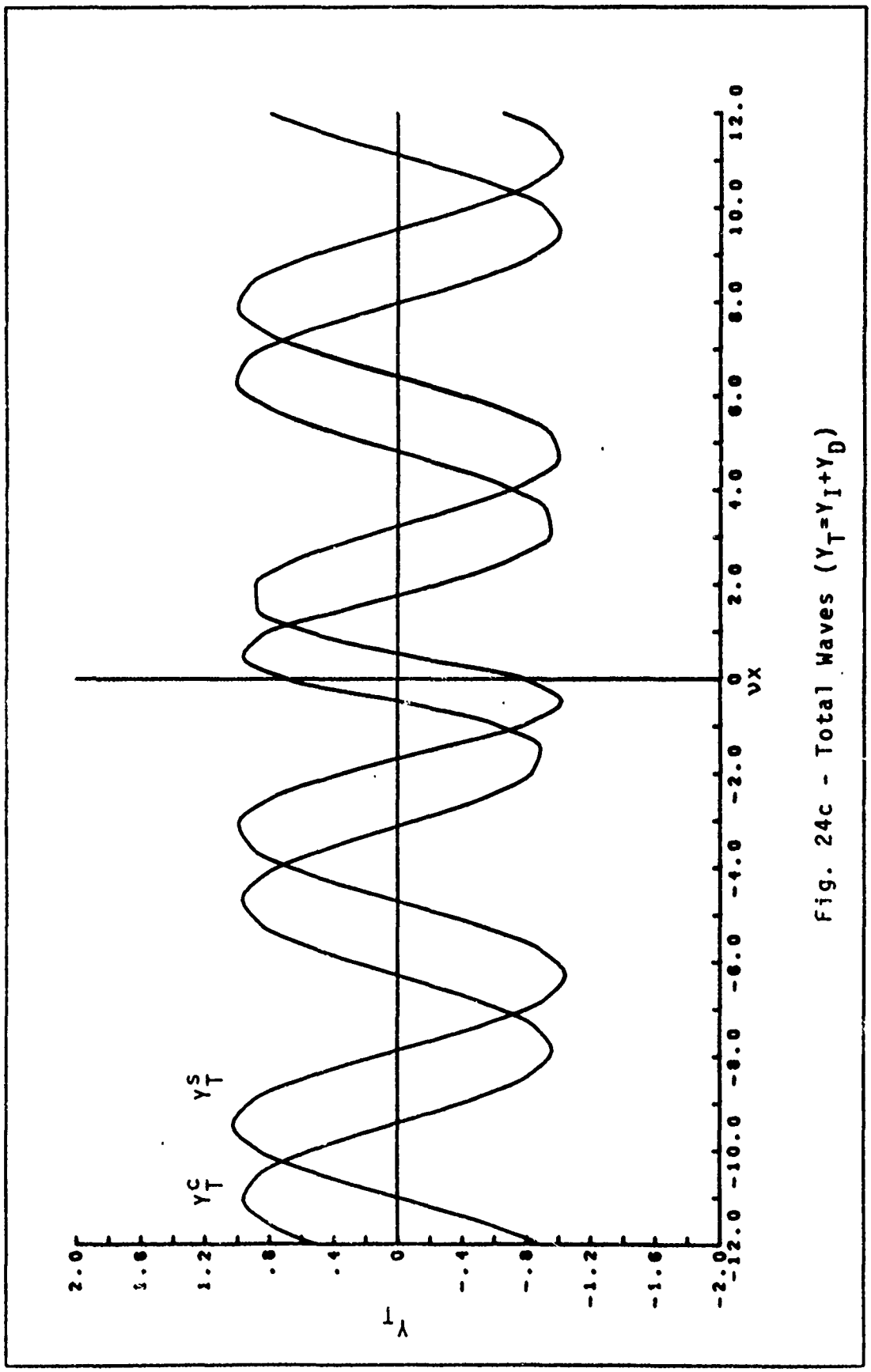

Fig. 24c - Total Waves ($Y_T=Y_I+Y_D$)

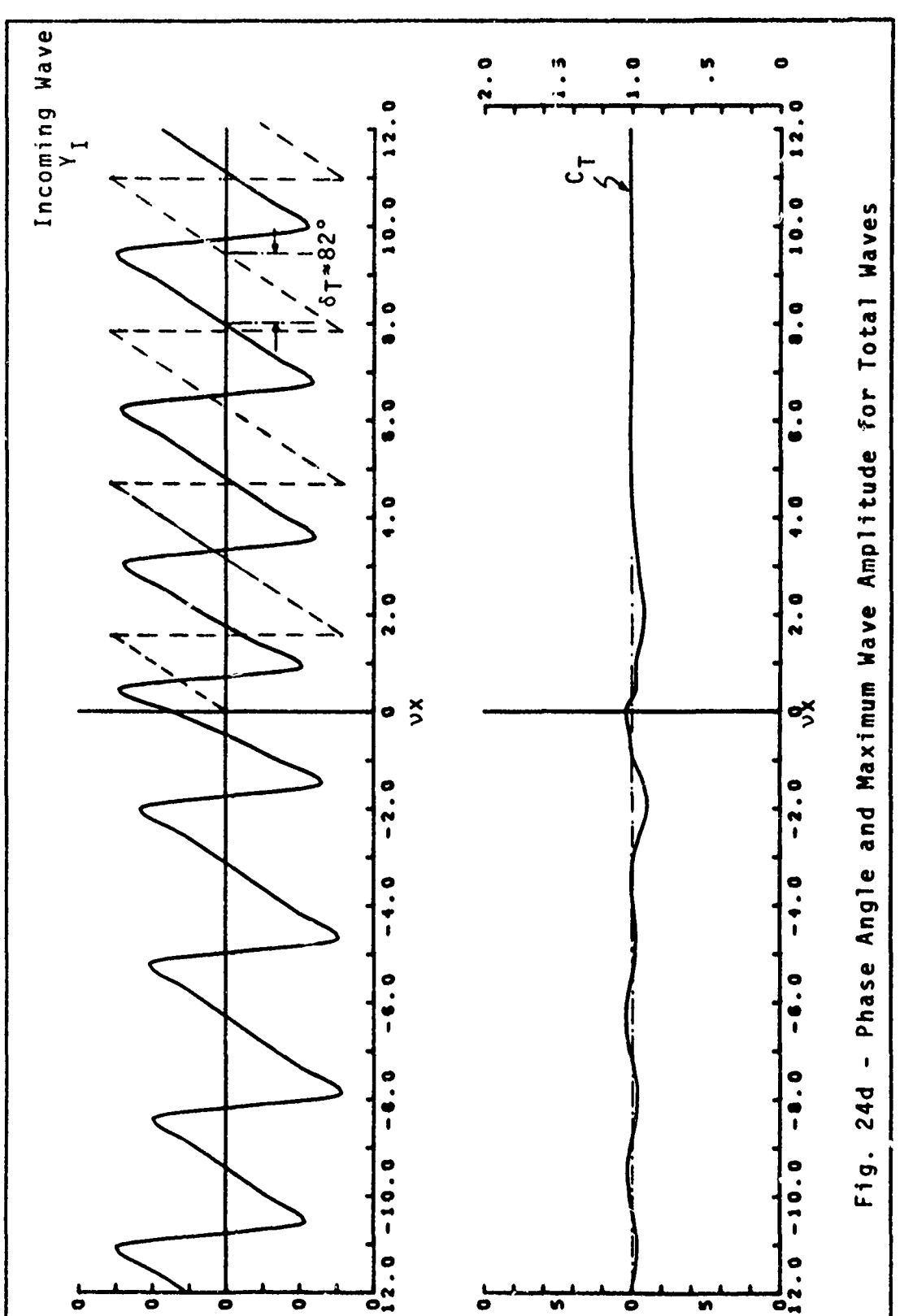

Fig. 24d - Phase Angle and Maximum Wave Amplitude for Total Waves

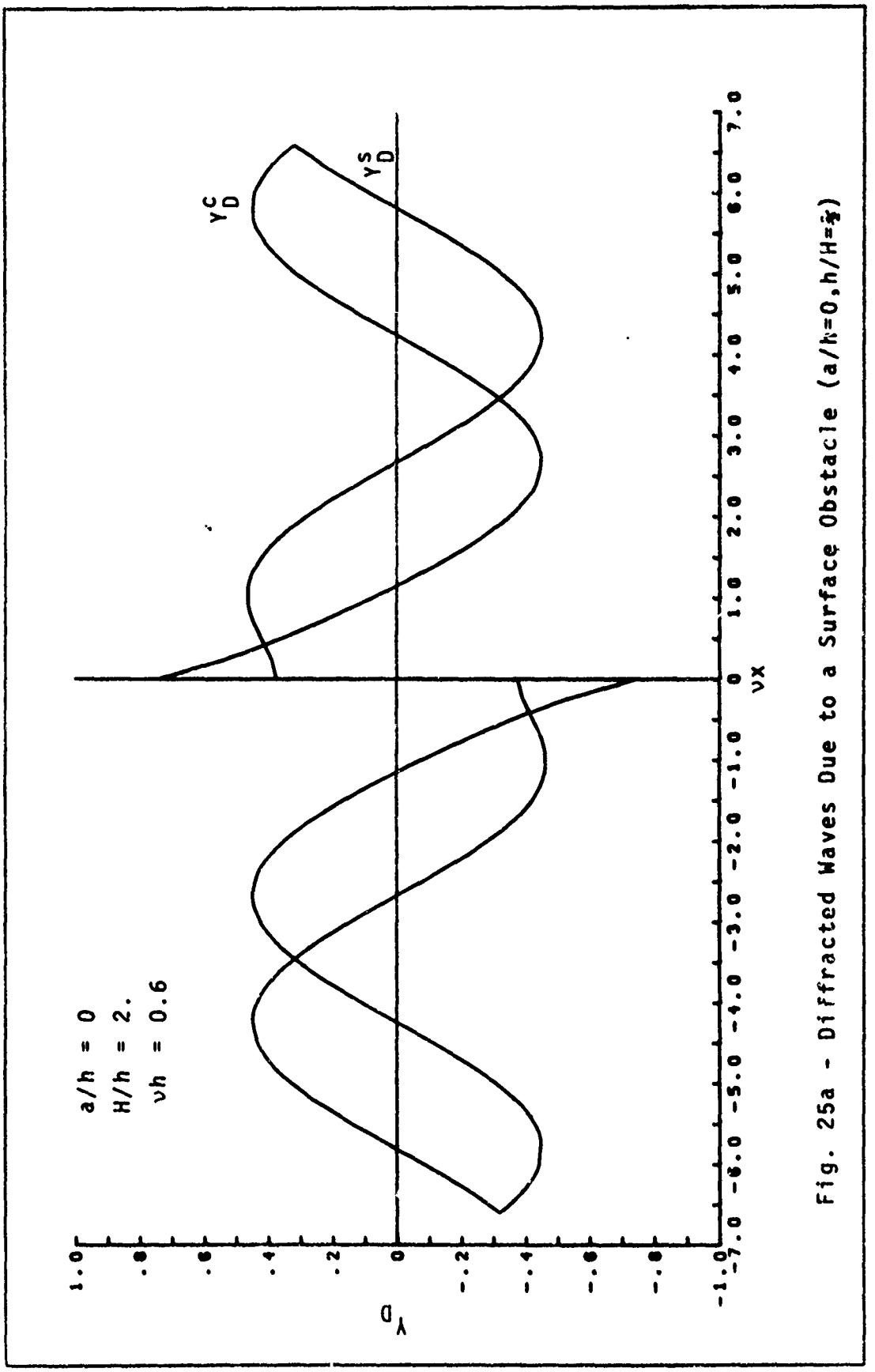

Fig. 25a - Diffracted Waves Due to a Surface Obstacle (a/h=0,h/H=½)

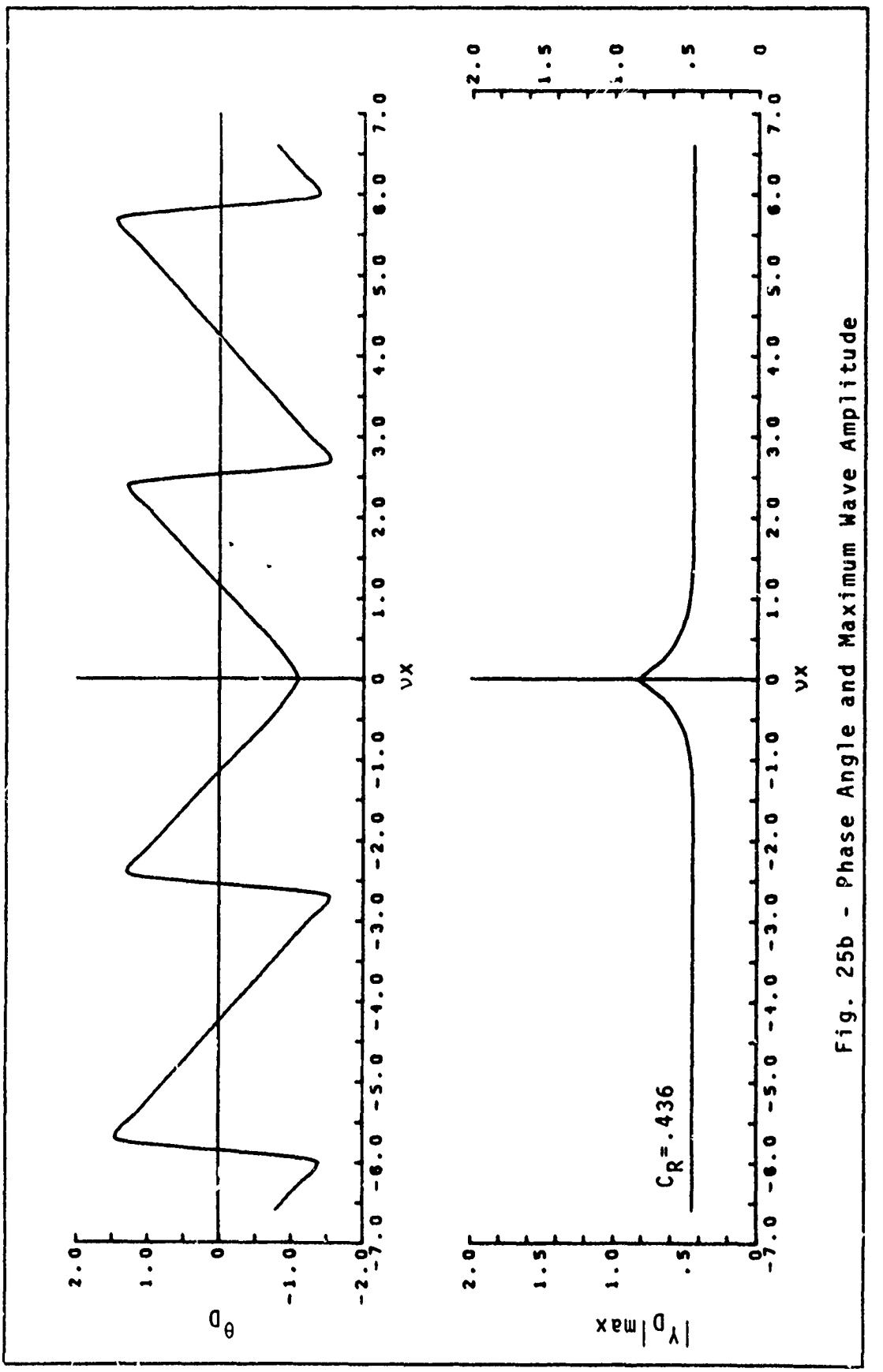

Fig. 25b - Phase Angle and Maximum Wave Amplitude

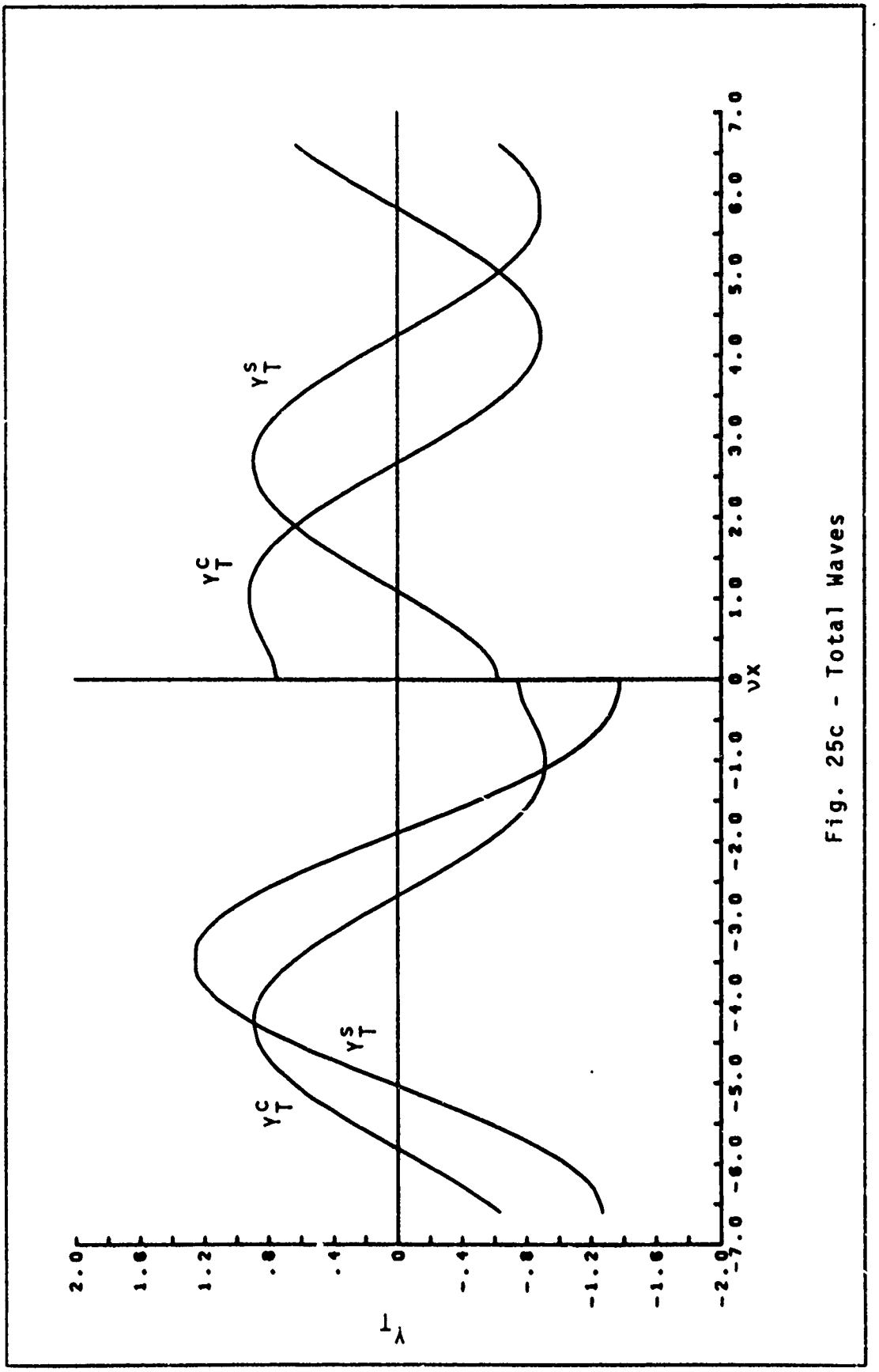

Fig. 25c - Total Waves

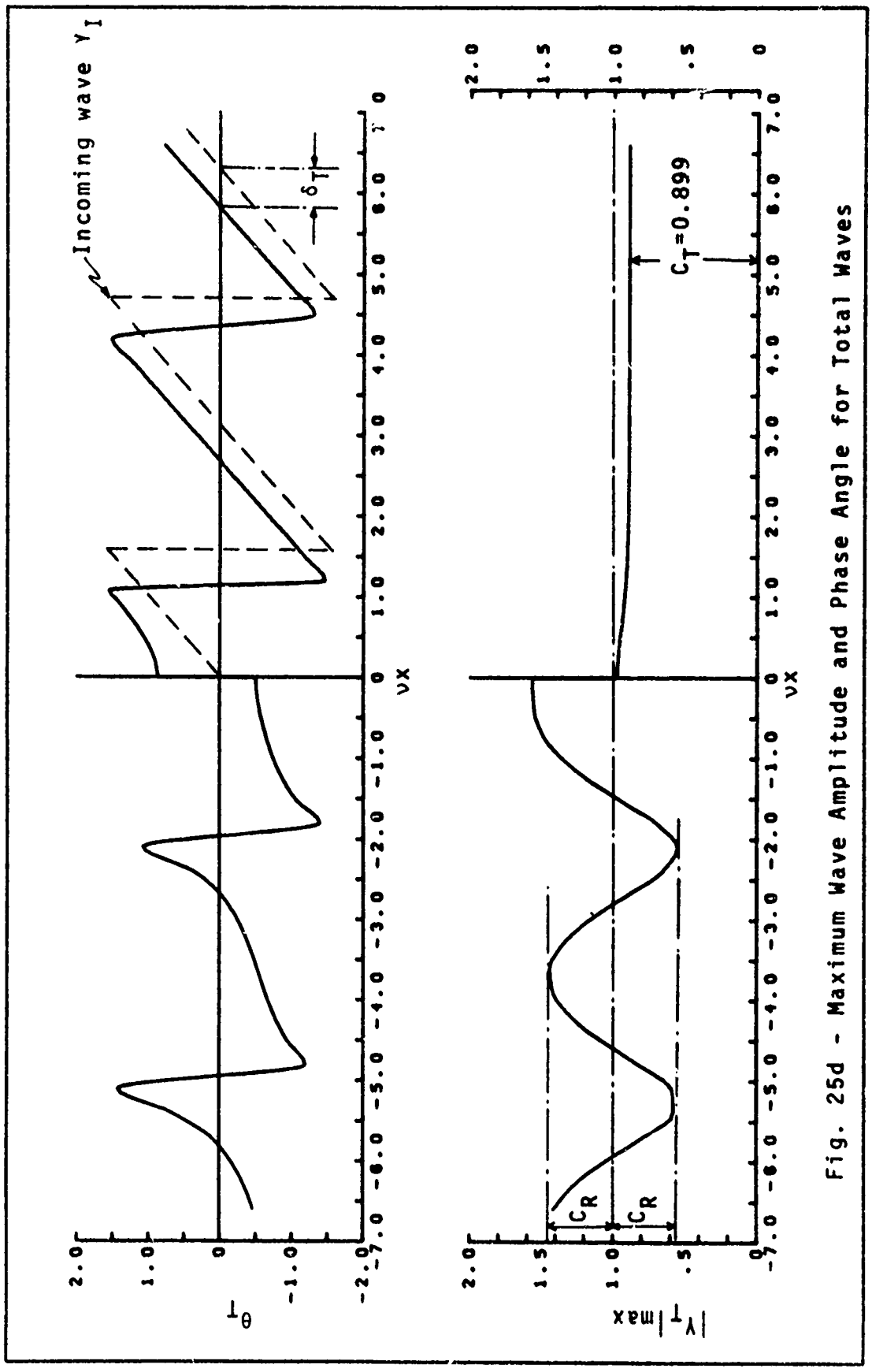

Fig. 25d - Maximum Wave Amplitude and Phase Angle for Total Waves

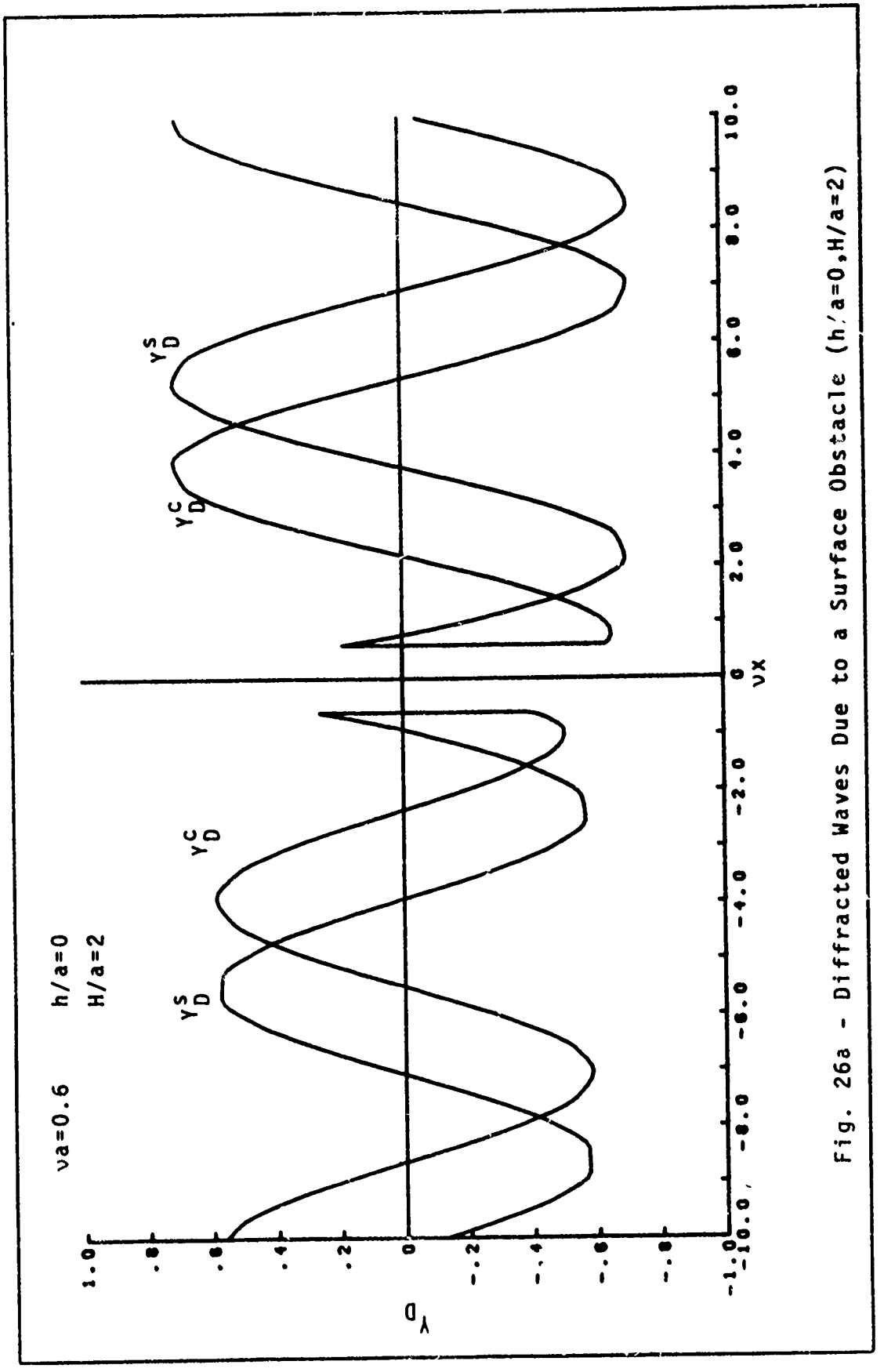

Fig. 26a - Diffracted Waves Due to a Surface Obstacle (h/a=0,H/a=2)

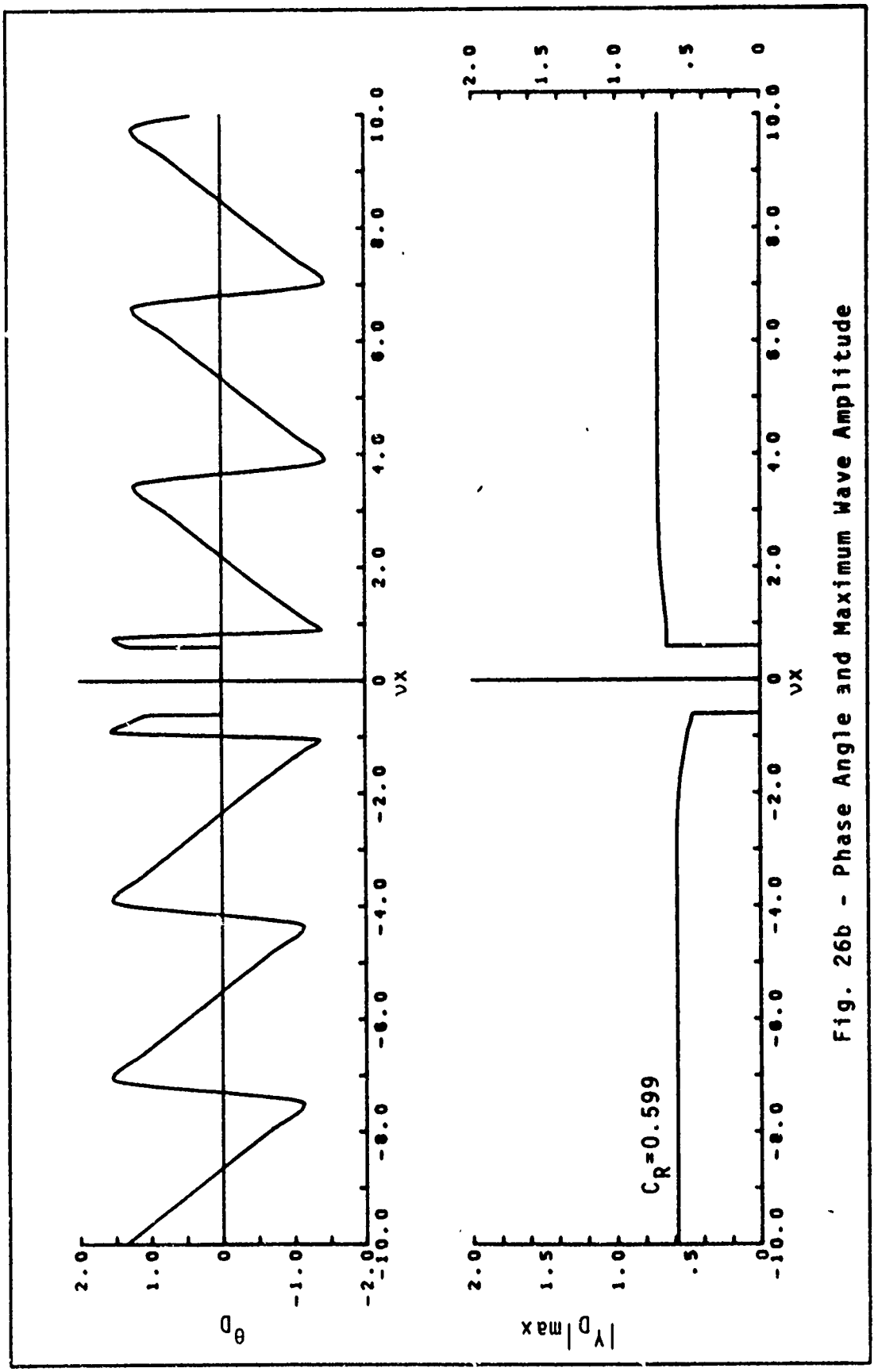

Fig. 26b - Phase Angle and Maximum Wave Amplitude

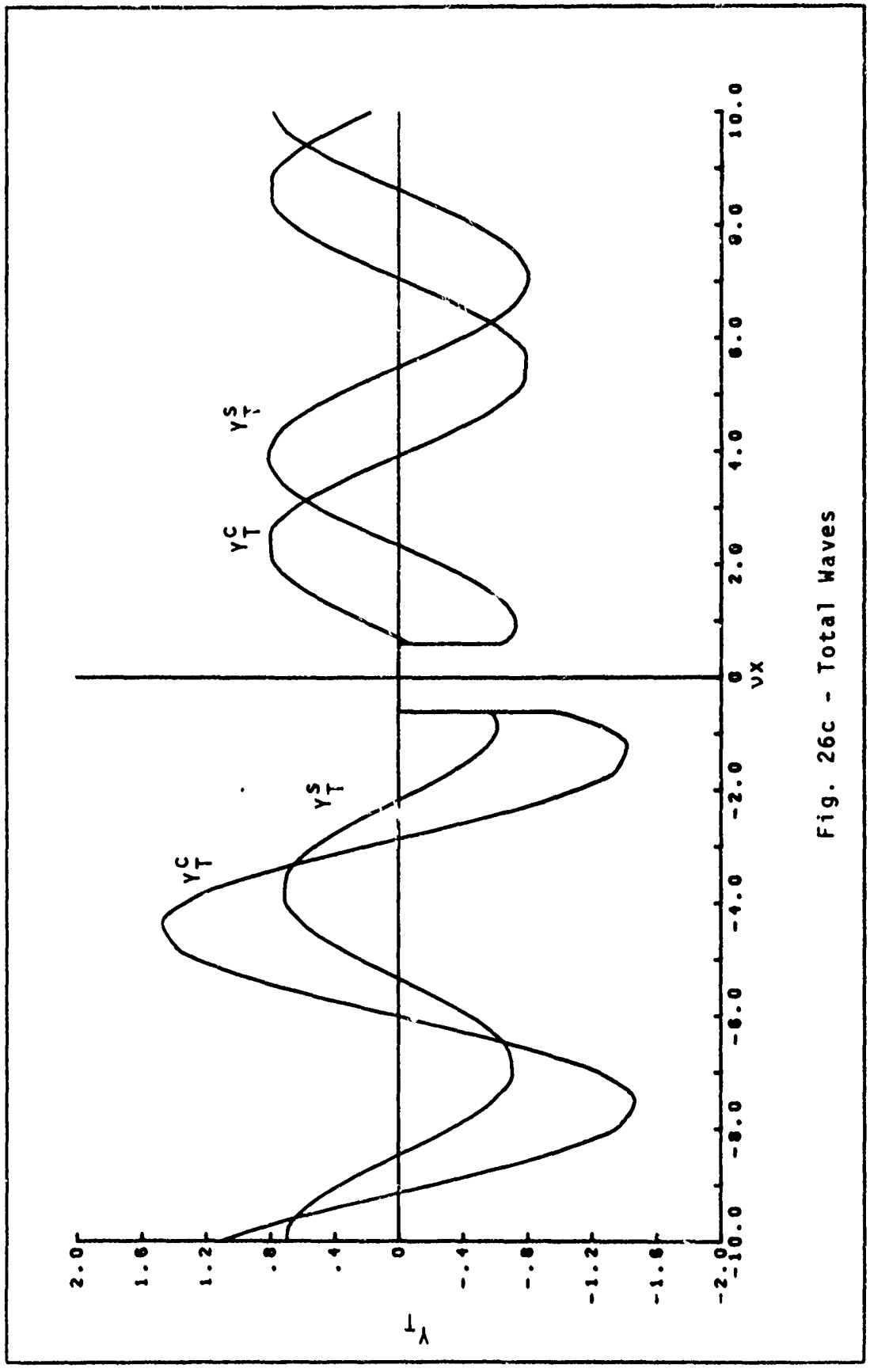

Fig. 26c - Total Waves

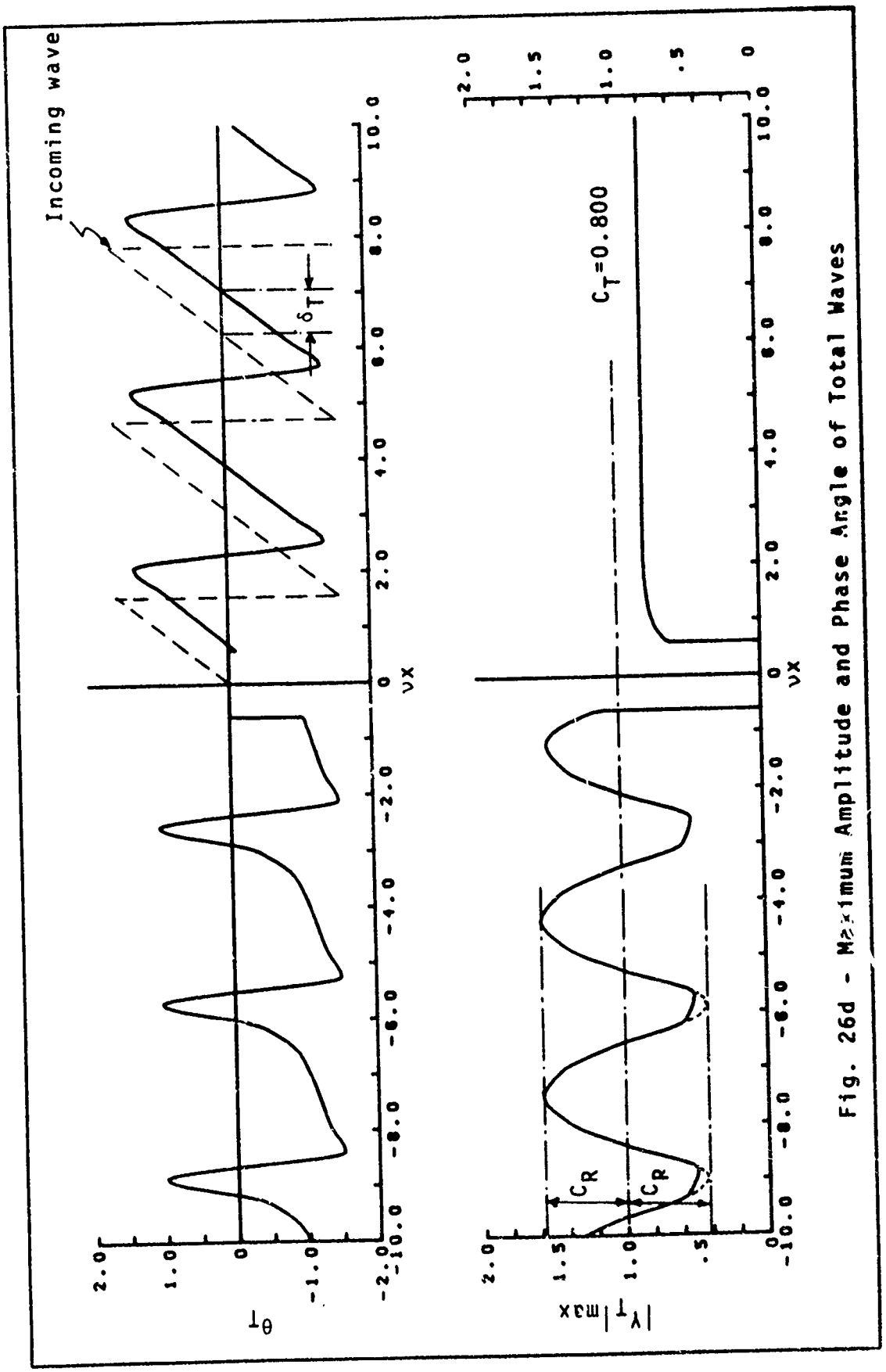

Fig. 26d - Maximum Amplitude and Phase Angle of Total Waves

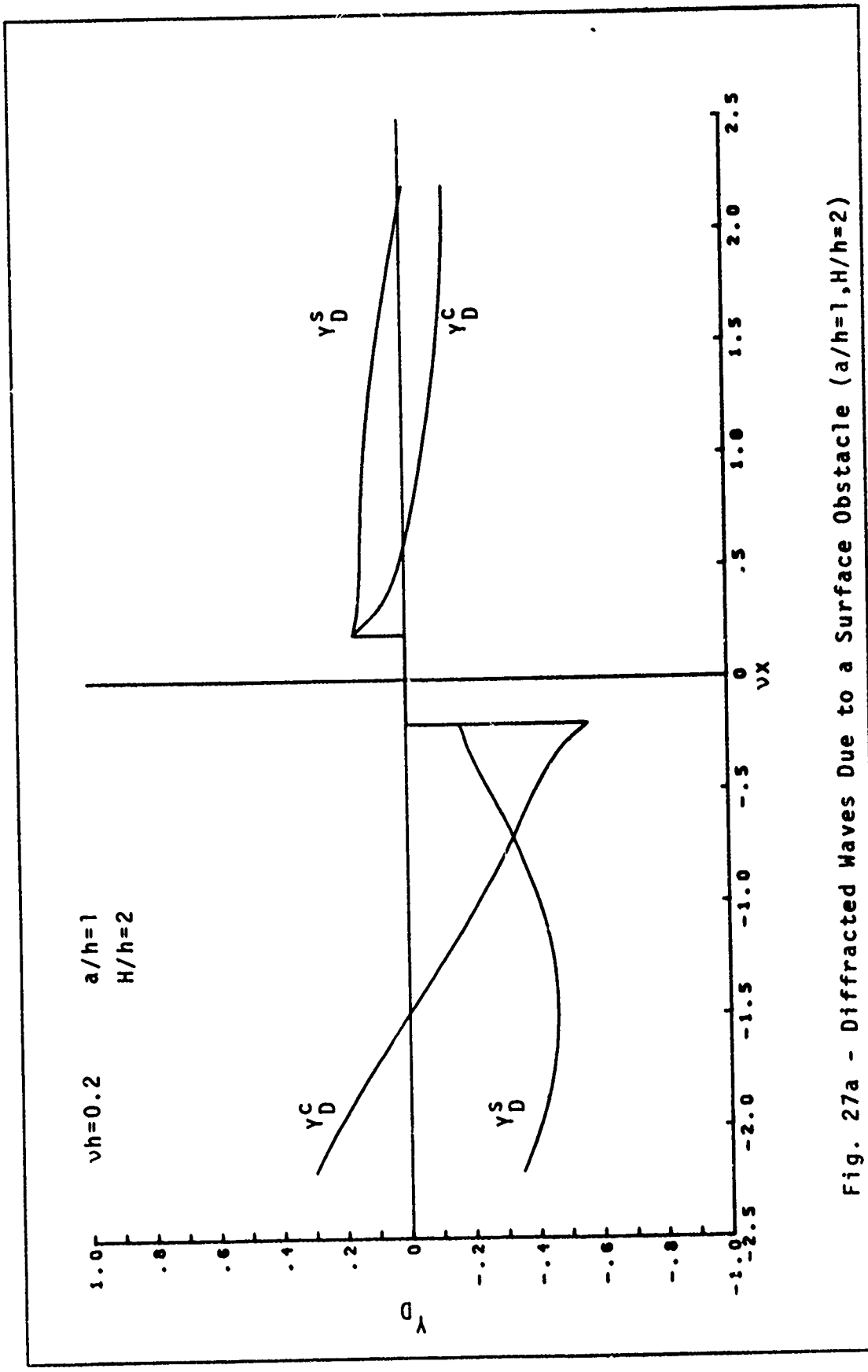

Fig. 27a - Diffracted Waves Due to a Surface Obstacle (a/h=1,H/h=2)

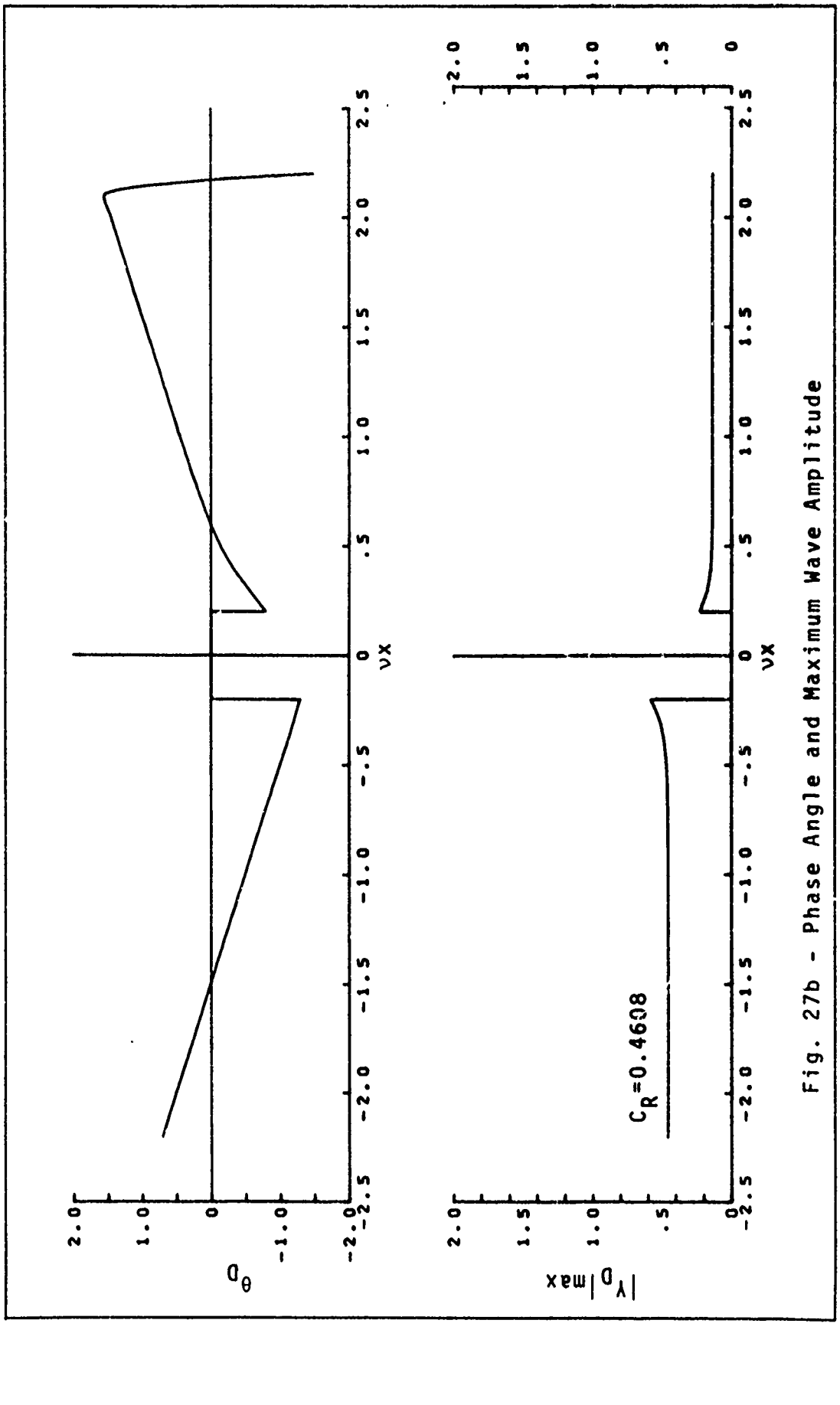

Fig. 27b - Phase Angle and Maximum Wave Amplitude

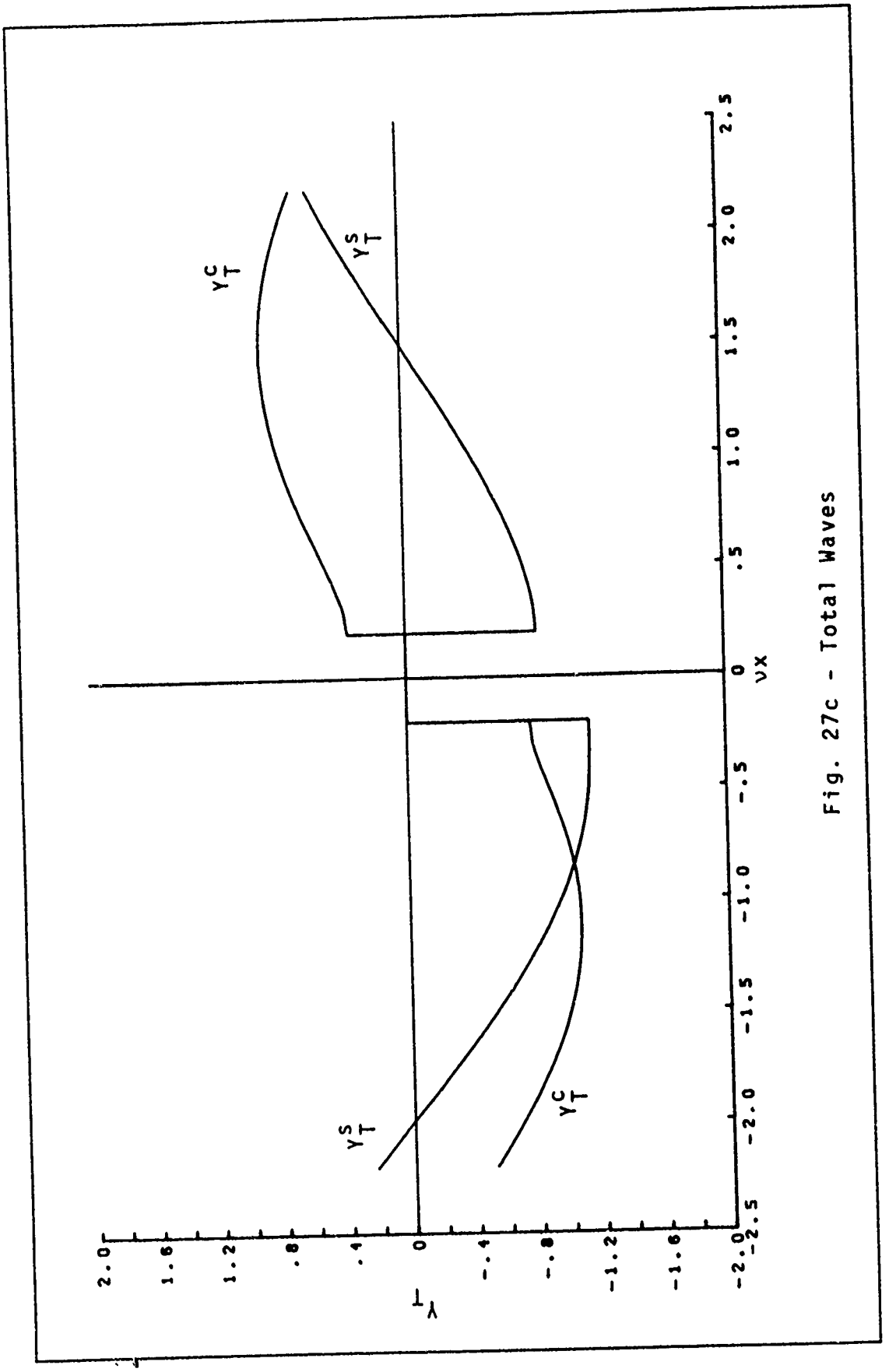

Fig. 27c - Total Waves

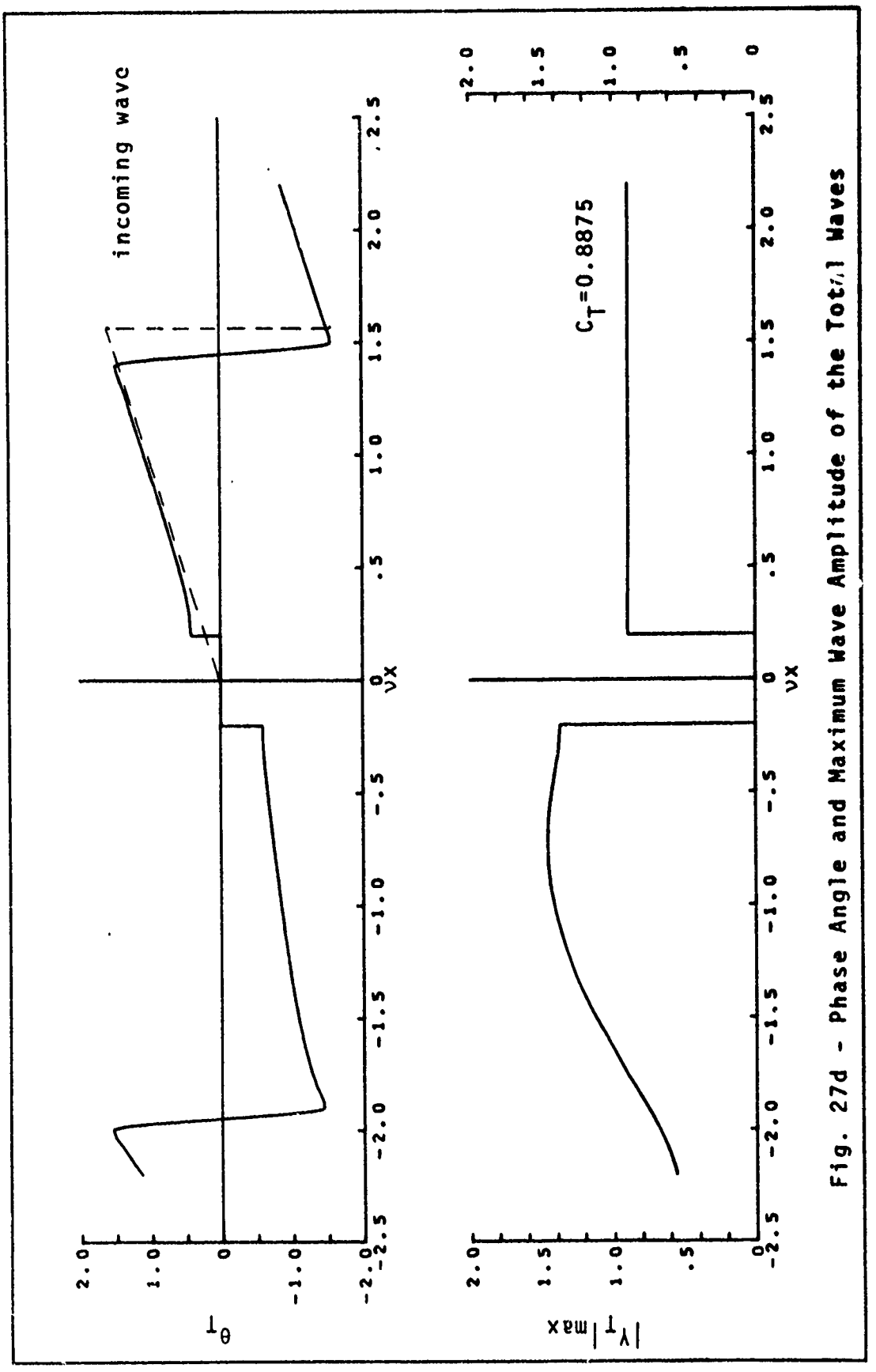

Fig. 27d - Phase Angle and Maximum Wave Amplitude of the Total Waves

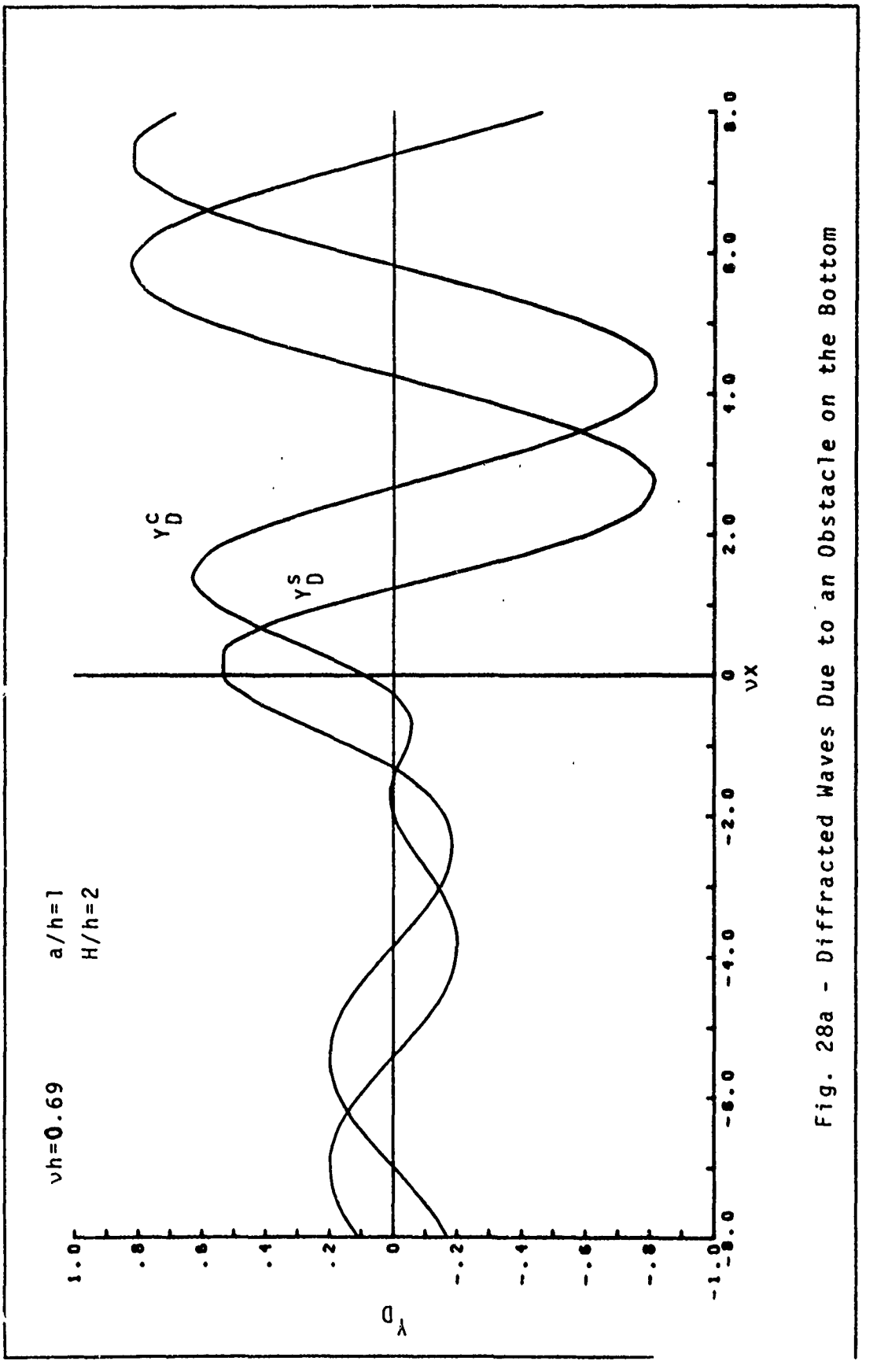

Fig. 28a - Diffracted Waves Due to an Obstacle on the Bottom

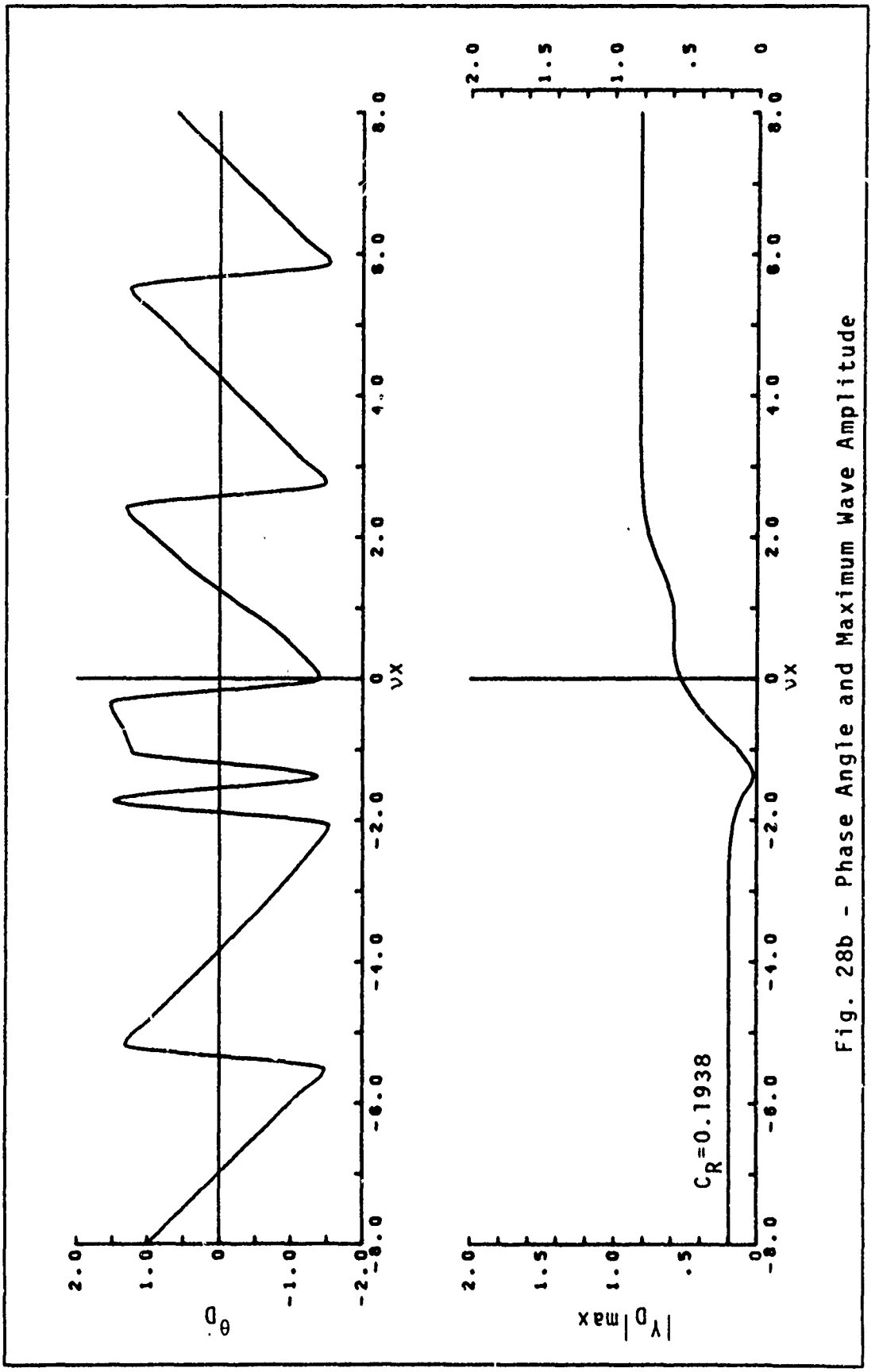

Fig. 28b - Phase Angle and Maximum Wave Amplitude

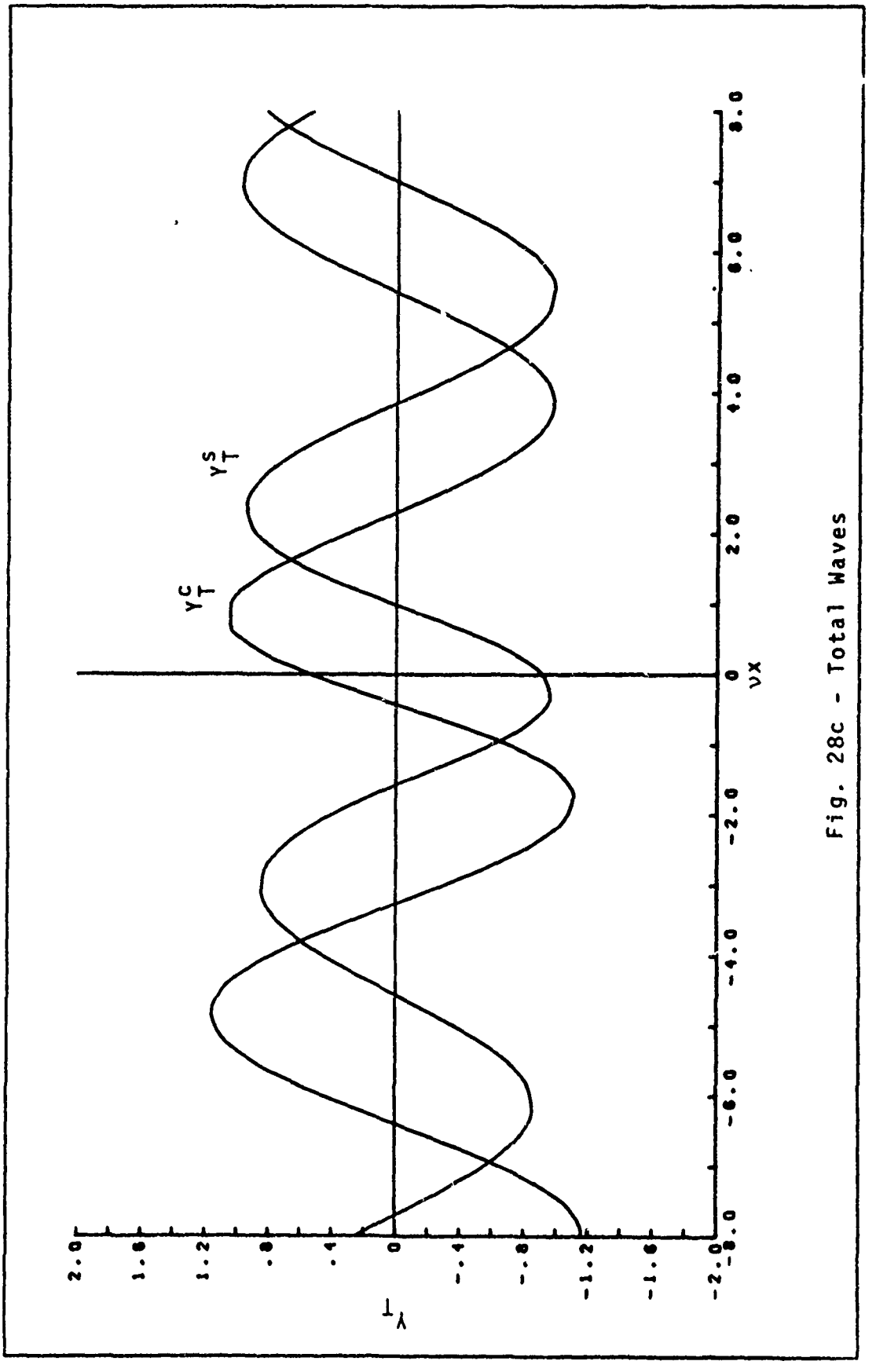

Fig. 28c - Total Waves

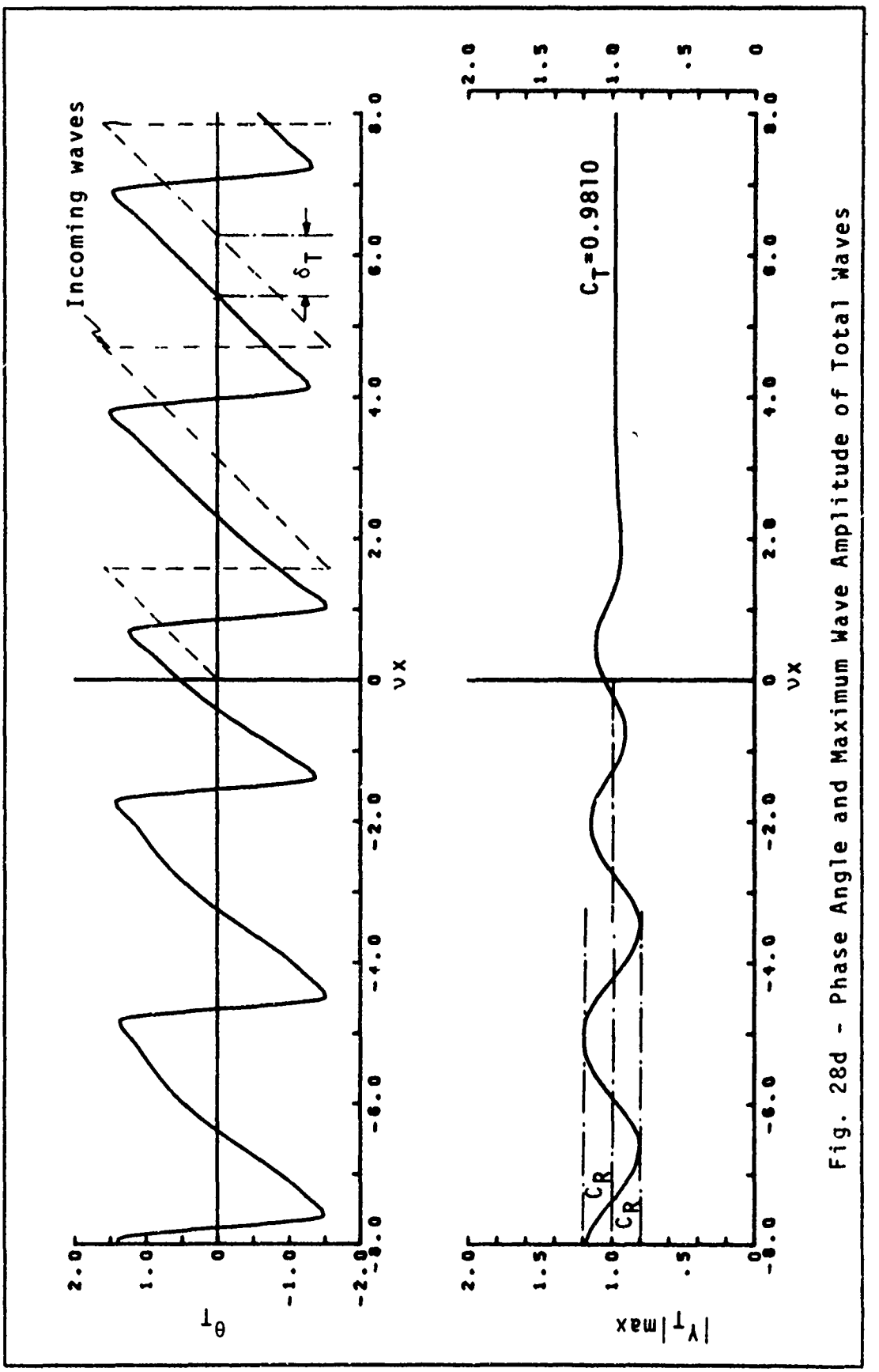

Fig. 28d - Phase Angle and Maximum Wave Amplitude of Total Waves

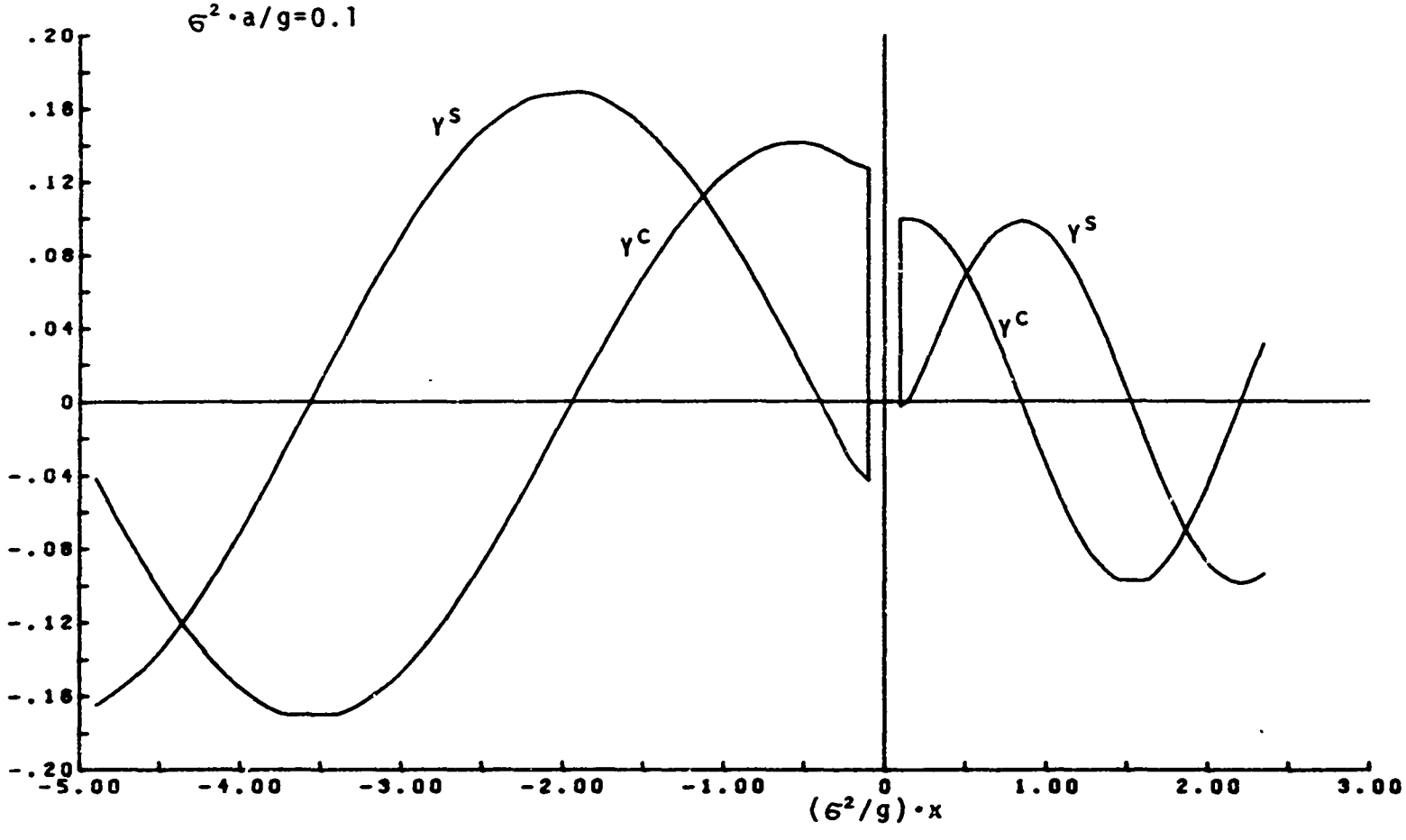

Fig. 29a - Wave Profiles Due to a Forced Motion of a Rectangular Cylinder

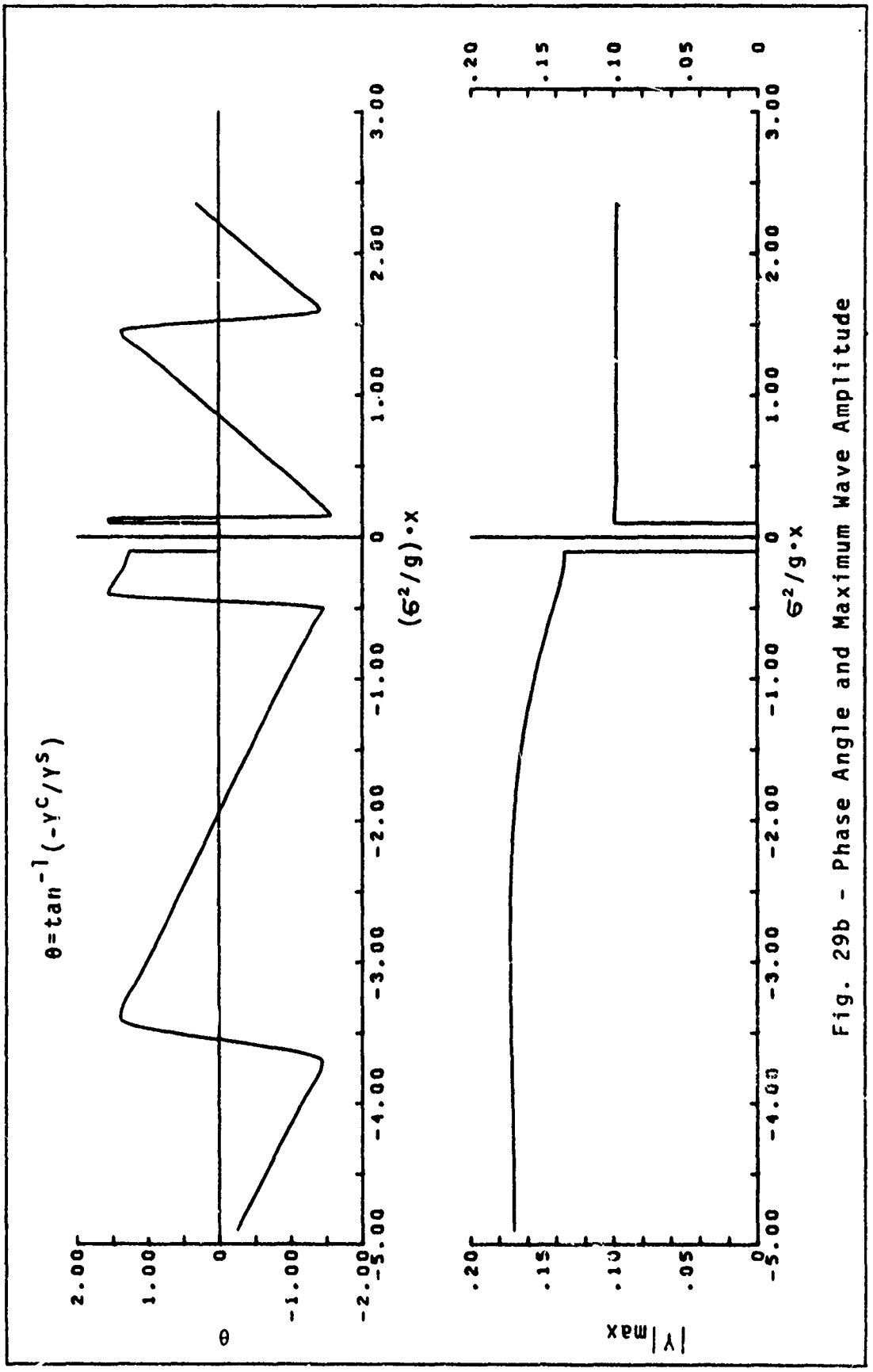

Fig. 29b - Phase Angle and Maximum Wave Amplitude

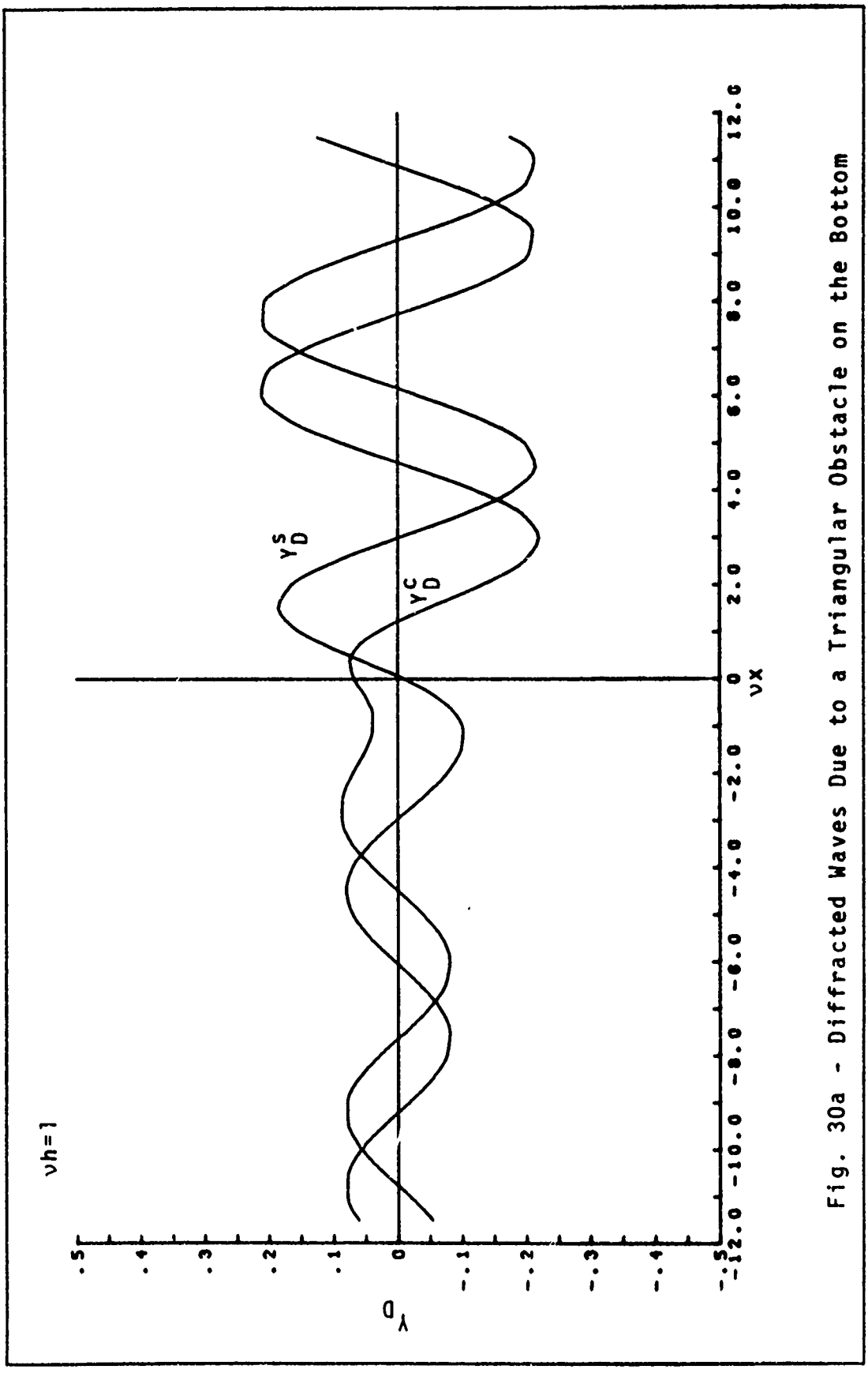

Fig. 30a - Diffracted Waves Due to a Triangular Obstacle on the Bottom

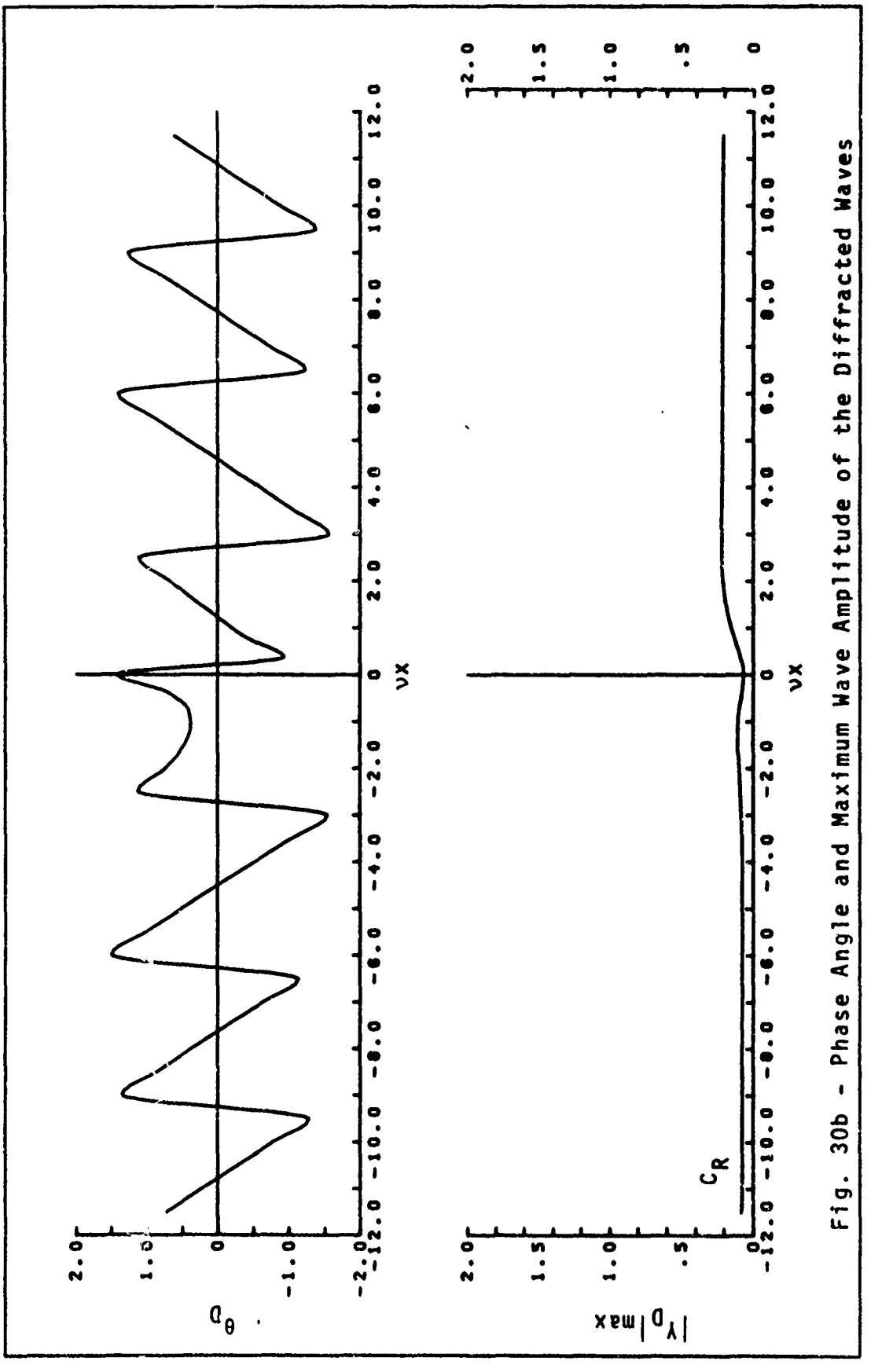

Fig. 30b - Phase Angle and Maximum Wave Amplitude of the Diffracted Waves

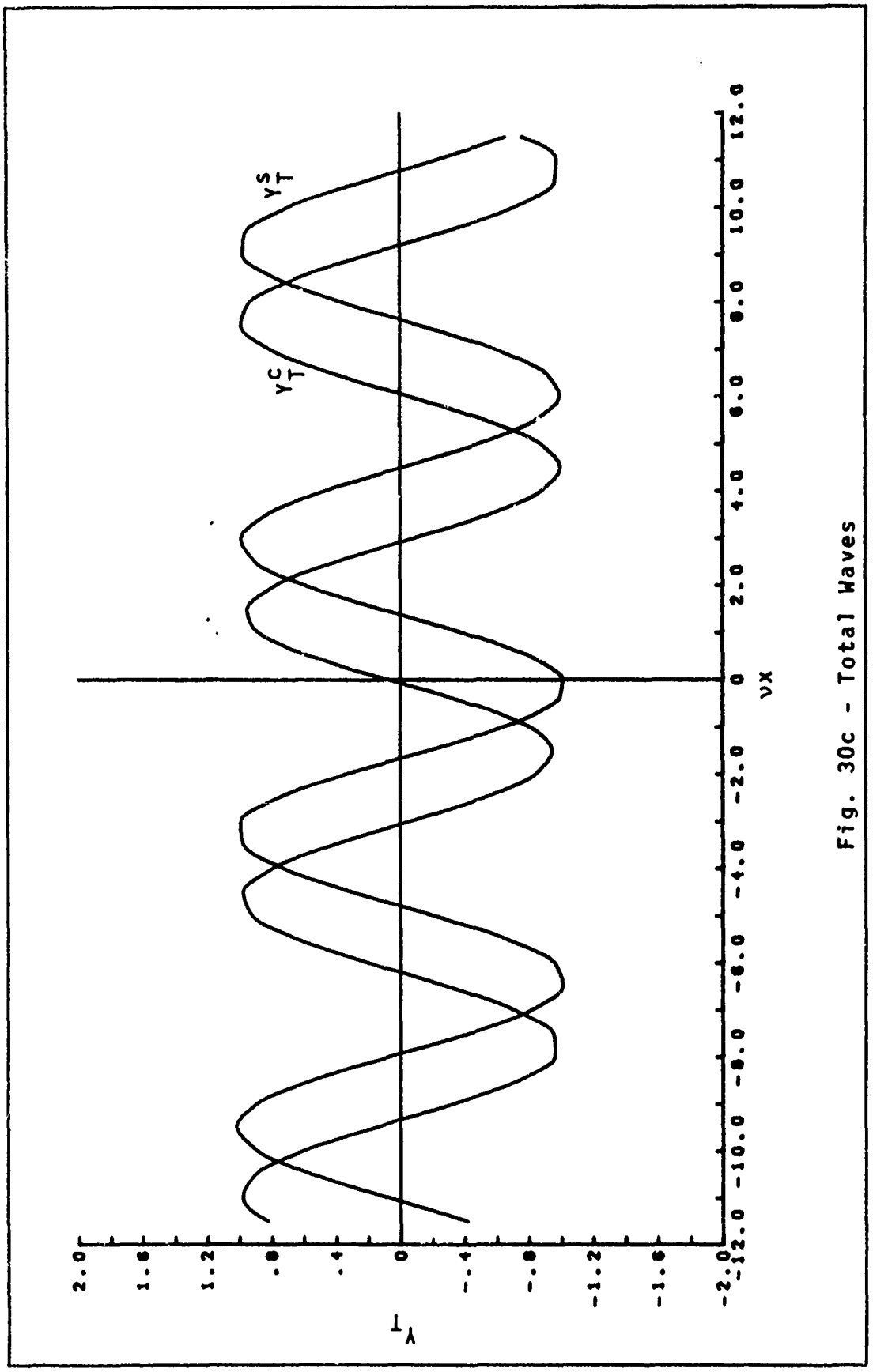

Fig. 30c - Total Waves

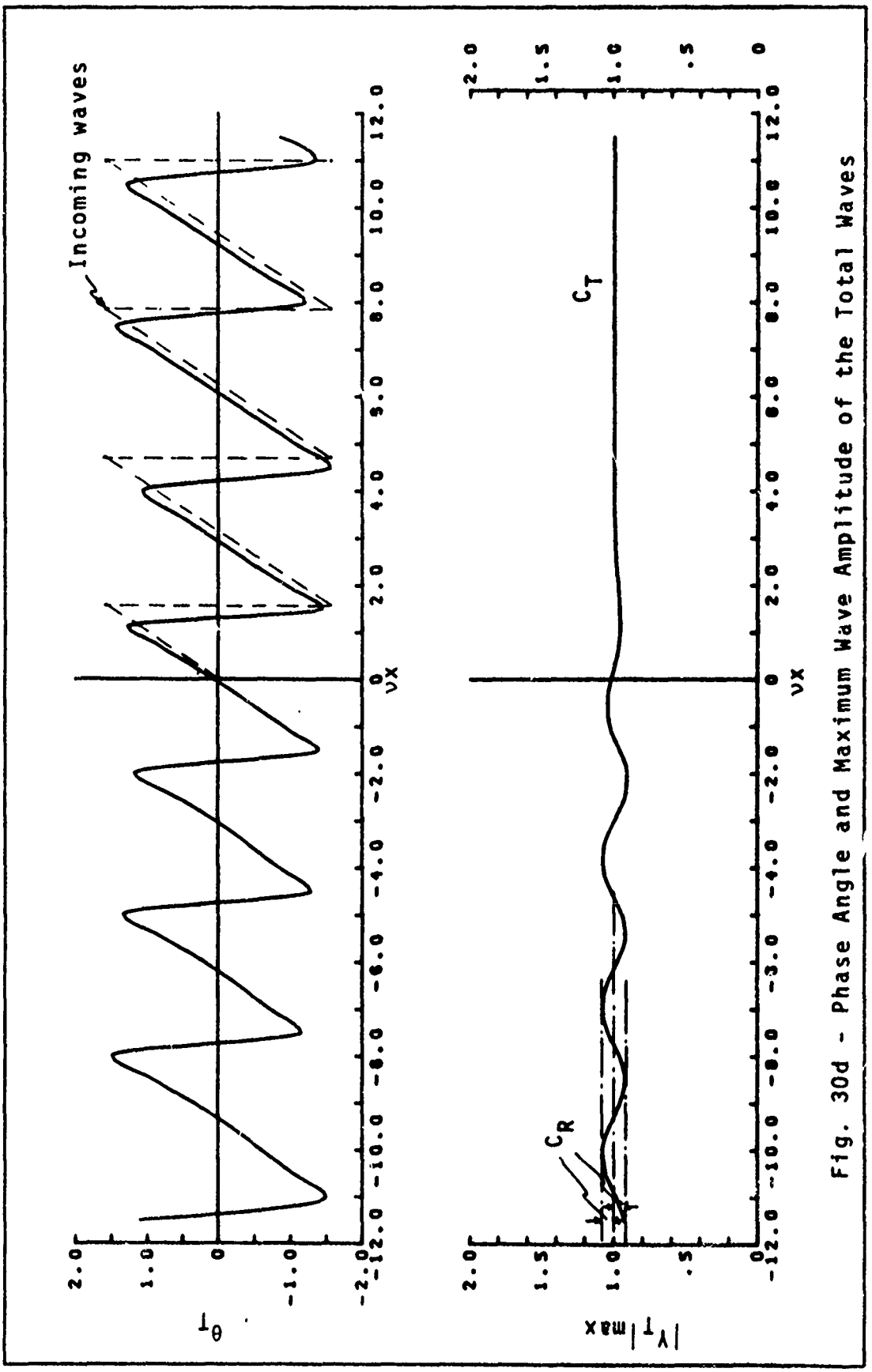

Fig. 30d - Phase Angle and Maximum Wave Amplitude of the Total Waves

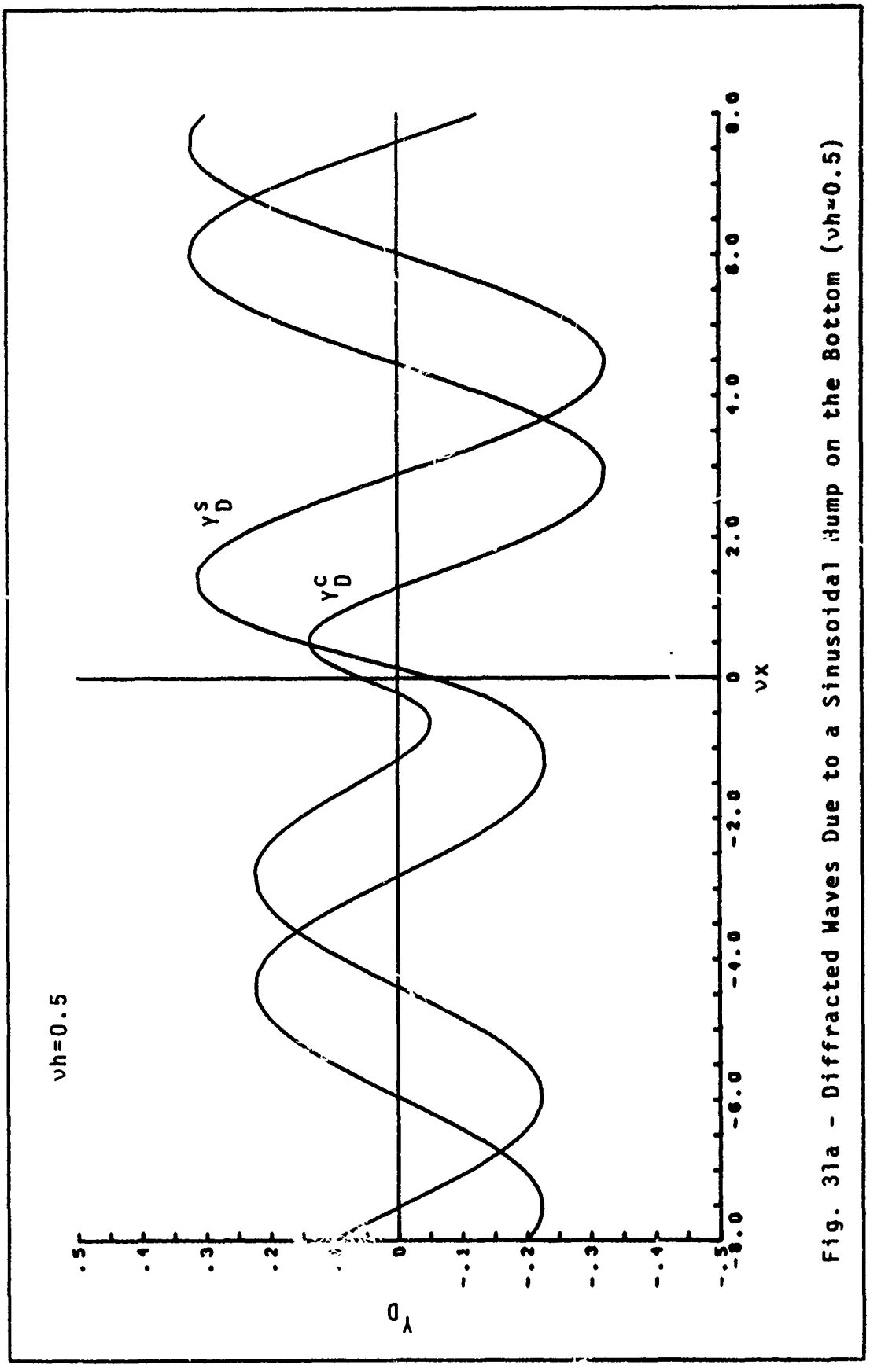

Fig. 31a - Diffracted Waves Due to a Sinusoidal Hump on the Bottom (νh=0.5)

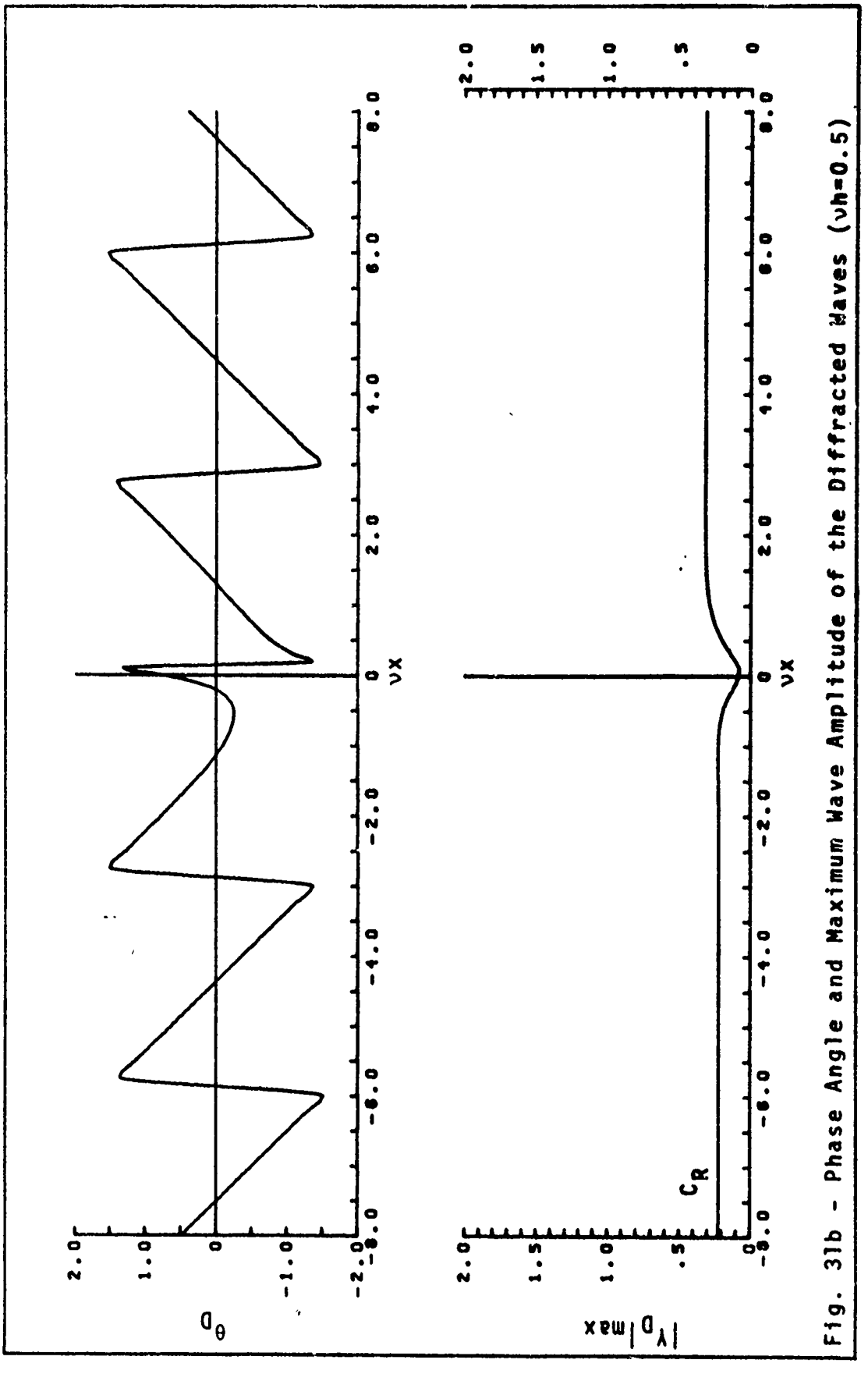

Fig. 31b - Phase Angle and Maximum Wave Amplitude of the Diffracted Waves (νh=0.5)

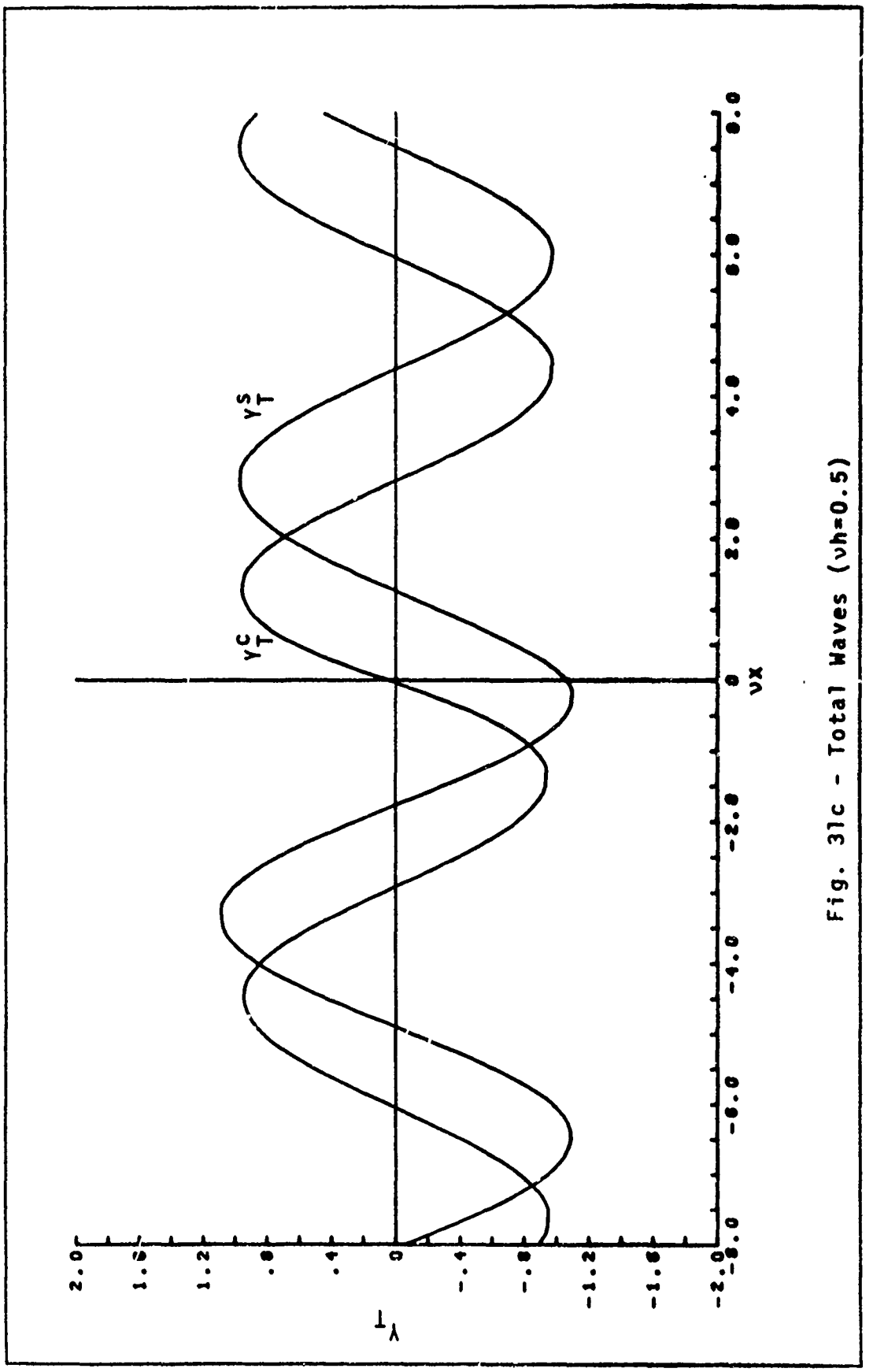

Fig. 31c - Total Waves (vh=0.5)

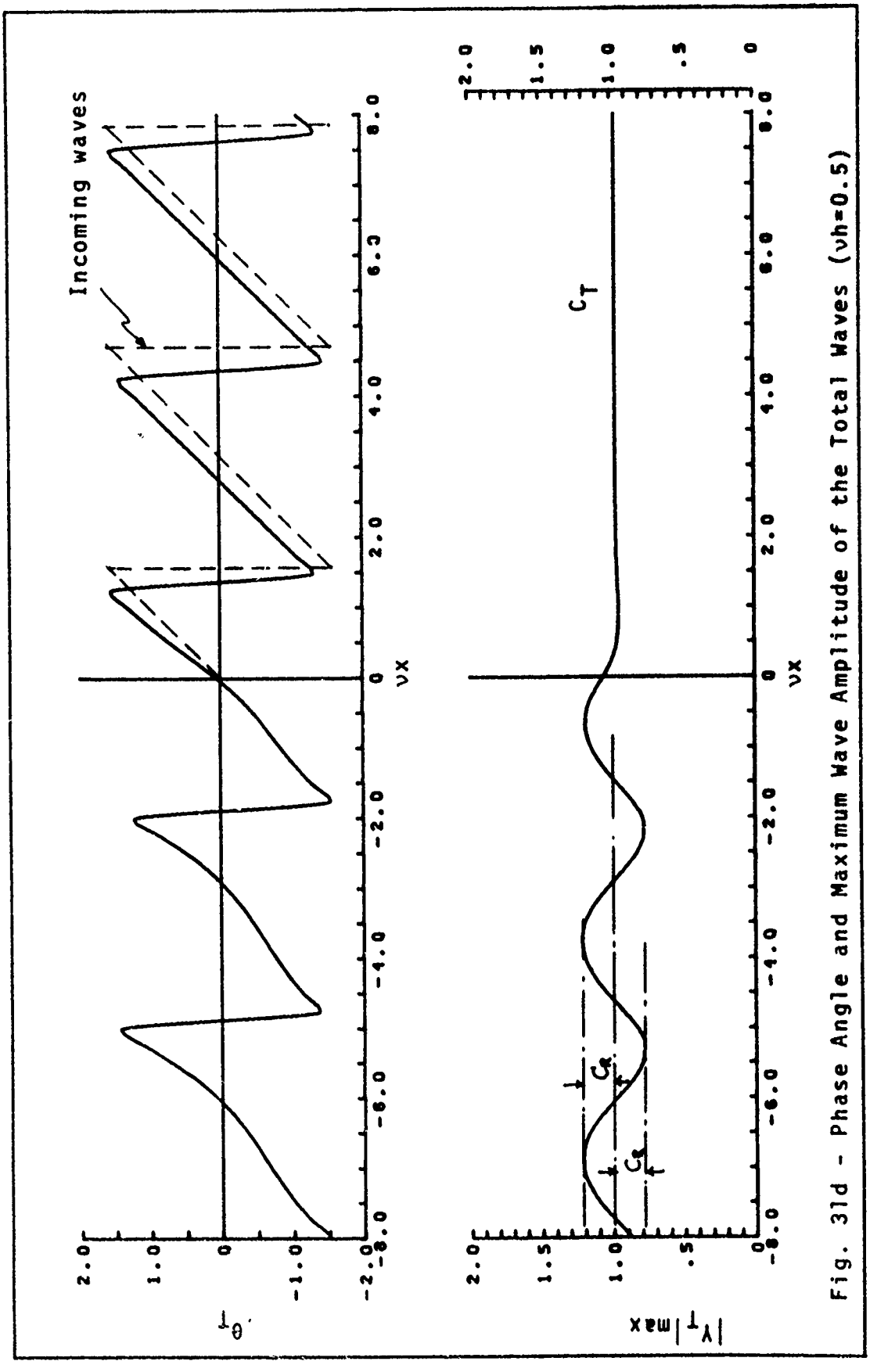

Fig. 31d - Phase Angle and Maximum Wave Amplitude of the Total Waves (νh=0.5)

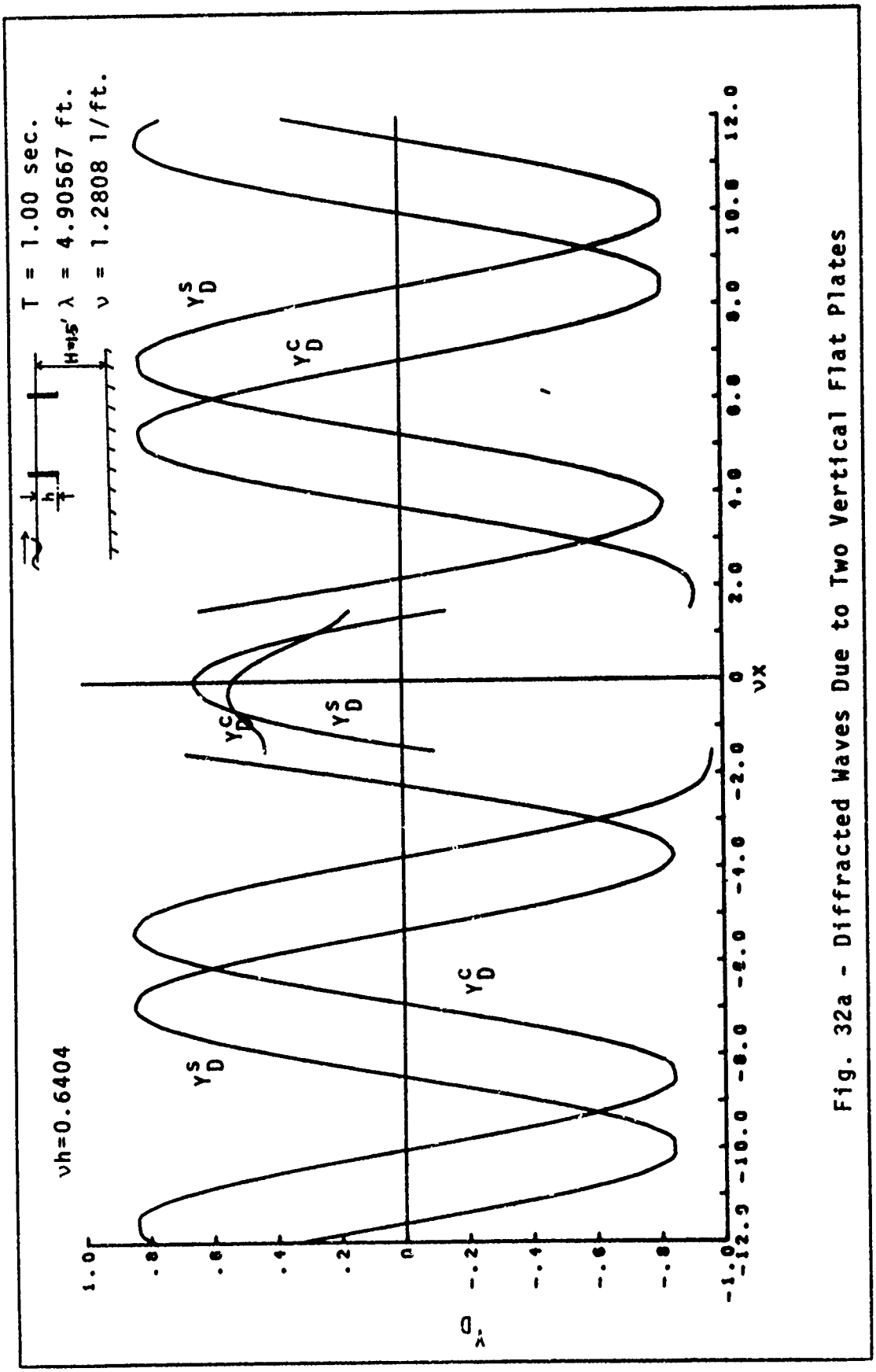

Fig. 32a - Diffracted Waves Due to Two Vertical Flat Plates

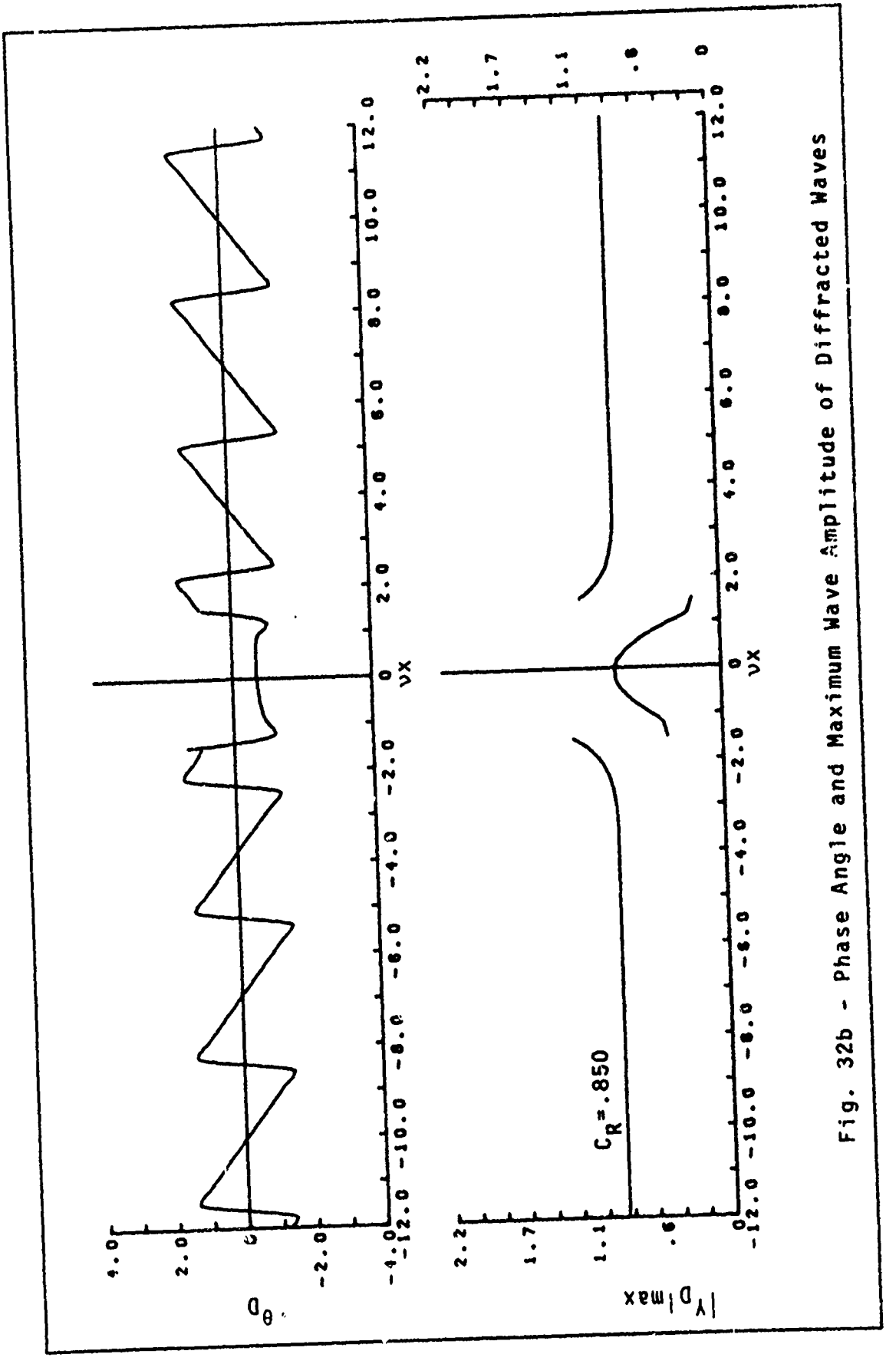

Fig. 32b - Phase Angle and Maximum Wave Amplitude of Diffracted Waves

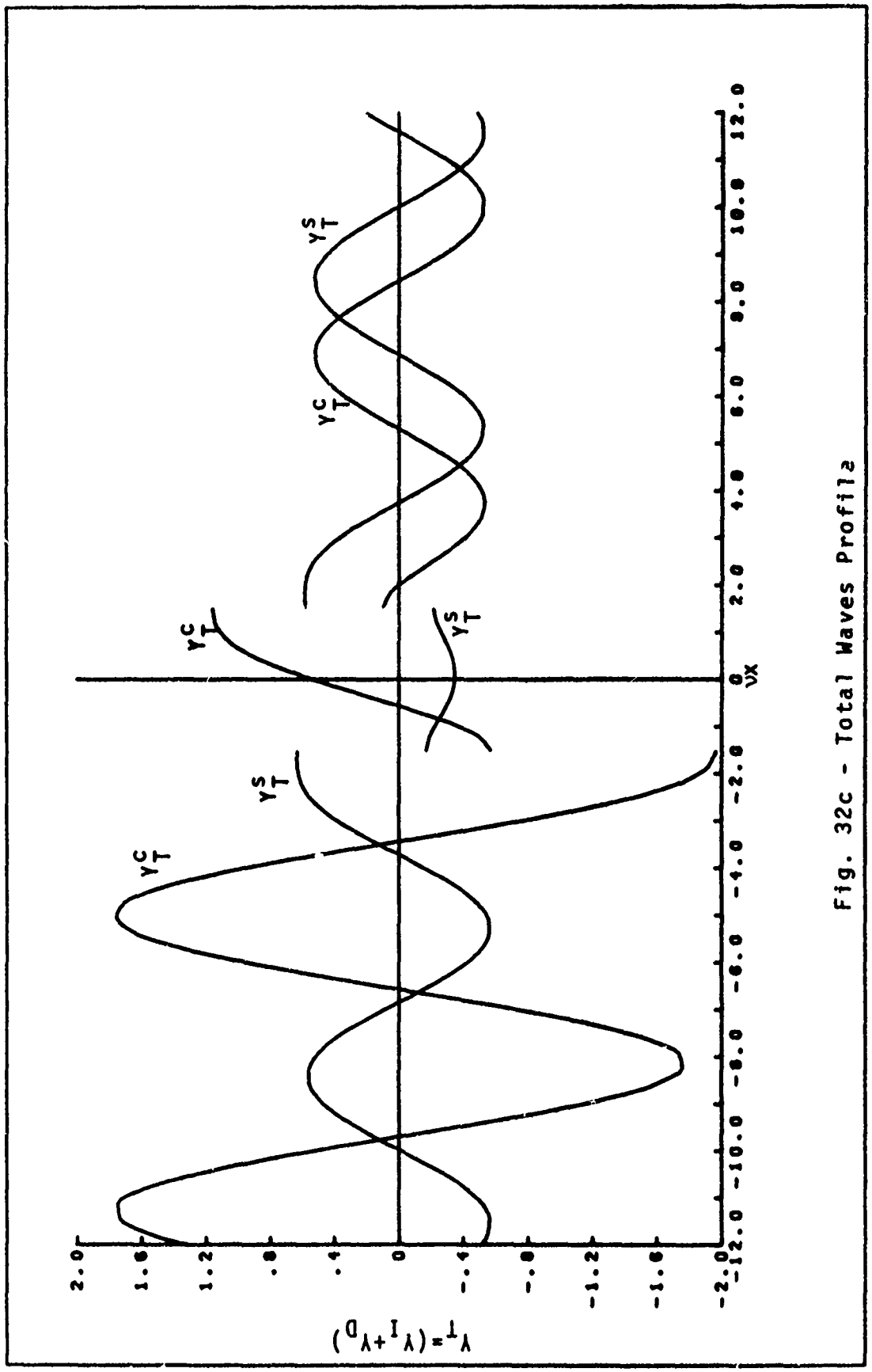

Fig. 32c - Total Waves Profile

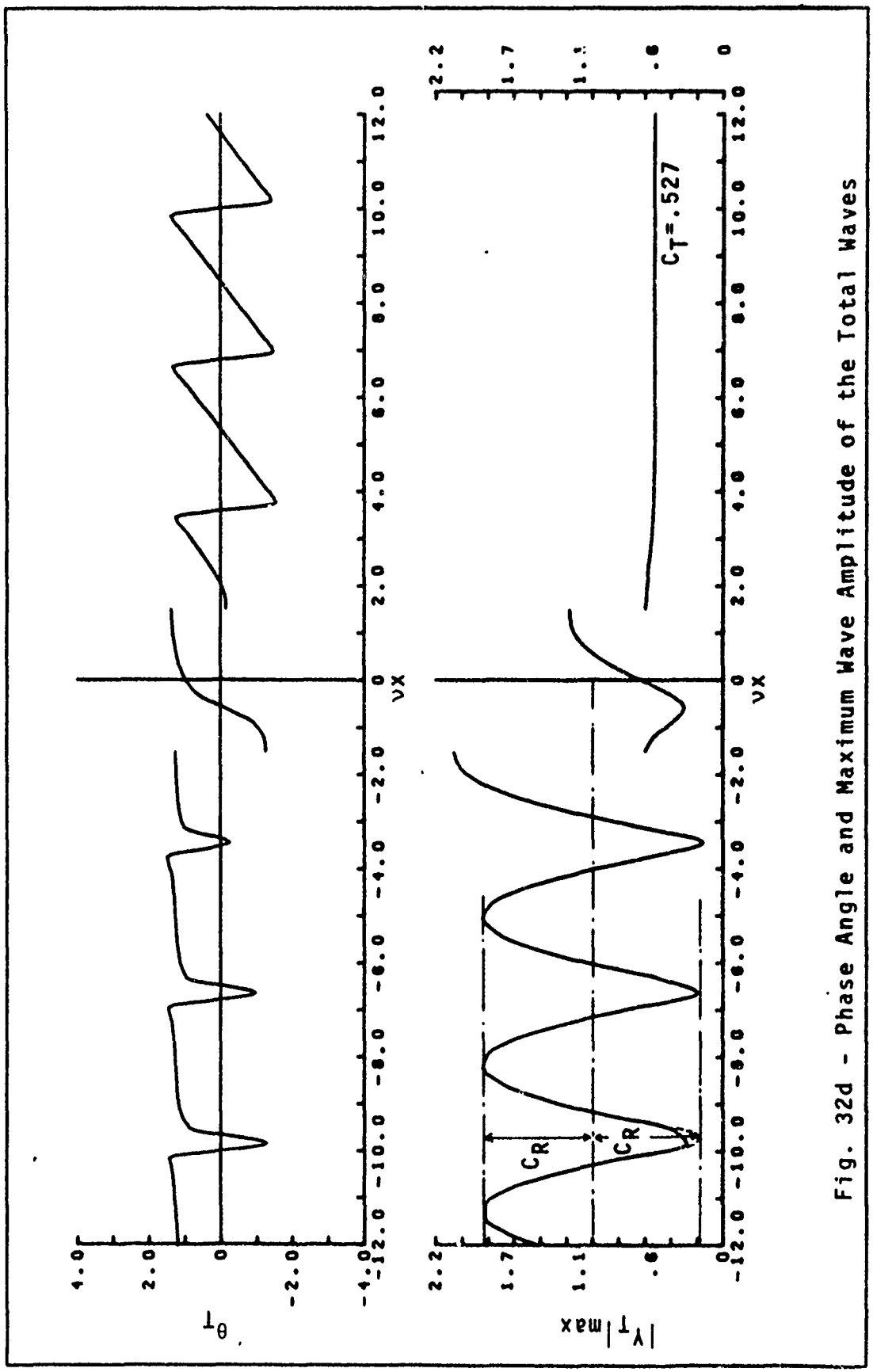

Fig. 32d - Phase Angle and Maximum Wave Amplitude of the Total Waves

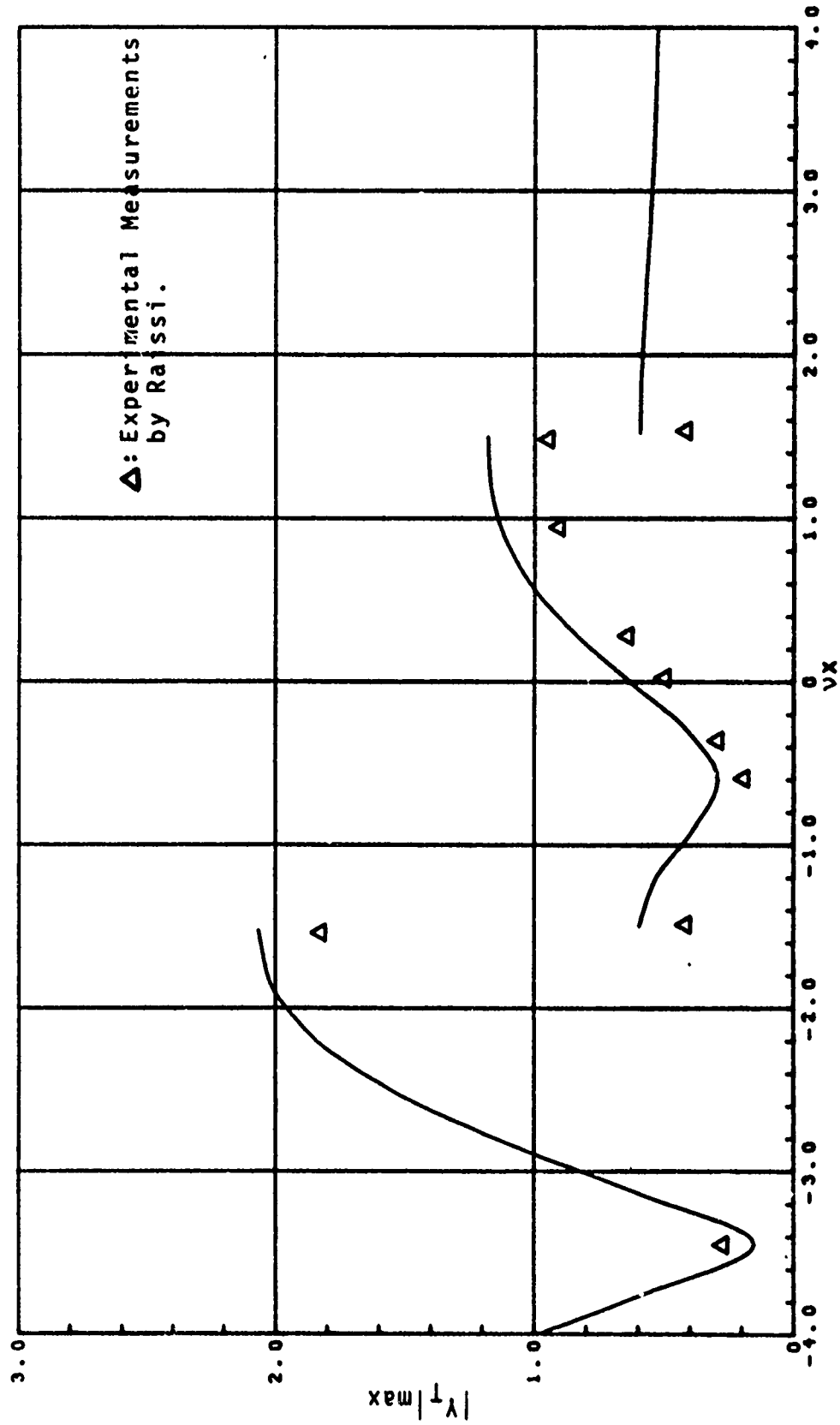

Fig. 32e - The Total Wave Amplitude

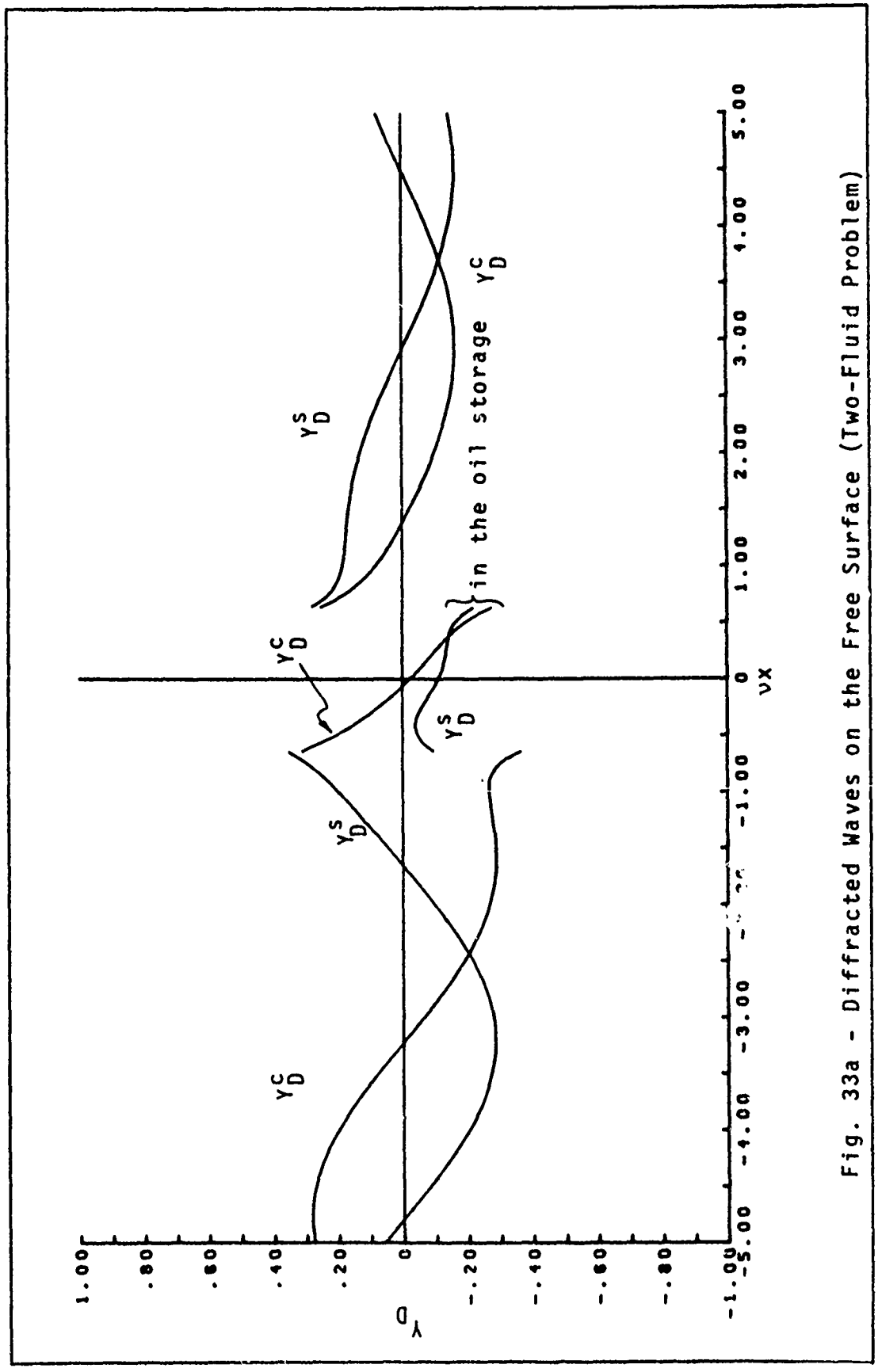

Fig. 33a - Diffracted Waves on the Free Surface (Two-Fluid Problem)

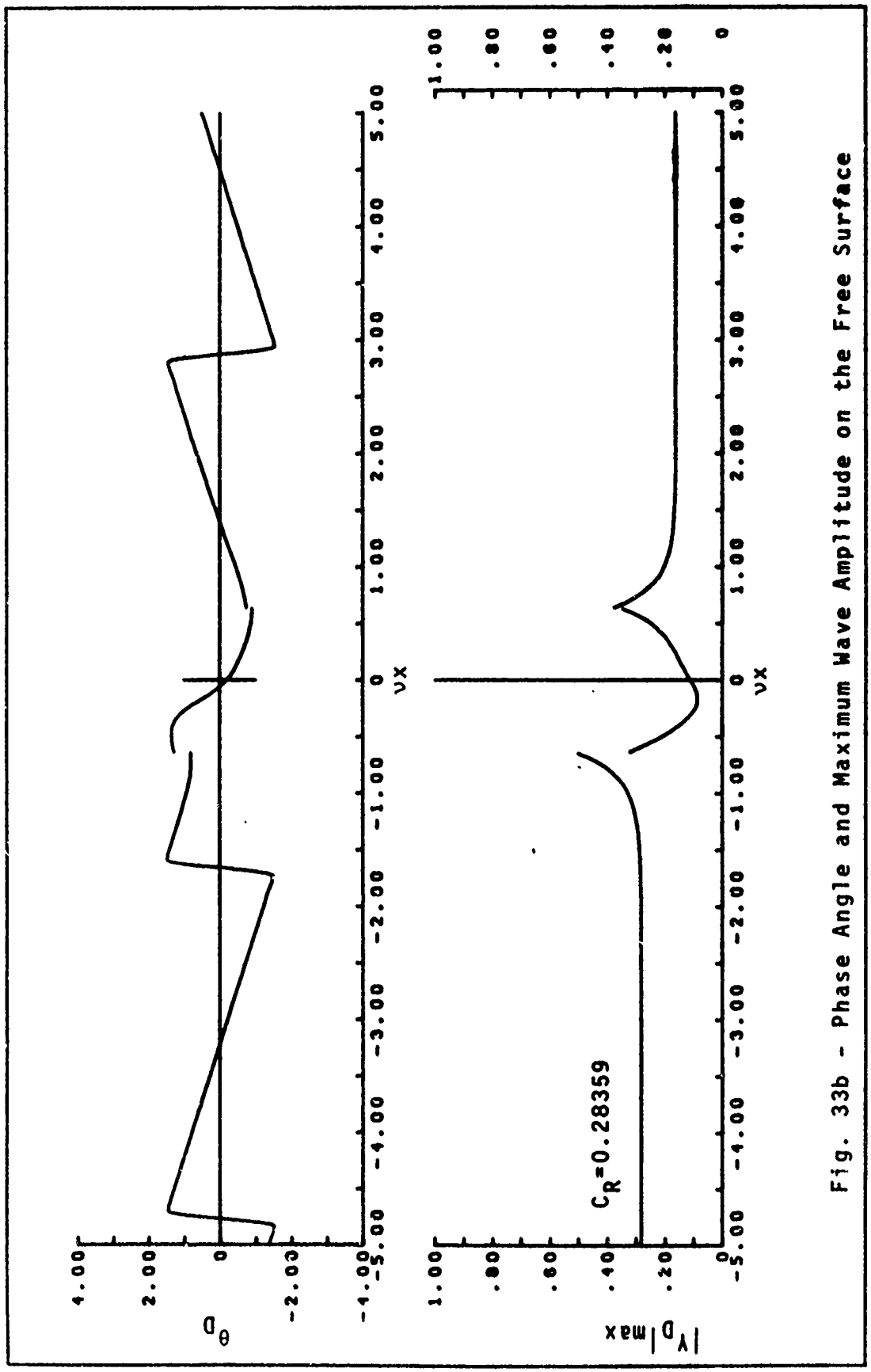

Fig. 33b - Phase Angle and Maximum Wave Amplitude on the Free Surface

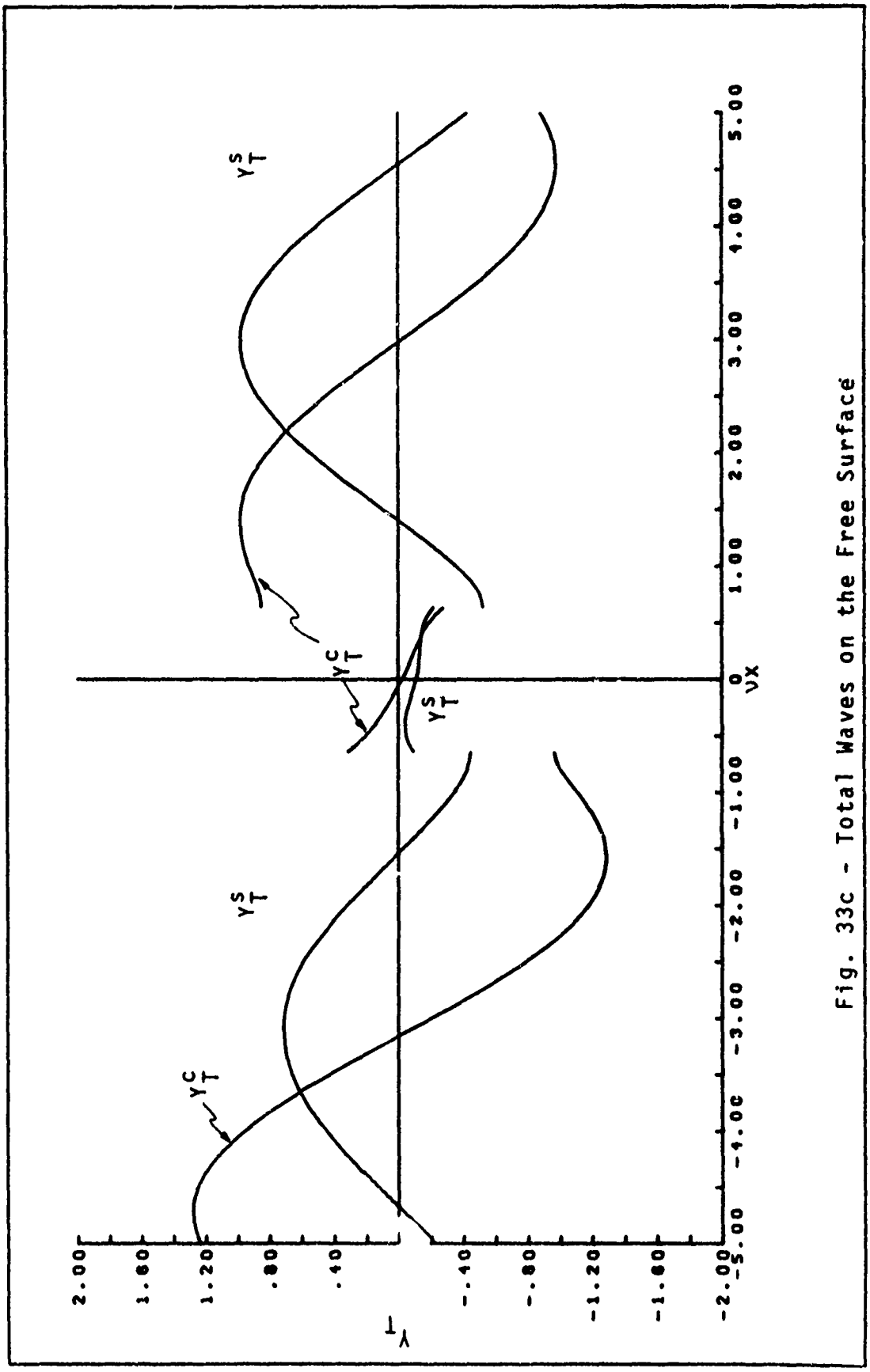

Fig. 33c - Total Waves on the Free Surface

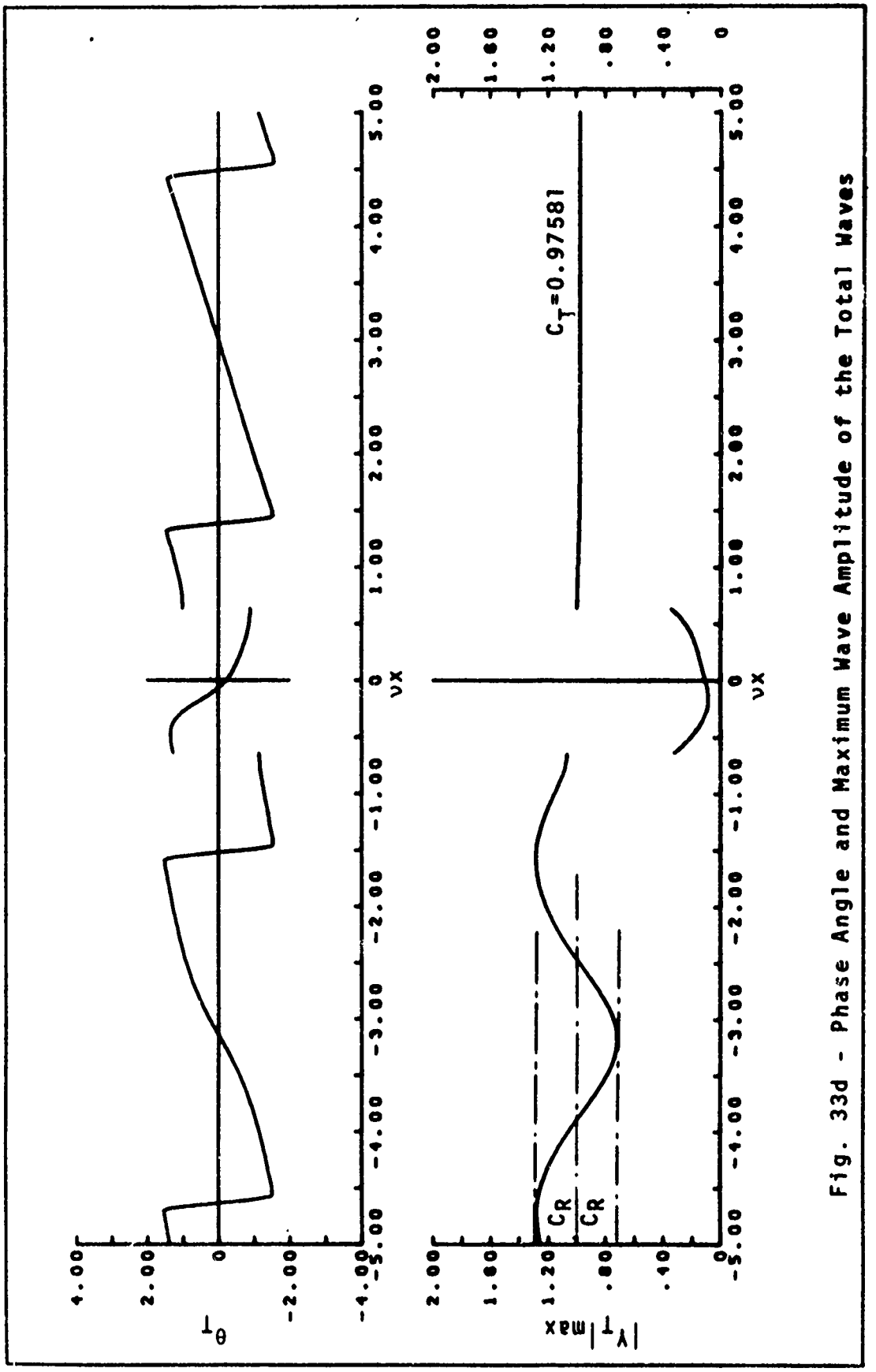

Fig. 33d - Phase Angle and Maximum Wave Amplitude of the Total Waves

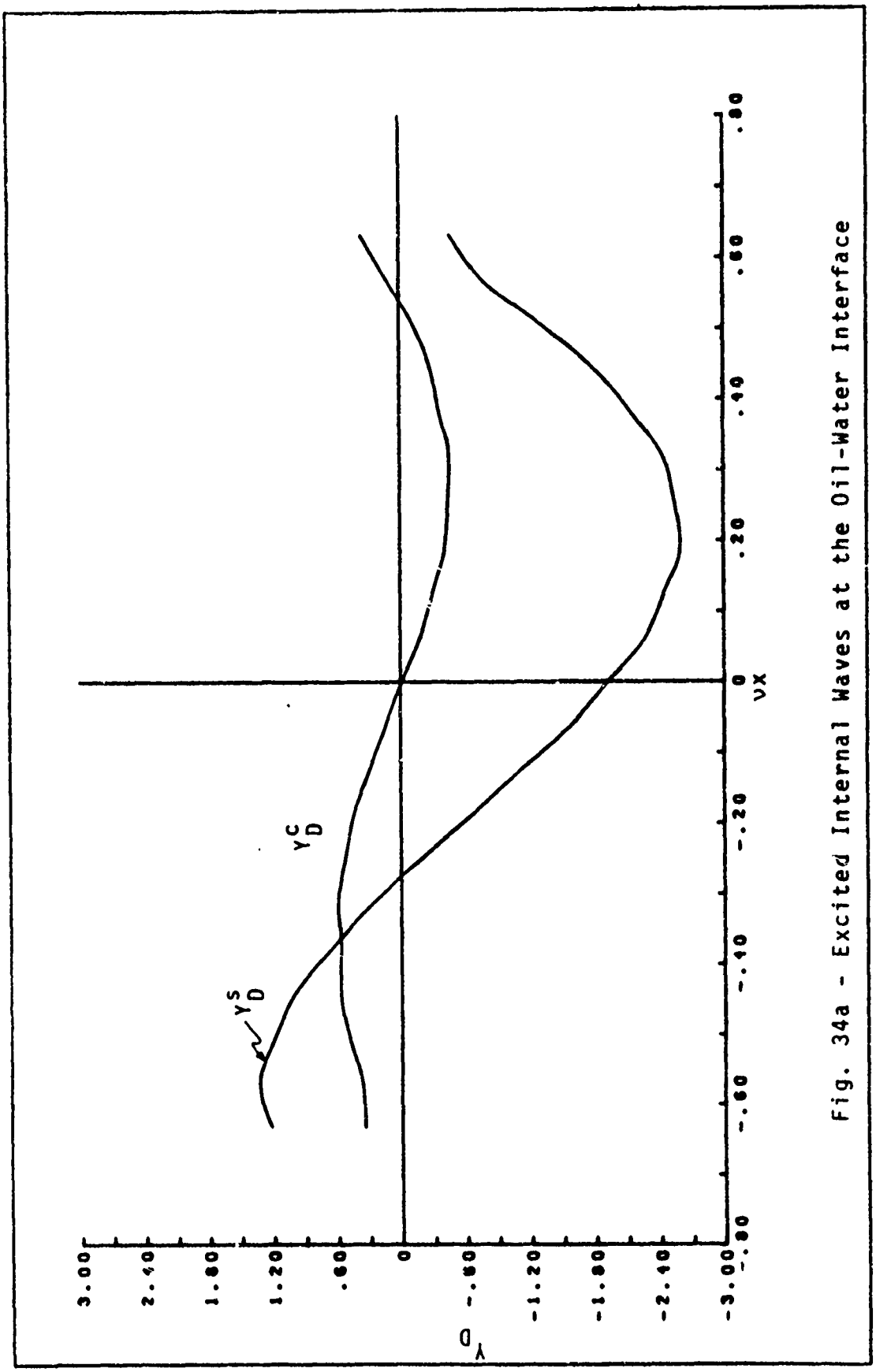

Fig. 34a - Excited Internal Waves at the Oil-Water Interface

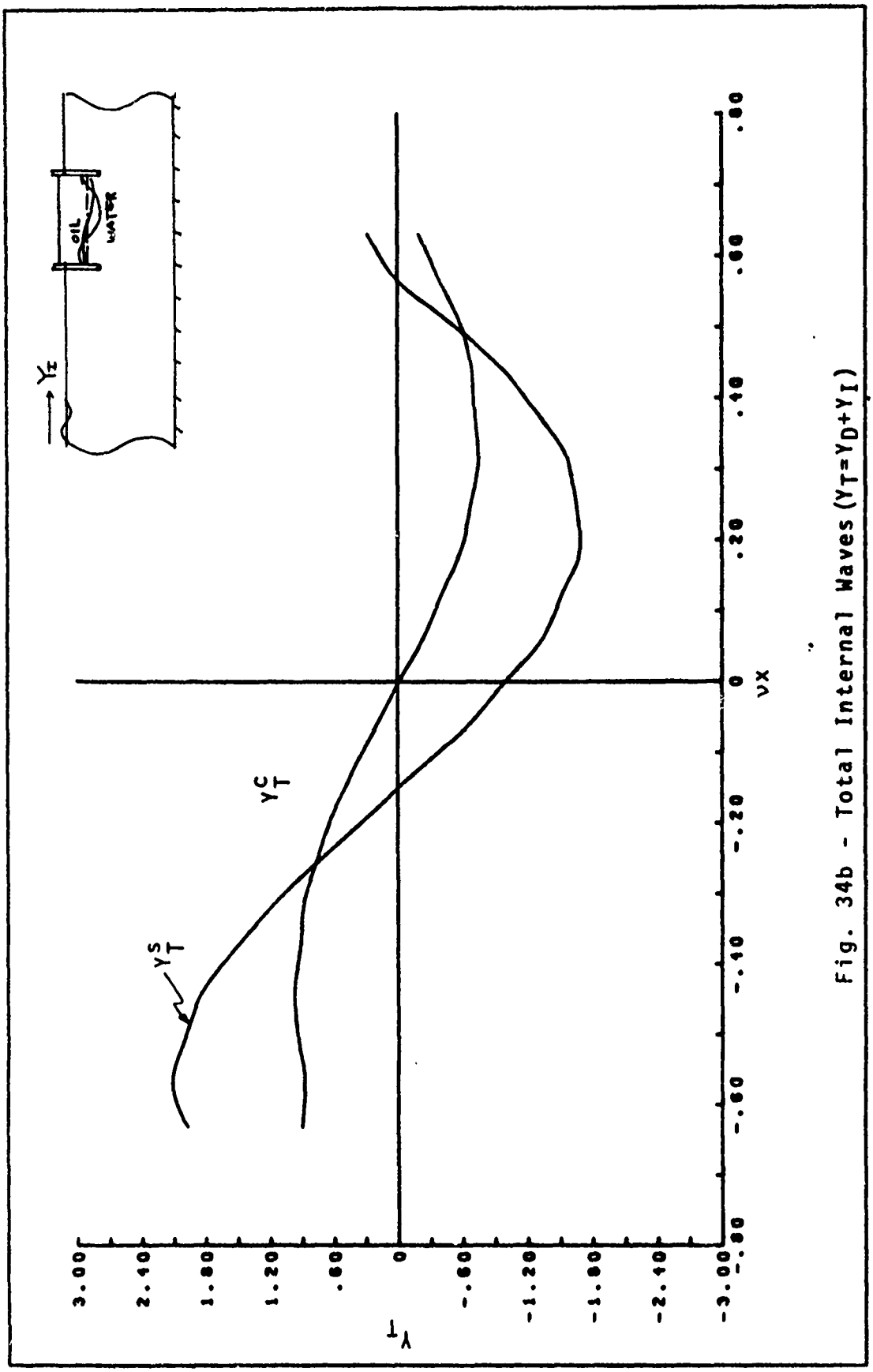

Fig. 34b - Total Internal Waves ($Y_T = Y_D + Y_I$)

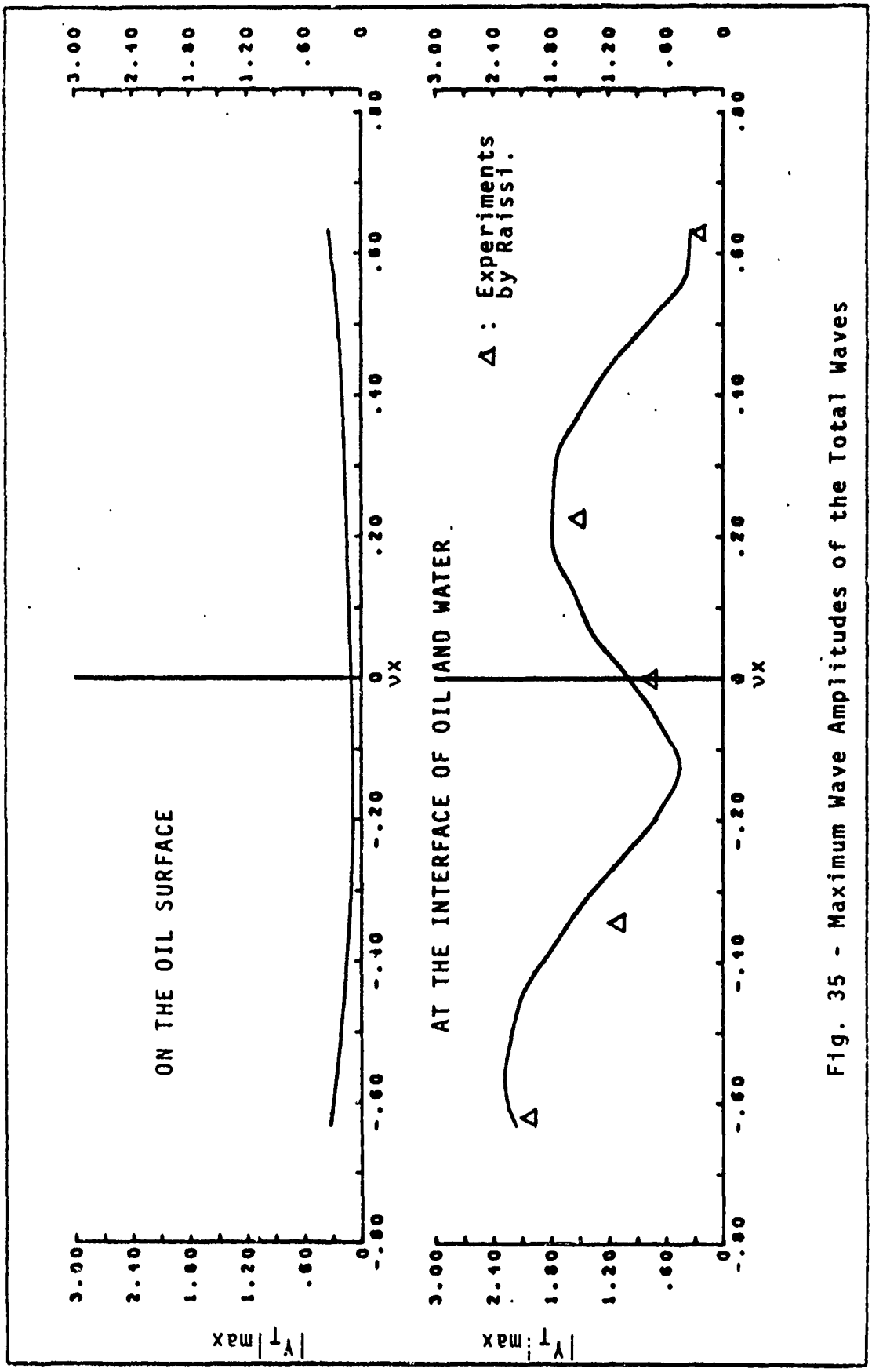

Fig. 35 - Maximum Wave Amplitudes of the Total Waves